Scientific Supervisors:
Prof. Zoltán Homonnay, professor and Prof. Azzedine Bousseksou, research director
Laboratory of Nuclear Chemistry, Institute of Chemistry
PhD School of Chemistry, Dr. György Inzelt
Theoretical and Physical Chemistry, Research of Material Structure PhD Programme,
Dr. Péter Surján
Eötvös Loránd University of Budapest, Hungary
"Switchable Molecular Materials" Group
Laboratory of Coordination Chemistry, CNRS, France
PhD School Material Science, Dr. Ronald Martino
Nanophysics PhD Programme Dr. Jean-Claude Ousset
Paul Sabatier University of Toulouse, France

DOCTORATE THESIS

of

Petra Ágota Szilágyi

Study of iron-chelates in solid state and aqueous solutions using Mössbauer spectroscopy

Submitted for the degree of PhD

2007

1 Acknowledgments

I dedicate this work to my family who have supported me all my life and have never let me down.

I am indebted for the multiple support of both of my supervisors Prof. Zoltán Homonnay and Dr. Azzedine Bousseksou.

I would also like to thank Dr. Gábor Molnár, Prof. Attila Vértes and Prof. Ernő Kuzmann for the very useful discussions and to all the help they provided me with.

Thanks are given to Dr. Jean-Marc Grenèche (Mössbauer measurements in an applied external magnetic field and at low temperature), Laboratoire de Physique de l'Etat Solide, Université du Maine, le Mans, France; to Dr. Roland Szalay (chemical syntheses) and to Dr. Zoltán Szakács (potentiometric titrations), Eötvös Loránd University, Budapest, Hungary; to Alain Mari (magnetic susceptibility measurements, ESR spectroscopy, Mössbauer spectroscopy), Jean-François Meunier (Mössbauer spectroscopy, thermal analyses), Lionel Rechignat (magnetic susceptibility measurements, ESR spectroscopy), Alix Saquet (electrochemistry) and to Laure Vendier (X-ray diffraction), LCC du CNRS, Toulouse, France, to Dr. János Madarász (thermal analyses), Technical University of Budapest, Budapest, Hungary, to Dr. Virender K. Sharma (Florida Institute of Technology, Florida, USA) and to all the staff at both institutions for their great scientific and technical support.

I wish to thank all my teachers who guided me in my studies, especially to Melinda Forró and to Attila Villányi.

I wish to acknowledge the warm collegial support during this research work to the other PhD students at both establishments, to Krisztina Kovács, Zoltán Németh, Szilvia Kárpáti, Saioa Cobo, Thomas Guillon and Sébastien Bonhommeau.

I wish to express my profound appreciation for the understanding and great support of my friends and of my boyfriend.

I also acknowledge the French Embassy in Hungary, especially Mr. Bob Kaba Lœmba and the Hungarian Ministry of Culture and Education for the scholarships that made this work possible.

2 General Introduction

The chelating agent ethylenediaminetetraacetic acid (EDTA; see molecular structure in Figure 2.1) is a compound of massive use world wide with household and industrial applications, being one of the anthropogenic compounds with highest concentrations in European inland waters. At a laboratory scale, degradation of EDTA has been achieved: however, in natural environments studies detect poor biodegradability. It is concluded that EDTA behaves as a persistent substance in the environment and that its contribution to heavy metals bioavailability and remobilisation processes in the environment is a major concern.

Metal ions cause detrimental effects in several industrial processes and in the formulation of many products. The presence of transition metal ions such as those of copper, iron, zinc and manganese may trigger chemical processes of corrosion, catalytic degradation, polymerisation inhibition, redox reactivity and changes in the colouring of products. In industrial processes these metal cations may come from the process waters, raw materials, equipment erosion and corrosion. They may also be added as specific metal species, but they may later suffer undesired alterations due to changes in concentration, pH, oxidation conditions, or reactions with other ingredients during the process. EDTA is a chelate ligand with a high affinity constant to form metal-EDTA complexes, being deliberately added to separate metal ions.

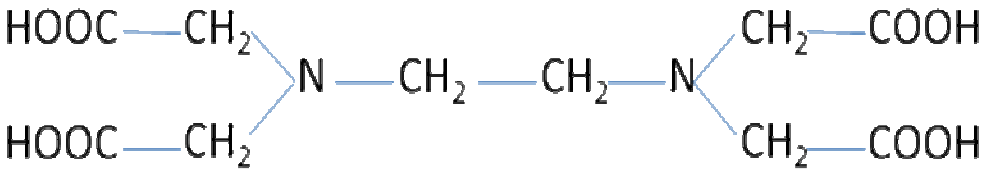

Figure 2.1 Molecular structure of the EDTA chelating agent.

EDTA is a powerful complexing agent of metals and a highly stable molecule, offering a considerable versatility in industrial and household uses (see in Table 2.1).

Table 2.1 Industrial and household uses of EDTA and its ligands (as percentage of the world market)

Use	% of world market
Detergents	33
Water treatment	18
Pulp and Paper Industry	13
Photography	5
Metal Cleaning	5
Cosmetics, foodstuffs, pharmaceuticals	5
Agrochemicals	4
Textile Industry	4
Printing Inks	3
Concrete admixtures	2
Miscellaneous	12

Annual consumption of EDTA was about 35000 tons in Europe and 50000 tons in the USA, in the year 1999.

In this work, the speciation of the ferric ethylenediaminetetraacetate in aqueous solutions, its photochemical properties, its reaction with hydrogen peroxide and its solid state behaviour have been studied. In order to obtain more information, some analogues, such as the ferric CDTA and EDDA complexes have been studied as well. The main method used was Mössbauer spectroscopy, which is a powerful method for studying iron complexes, especially in the case of solution samples where no crystallographic data can be obtained of the structure of complexes. In general, a major problem is how to correlate the structure in the solid state with the structure in solution. Investigations of the structure in solution are rather difficult, because various species can be present, which often exhibit similar spectroscopic properties, so that distinguishing them is not an easy task. An advantage of Mössbauer spectroscopy is that this method is very sensitive to small changes in the microenvironment and electronic structure of the Mössbauer active species (in our case, the iron-containing species) and thus provides high resolution to identify different species of iron.

In order to better understand this method, a short description of the principles of Mössbauer spectroscopy as well as of the hyperfine parameters and of the standard

Mössbauer measuring technique is given in Chapter 4 of this work, with special regard to the paramagnetic spin relaxation phenomenon, which often occurs in aqueous solutions of high spin (S=5/2) ferric compounds.

In Chapter 5, the studies carried out in order to investigate pH dependence of aqueous solutions of Fe^{III}EDTA, -CDTA and -EDDA using Mössbauer spectroscopy with and without an external magnetic field, ESR spectroscopy and magnetic susceptibility measurements are reported. The speciation of the ferric-ethylenediaminetetraacetate has been investigated previously by many workers and, since it is a very difficult task to recognise the species being present in a solution unambiguously (delicate acid-base reactions can take place, resulting in species with very similar spectroscopic parameters) contradictory hypotheses have been established to describe the system. It is known that ferric EDTA undergoes dimerisation and the dimeric species is well described spectroscopically, we aimed to induce the same process for the ferric CDTA and EDDA species as well.

In Chapter 6 Mössbauer studies of photodegradation of ferric-EDTA and the autoxidation of ferrous-EDTA are presented. This photoreduction has been investigated in the past decades and there are still some problems that need further investigation, such as the catalytic effect of the ferric oxy(hydroxy) precipitation on the reaction or the photoreactivity of the dimeric species. This reaction also affects the reaction of the iron/EDTA system with hydrogen peroxide; therefore its mechanism is interesting from this point of view as well as from the point of view of possible industrial applications.

Chapter 7 covers our experimental results on the reaction taking place between the Fe^{III}-EDTA/CDTA/EDDA system and hydrogen peroxide. In the case of the EDTA complex, the effect of its photodegradation on the reaction pathway has been studied. Structures of intermediate species as well as a scheme for the reaction paths have been proposed. The possibility of further application of the reaction taking place between the EDTA complex and hydrogen peroxide is obvious, since the species formed in the course of these reactions are known to be good model compounds, "*mimics*", for certain enzymes. However, the reaction pathway has not been completely discovered, nor have the intermediate species. We aimed to further study the pathway of the reaction, and also the reactions taking place between hydrogen peroxide and the ferric CDTA or

EDDA complexes in a qualitative way, so we had been focussing on the intermediate species generated in the course of these reactions.

Chapter 8 shall describe our Mössbauer (with and without an external magnetic field), magnetic susceptibility and crystallographic results on solid NaFeEDTA·3H_2O, as well as our Mössbauer spectroscopic and thermal analysis on the same compound. In this latter study, the further decay of the degradation products has also been studied and an oxidation mechanism proposed. The Mössbauer spectrum of the NaFeEDTA·3H_2O has been known since the middle of the seventies. Despite the well-known spectrum, the origin of its typical relaxation line shape has not been properly described. In this work, we aimed to determine the cause of the wide temperature range relaxation.

2.1 List of Abbreviations

EDTA – ethylenediaminetetraacetate

CDTA – cyclohexanediaminetetraacetate

ED3A – ethylenediaminetriacetate

EDDA – ethylenediaminediacetate(generally N,N'-)

EDMA – ethylenediaminemonoacetate

IMDA – iminodiacetate

NTA – nitrilotriacetate

MIDA – methyliminodiacetate

DPTA – diethylenetriaminepentaacetate

HEDTA – abbreviation is rather ambiguous in the literature, it usually refers to hydroxyethylethylenediaminetriacetate but there are also numerous publications which use it as a reference for the protonated form of EDTA. In this work, since mostly EDTA chelating agent was used, this abbreviation will refer for this latter one. However, if it means the hydroxylethylethylenediaminetriacetate, it will be mentioned in the text.

ESR – electron spin resonance spectroscopy

GC-MS – gas chromatography equipped with a mass spectrometer detector

3 Table of Content

4 Mössbauer spectroscopy

4.1 The Basic Phenomenon: The Mössbauer Effect

The resonance absorption of electromagnetic radiation is well known and widely used in different spectroscopic methods. The Mössbauer effect is based on the nuclear resonance absorption of γ-photons. The conditions of the resonance absorption of high-energy photons in nuclei are not as obvious as those of the absorption of low energy light (VIS, UV) in atoms. The basic difference between these two cases is due to two physical parameters. On the one hand, the lifetime of the excited states for atomic orbitals is relatively short, therefore the theoretical linewidth (Full Linewidth at Half-Maximum, FWHM or Γ) of the resonant radiation is large, but for nuclear levels the situation is the opposite (see Table 4.1.1). The uncertainties in energy and in time are related to Planck's constant $h = 2\pi\hbar$ by the Heisenberg uncertainty principle

$$\Delta E \Delta t \geq \hbar. \tag{4.1.1}$$

The ground-state nuclear level has an infinite lifetime and hence a zero uncertainty in the energy. However, the excited state of the radiation source has a mean lifetime τ of a microsecond or less, so that there will be a spread of γ-ray energies denoted by Γ_s

$$\Gamma_s \tau = \hbar. \tag{4.1.2}$$

On the other hand, the energy of a γ-ray quantum is of the magnitude of a few keV, while the energy of the photons responsible for atomic excitations is only about a few eV or less.

The energy of the emitted radiation, E_γ, defines the magnitude of the recoil energy, E_R, according to the principle of conservation of momentum

$$\frac{E_\gamma}{c} = Mv, \tag{4.1.3}$$

where v is the speed of the recoiled mass, M is the mass after the recoil event and c is the speed of light. Thus the recoil kinetic energy of the nucleus

$$E_R = \frac{E_\gamma^2}{2Mc^2}. \tag{4.1.4}$$

Obviously, raising E_γ, E_R can reach extremely high values since this latter one proportional to the square of the gamma energy.

Table 4.1.1 The recoil energy and half-linewidth at two typical photon energies[a]

	E_γ (eV)	E_R (eV)	Γ (eV)
(1)	1	$\sim 10^{-11}$	$\sim 10^{-5}$
(2)	$\sim 10^{5}$	$\sim 10^{-3}$	$\sim 10^{-9}$

[a] (1): atomic transition, (2): nuclear transition

To be able to take advantage of the extremely narrow linewidth of γ-radiation and, thus to be able to measure energy with an extremely high precision, at first, one has to get rid of the recoil energy. In 1957, Rudolf Mössbauer, discovered that the probability of the nuclear resonance absorption – in contrast to the try-outs made up to that time – is higher at lower temperature, in solid state. The phenomenon of the emission or absorption of a γ-photon without loss of recoil energy and without thermal broadening is known as the Mössbauer effect. Its unique feature is the production of monochromatic electromagnetic radiation with a very accurately defined energy spectrum, so that it can be used to resolve minute energy differences.

The Mössbauer effect is a quantum phenomenon, a direct consequence of the fact that lattice vibrations are quantised. A γ-photon can transmit its recoil energy to the system it was produced in by two basic mechanisms. Since the nucleus itself emits the γ-photon, this is the first target of the recoil energy. The recoil increases the kinetic energy of the vibrating nucleus and, since the nuclei are bound in a lattice, a phonon may be emitted, (the very unlikely event when the recoiled atom is ejected from the lattice can be safely excluded). In other words, the lattice vibrations may absorb the recoil energy. However, if the recoil energy is not high enough to excite the lowest energy vibration quantum available at the given temperature, the whole crystal, as a rigid body, will absorb the recoil energy, *i.e.* if the emitting atom is unable to recoil freely because of chemical binding, the recoiled mass can be considered to be the mass of the of the whole crystal rather than the mass of one single emitting atom (in a certain percentage of the events). Equation 4.1.4 will still apply, but the mass M is now that of the whole crystallite which even in a fine powder contains at least 10^{15} atoms, a huge mass in the relative sense, which results in negligible recoil energy. This phenomenon is called recoilless emission. The same phenomenon occurs during the absorption.

The probability of the recoilless events can be calculated using the Debye-model this model embodies a continuum of oscillator frequencies (ω) ranging from 0 to a

maximum ω_D (see Figure 4.1.1). This describes basically the above-mentioned phenomenon by defining a temperature, the Debye-temperature that is a unique parameter for each compound, below which the lattice vibrations are quantised, thus a phonon may be produced instead of the free recoil of nuclei. Excitation of phonons, because of quantum mechanical reasons, can be discussed only on a probability basis and not in a deterministic way. Consequently, the Mössbauer measurement requires relatively high threshold energy for exciting phonons.

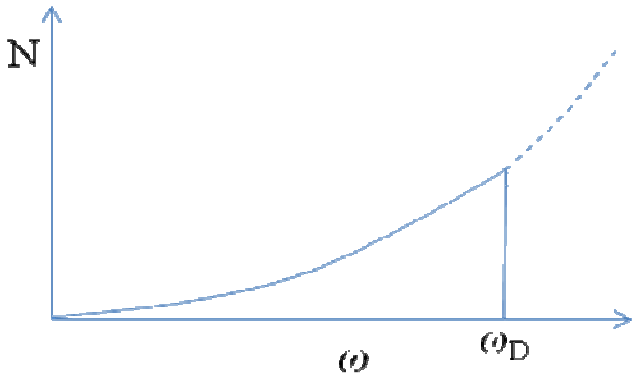

Figure 4.1.1 Number of freedom degrees of the lattice *vs.* frequency of the lattice vibration.

The probability of the Mössbauer effect is given by the Mössbauer-Lamb factor:

$$f = e^{-\frac{6E_R}{k\theta_D}\left\{\frac{1}{4}+\left(\frac{T}{\theta_D}\right)^2 \int_0^{\frac{\theta_D}{T}} \frac{x/dx}{e^x-1}\right\}}, \qquad (4.1.5)$$

where k is the Boltzmann constant, Θ_D is the Debye-temperature ($\Theta_{D,\text{ defined by }} \hbar\omega_D = k\Theta_D$) of the solid, T is the temperature and E_R is the recoil energy.

This recoilless nuclear resonance absorption is a powerful tool to study hyperfine interactions. A phase transition is always followed by the change of the Θ_D and of the f factor consequently. This change can be measured and the phase transition can be identified (references are given in Bibliography).

4.1.1 The ^{57}Fe-Mössbauer Measurement

The direct application of the Mössbauer effect to chemistry arises from its ability to detect the slight variations in the energy of interaction between the nucleus and the extra-nucleus electrons, variations which had previously been considered negligible. The Mössbauer measurement is a measurement of the absorption of the γ-rays as a function of energy (on an extremely fine scale). The photon in the case of ^{57}Fe is provided by a ^{57}Co source (See Figure 4.1.2). Following the electron capture (EC) and the emission of a photon of 122 keV, the excited state of the ^{57}Fe nucleus with I=3/2 nuclear spin is produced with the highest probability and this will emit the 14,4 keV photon that is able to excite another ^{57}Fe in ground state (I=1/2) if recoilless emission and adsorption as well as other conditions are met.

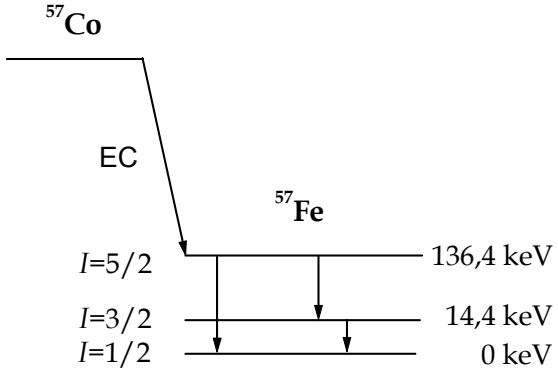

Figure 4.1.2. Decay scheme for a ^{57}Co nucleus.

During the emission of γ-rays, the excited state with a lifetime of about 10^{-7} s relaxes and the multitude of the ^{57}Fe nuclei emits an electromagnetic radiation that corresponds – approximately – to a function falling off exponentially in time, with an amplitude (intensity), modulated by a function representing the hyperfine interaction(s) as well. The energy distribution of the γ-ray (line shape) can be given by Fourier transformation and it results in a Lorentzian. The position of the observed resonant line is given by the frequency of the radiation (modulated by the hyperfine interactions); while the line width is given by the slope of the falling off of the exponential.

The change of the environment within the characteristic time of the hyperfine interactions can cause line distortions (in the case of paramagnetic spin relaxation, for instance).

4.1.2 Hyperfine Interactions

The energy of an electrically charged particle depends on the electromagnetic interactions in which it participates. The nucleus interacts with the electric field as a monopole and as a quadrupole, while it interacts with the magnetic field as a dipole; the terms of higher order are negligible, as their effect cannot be observed in the spectra.

Interaction with the electric field can be described as follows:

$$\Delta E = \int \rho_{nuc}(\mathbf{r}) V_{\mathrm{el}}(\mathbf{r}) \mathrm{d}\tau \,, \tag{4.1.6}$$

where the integration runs over the whole space. $\mathrm{d}\tau$ denotes the volume unit, ρ_{nuc} (hereinafter simply: ρ) is the charge density in the nucleus, V_{el} (hereinafter: V) the electric potential of the field created by the surrounding charges (atomic electrons).

Developing the potential into a Taylor series around the origin ($\mathbf{r}$=0) is sufficient up to the quadratic term since the volume of the nucleus is small:

$$\Delta E \approx V_0 \int \rho(\mathbf{r}) \mathrm{d}\tau + \sum_{i=1}^{3} \left(\frac{\partial V}{\partial x_i}\right)_0 \int \rho(\mathbf{r}) x_i \mathrm{d}\tau + \frac{1}{2} \sum_{i,j=1}^{3} \left(\frac{\partial^2 V}{\partial x_i \partial x_j}\right)_0 \int \rho(\mathbf{r}) x_i x_j \mathrm{d}\tau \,. \tag{4.1.7}$$

In this expression, the first term describes the interaction by an approximation where the nucleus is considered as a point charge in constant field, this approximation results equal energy affix to the ground and excited states, since the integral gives the charge of the nucleus. The second term always equals zero, since, according to the parity conservation law, a nucleus cannot have a dipole moment. For describing hyperfine interactions, the third term of the series is the most interesting one, which can be written as follows after diagonalising V to describe the charge distribution as a combination of spherical and diverging terms:

$$E_3 = \frac{1}{2} \sum_{i=1}^{3} V_{ii} \int \rho(\mathbf{r}) \frac{r^2}{2} \mathrm{d}\tau + \frac{1}{6} \sum_{i=\&}^{3} V_{ii} \int \rho(\mathbf{r}) (3x_i^2 - r^2) \mathrm{d}\tau \,. \tag{4.1.8}$$

The first part of this expression is related to the isomer shift, while its second part is related to the quadrupole splitting.

4.1.2.1 The Isomer Shift

For many purposes it is adequate to consider the nucleus as a point charge that influences the electrons via the Coulombic potential. However, the nucleus has a finite volume, and this must be taken into account when considering nucleus-electron interactions because an *s*-electron wavefunction implies a non-zero charge density within the nuclear volume, as described by equation 4.1.9 (see below). This is the electric monopole interaction, or the Coulomb-interaction, which alters the energy separation between the ground state and the excited state of the nucleus, thereby causing a slight shift in the position of the observed resonant line (E_δ). (For typical isomer shift values of iron compounds in versatile oxidation and spin state at room temperature see Figure 4.1.3.)

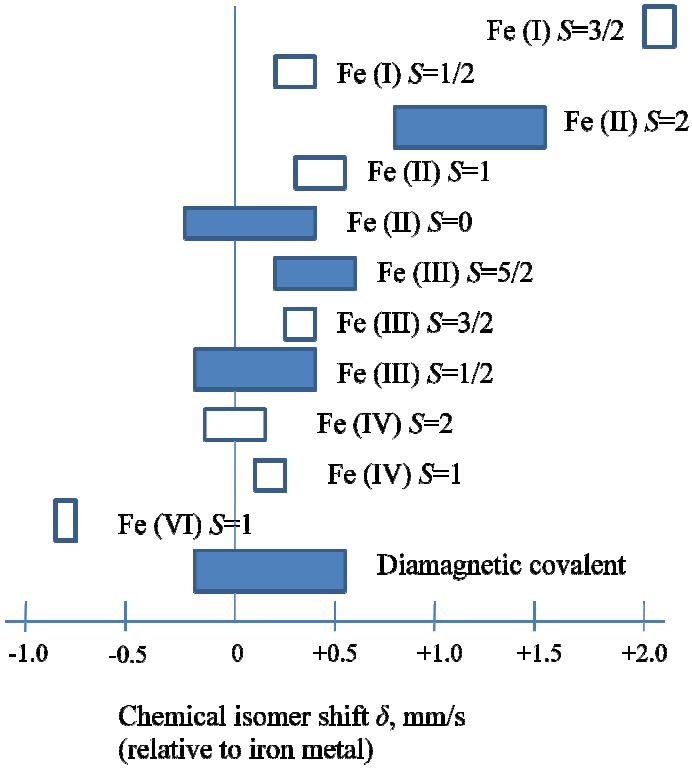

Figure 4.1.3 Typical isomer shift values of iron compounds in versatile oxidation and spin state at room temperature.

It can be demonstrated that integrating the first term of equation 4.1.8 the energy of the interaction is given as follows:

$$E_\delta = \left(\frac{2\pi}{5}\right) Ze^2R^2|\Psi(0)|^2, \quad (4.1.9)$$

where R is the nuclear radius and Ψ refers to the wave function of the *s* electrons.

Since the isomer shift is given by definition as:

$$\delta = E_{\delta,abs} - E_{\delta,source} = \left(E_{exc} - E_{ground}\right)_{abs} - \left(E_{exc} - E_{ground}\right)_{source}, \quad (4.1.10)$$

Therefore

$$\delta = \frac{2\pi Ze^2}{5}\left(R_{exc}^2 - R_{ground}^2\right)(|\Psi_{\text{abs}}|^2 - |\Psi_{\text{source}}|^2), \quad (4.1.11)$$

The isomer shift is a relative quantity: since one cannot measure this energy change directly, in an absolute way, it is only possible to compare it by means of a suitable reference which can either be the γ-source used in recording the Mössbauer spectra or another absorber (natural iron).

The Isomer Shift of a compound always displays a variation as a function of temperature; this effect is called the Second Order Doppler Effect:

4.1.2.1.1 *Second Order Doppler Shift*

The Second Order Doppler Shift is a temperature-dependent effect on the centre shift of a Mössbauer spectrum. Above 0 K, atoms in lattice oscillate about their mean position. The frequency of this oscillation is of the order of 10^{-12} Hz, meaning that the average displacement during the lifetime of a Mössbauer event is zero. However, the second term in the Doppler shift depends on v^2 leading to the mean square displacement being non-zero. This energy shift is given by:

$$\frac{\delta E_\gamma}{E_\gamma} = -\frac{\langle v^2 \rangle}{2c^2}. \quad 4.1.12$$

For ^{57}Fe in the high temperature limit this gives a change of $7*10^{-2}$ mm/sK, approximately.

4.1.2.2 The Quadrupole Splitting

The quadrupole moment of the nucleus makes an electric quadrupole interaction with the electric field gradient (**EFG**) created by the surrounding charges possible, thus the resonant lines split in the spectrum (see Figure 4.1.3/1).

Using the second term of equation 4.1.6, the quadrupole interaction can be expressed for the I=3/2→1/2 nuclear transition in an analytical form as follows:

$$E_{\mathrm{Q}} = \frac{e^2qQ}{4I(2I-1)}\left[3m_{\mathrm{I}}^2 - I(I+1)\right]\left(1+\frac{\eta^2}{3}\right)^{\frac{1}{2}}, \tag{4.1.13}$$

where η is the asymmetry parameter (in the axial symmetrical case η=0), Q is the quadrupole moment of the nucleus, I is the nuclear spin, m_{I} is the magnetic quantum number and eq is the zz component of the electric field gradient,

$$eq = V_{zz} = -\frac{\partial^2 V}{\partial z^2}. \tag{4.1.14}$$

The electric field gradient (**EFG**) is a second order tensor defined by the matrix below:

$$\mathbf{EFG} = -\begin{bmatrix} \frac{\partial^2 V}{\partial x^2} & \frac{\partial^2 V}{\partial x \partial y} & \frac{\partial^2 V}{\partial x \partial z} \\ \frac{\partial^2 V}{\partial y \partial x} & \frac{\partial^2 V}{\partial y^2} & \frac{\partial^2 V}{\partial y \partial z} \\ \frac{\partial^2 V}{\partial z \partial x} & \frac{\partial^2 V}{\partial z \partial y} & \frac{\partial^2 V}{\partial z^2} \end{bmatrix}. \tag{4.1.15}$$

The asymmetry parameter can be written as follows,

$$\eta = \frac{V_{xx}-V_{yy}}{V_{zz}}, \tag{4.1.16}$$

where

$$|V_{zz}| \geq |V_{yy}| \geq |V_{xx}|, \tag{4.1.17}$$

by definition.

The quadrupole splitting results in one doublet for the case of ^{57}Fe, which is generally symmetrical (if the sample does not have a texture effect[1] for instance).

The measurement of these interactions can provide important chemical information.

[1] A single-crystal absorber, unlike a polycrystalline one, has angular properties, and the intensity of the hyperfine lines will vary according to orientation. A dipole 3/2→1/2 transition shows 1:1 intensity for a polycrystalline sample, and 5:3 and 1:3 intensity ratios for a single crystal with the γ-ray axis perpendicular and parallel to the principal axis of a symmetric electric field gradient tensor.

The isomer shift is very sensitive to the oxidation state (see Figure 4.1.3), for the donor-acceptor properties of the ligands, and one can also get information concerning ligand field strength and the spin state of complexes, etc.

The quadrupole splitting provides data about the symmetry of the electric field around the studied atom, since the non-zero **EFG** is due to the deviation distribution of the electrons or the ions from the spherical or the highest crystallographic symmetry. The quadrupole splitting is a sensitive measure of the valence state of iron since the $3d^5$ and $3d^6$ electronic configurations for the Fe^{3+} and Fe^{2+} ions, respectively, have markedly different symmetry. The variation of the spin state also causes dramatic change for a similar reason.

4.1.2.2 The Magnetic Splitting

The third important hyperfine interaction is the Zeeman effect that occurs when there is a magnetic field at the nucleus. Since the nucleus acts as a magnetic dipole, the magnetic field splits the nuclear level of spin I into $(2I+1)$ equidistant, non-degenerated substates (in the case of ^{57}Fe the ground state splits into two, while the excited state splits into four levels); the magnitude of the splitting is related to the strength of the magnetic field (see Figure 4.1.4/2).

The selection rules ($\Delta m=0,\pm1$) permit only six from the eight possible transitions (note that the selection rules are derived from the principle of the conservation of momentum). The value of the nuclear energy levels is

$$E_{\mathrm{m}} = \frac{-\mu H m_{\mathrm{I}}}{I}\,, \tag{4.1.18}$$

where m_{I} is the magnetic quantum number representing the z component of I (*i.e.* $m_{\mathrm{I}} = I, I-1 \ldots -I$), μ is the nuclear magnetic moment and H is the magnetic field at the nucleus. The relative intensity of absorption lines in the ideal randomly homogenised material it is: 3:2:1:1:2:3.

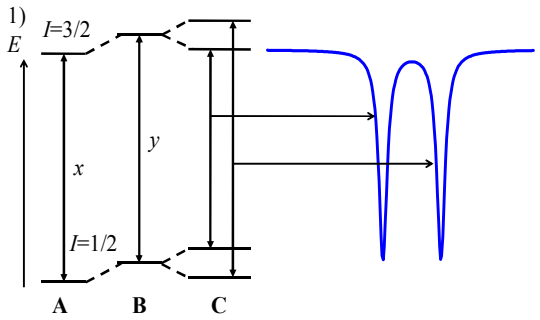

Figure 4.1.4/1

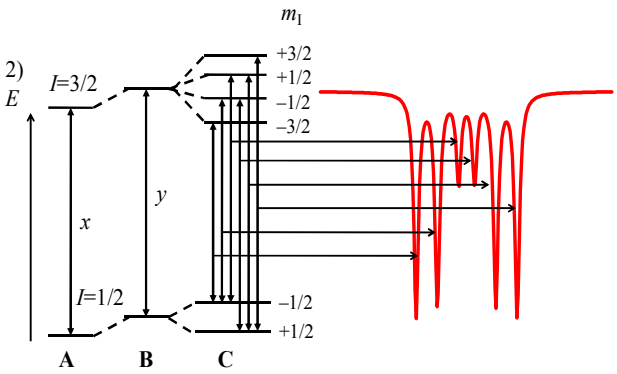

Figure 4.1.4/2

Energy levels of hyperfine interactions (the isomer shift is given by the subtraction $y_{absorber}-y_{source}$, $x \neq y$) and the possible transitions:

A: Energy levels of a nucleus in a nuclear transition, without external Coulomb field,

B: Energy levels of a system consisted of a nucleus and other charges (*e.g.*, nucleus in an atom) in a nuclear transition,

C: 1) Energy levels in the case of electric quadrupole interaction. 2) Energy levels in the case of magnetic dipole interaction.

4.1.3 Paramagnetic Relaxation Effects

The studied nucleus is *a priori* in a magnetic field when the unpaired electrons of the cores are ordered, so the matrix is either ferro-, ferri- or antiferromagnetic (not to mention more complicated cases), thus a permanent magnetic field is present. But, since the characteristic time of the interaction (Larmor-precession) is short, one can obtain spectra with magnetic splitting in the case of fluctuating magnetic field as well. Paramagnetic matters produce such a fluctuating field, where the spins flip in an unordered way (relaxation). If the frequency of the Larmor-precession of the interacting nucleus is considerably higher than the frequency of the spin relaxation, one obtains a pure magnetically split subspectrum (see in Figure 4.1.5a)). In the opposite case when the relaxation frequency is much higher than that of the Larmor-precession, a doublet can be observed in the Mössbauer spectrum (see in Fig. 4.1.5b)). More complicated spectra are obtained when the two speeds are from the same magnitude, which results in broadened lines in the spectrum (relaxation broadening/distortion, see in Fig. 4.1.5c)).

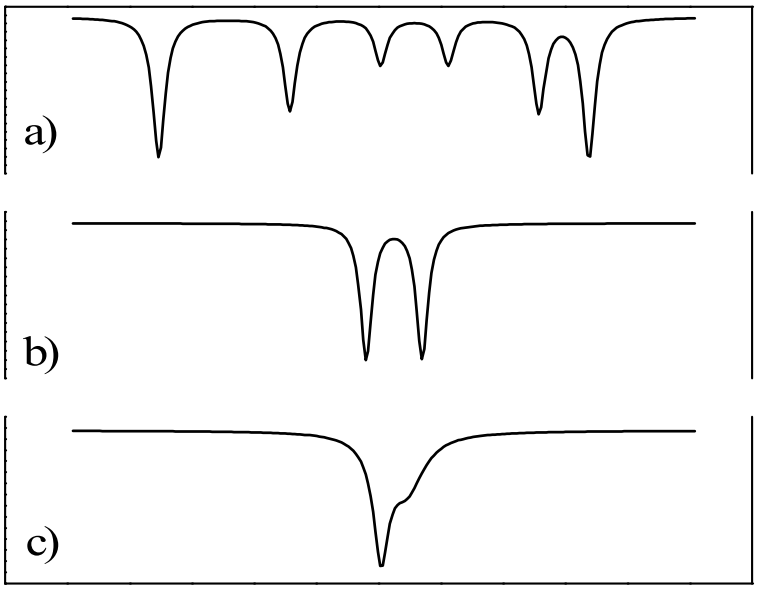

Figure 4.1.5 Simulated Mössbauer spectra at various spin-flip frequency/Larmor precession frequency relations (a) $\nu_{sf} << \nu_L$; b) $\nu_{sf} >> \nu_L$; c) $\nu_{sf} \sim \nu_L$). (Simulations were done by the MossWinn3.0 software package.)

4.1.3.1 Relaxation Mechanisms

The static hyperfine fields involve time-independent Hamiltonians. This approximation fails when the hyperfine fields fluctuate owing to electronic relaxation processes. Generally in paramagnetic systems, the lattice electronic or interionic electron spin-spin interactions are stronger than the intraionic hyperfine interactions. Much of the relaxation literature is concerned with the transfer of electronic Zeeman energy either from a "spin system" to lattice modes of vibration, called *spin-lattice relaxation* with a characteristic time T_1, or between individual members of the spin system, the latter considered as a separate energy system. The term *spin-spin relaxation* refers to processes establishing an equilibrium condition within this spin system. Its characteristic time is T_2.

In either case an external field is often implicitly assumed. Mössbauer experiments are commonly performed in the absence of such a field and the spin system consists of a set of crystal field levels (perturbed to varying degrees by local fields). In what follows, a spin system denotes a generic set of ionic levels, although they may not correspond to Zeeman levels.

A third type of relaxation, having many nuances, has been termed “cross relaxation” and basically involves exchange of energy between two “different” spin systems.

4.1.3.1.1 *Spin-Lattice Relaxation*

T_1, the mean time between electronic transitions may be expressed in terms of transition probabilities computed by first- and second-order, time-dependent perturbation theory. The general form for $\mathcal{H}_{\mathrm{OL}}$, the perturbation coupling the lattice and spin system can be written as an expansion of multiple operators as follows:

$$\mathcal{H}_{\mathrm{OL}} = \sum_k \mathbf{A}_{\mathrm{O}}^{[k]} \cdot \mathbf{B}_{\mathrm{L}}^{(k)} \tag{4.1.19}$$

Where $\mathbf{A}_{\mathrm{O}}^{[k]}$ operates on orbital states and $\mathbf{B}_{\mathrm{L}}^{(k)}$ on lattice oscillator states.

General types of spin-lattice relaxation processes:

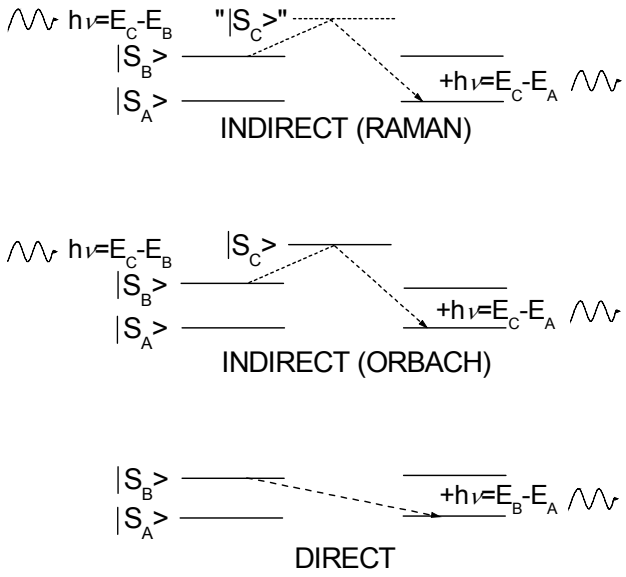

Figure 4.1.7 General types of spin-lattice relaxation processes

Direct or first-order process involves a transition in the spin system from an $|S_B\rangle$ to an $|S_A\rangle$ state, with the simultaneous creation of a lattice phonon of energy E_B–E_A. An indirect, or second-order process consists of three or more spin levels and two or more phonons, corresponding to inelastic phonon scattering, thus, a transition from an $|S_B\rangle$ to an $|S_C\rangle$ state occurs with the annihilation of a phonon of energy E_B–E_C, while the transition from an $|S_C\rangle$ to an $|S_A\rangle$ state creates a phonon of energy E_C–E_A. When the level $|S_C\rangle$ is a well-defined eigenstate of $\mathcal{H}_1$ the relaxation is called an Orbach process,

while when $|S_C\rangle$ is a virtual state, *i.e.*, the entire phonon spectrum is available for the scattering process, the relaxation is called Raman process.

A direct process involves a first-order calculation with the probability per unit time of a transition from $|A, l\rangle$ to $|A', l'\rangle$ given by

$$P_{AA'} = (\frac{2\pi}{h})|\langle A', l'|\mathcal{H}_{\mathrm{OL}}|A, l\rangle|^2\rho(E), \tag{4.1.20}$$

where l denotes a lattice state and $\rho(E)$ is the density of final states. Indirect processes involve $\mathcal{H}_{\mathrm{OL}}$ acting more than once therefore second-order formulas apply. Temperature and magnetic field dependences are usually not the same for direct and for indirect processes; at low temperatures, direct process dominates, while raising the temperature, indirect processes have faster rate.

Two different spin-lattice relaxation processes are known; the first involves the modulation of the dipole-dipole interaction and is concentration dependent, while the second (Kronig–Van Vleck process) involves relaxation transitions of the electron spin which are induced by fluctuations in the electrostatic crystal field potential and are sensed by the spins by spin-orbit coupling. Generally, this latter one is considered as a better approximation.

An additional possibility for direct relaxation involves admixtures of higher states by the hyperfine interaction A**I•S**. This mechanism is not concentration dependent and the ratio of the hyperfine structure spin-lattice process is given as

$$(AI|g_{\mathrm{L}}\beta H)^2 \tag{4.1.21}$$

and at low fields will dominate the Kronig–Van Vleck process. The selection rules involved are $\Delta M_S = \pm 1$ and $\Delta m_I = \mp 1$.

At higher temperatures Raman relaxation becomes dominant. The relaxation for the case of iron is largely of a quadrupole nature, *i.e.*, spin-lattice relaxation between levels $|A\rangle$ and $|B\rangle$ of spin Hamiltonian will be possible only when the matrix element $\langle A|S_{\mp}^2|B\rangle$ is nonvanishing.

According to the Kronig–Van Vleck mechanism, the lattice vibrations couple with the spins through the spin-orbit interaction λ**L•S**, so when ⟨**L**⟩ is crystal field of large level, the relaxation is fast (in comparison with the Larmor precession); this is the case for high spin Fe^{2+}, for instance. These fast rates have also been observed in

covalent Fe^{III} compounds where $\langle \mathbf{L} \rangle$ is nonvanishing again, and bonding effects may enhance relaxation. On the other hand, Fe^{3+} shows characteristically long spin-lattice relaxation.

A different relaxation mechanism involves the modulation by the phonons of spin-spin couplings of the core electrons via the action of the crystal field modulation on the orbital moment of the electrons; this process may sometimes dominate the Kronig–Van Vleck mechanism in direct processes.

4.1.3.1.2 *Spin-Spin Relaxation*

When the spin-lattice relaxation times in a compound are "long", it is common for an equilibrium state to be reached within a two-level system (in a time $T_2 \ll T_1$) which is characterised by a "spin-temperature", different from that of the lattice.

In the case where hyperfine energies are smaller than spin-spin interactions described by $\mathcal{H}_{SS}$ a relaxation process involves mutual spin flips, induced by $S_{1+}S_{2-}$, on neighbouring ions. If a doublet is split by local or external fields $\mathcal{H}_{SS}$ may induce direct relaxation in a way similar to spin-lattice relaxation. The analogue of the phonon is a neighbouring flip. For direct process $\langle + | S_+ | - \rangle \neq 0$ for a doublet $|\pm\rangle$, while for indirect spin relaxation becomes important when $\langle + | S_+ | - \rangle = 0$. In both cases, spin relaxation is concentration dependent. $\mathcal{H}_{SS}$ is temperature independent, but the populations amongst the crystal field levels vary with temperature. In the case where indirect spin relaxation is dominant, typical exponential temperature dependence is expected, when T is of the order of the first excited level.

When a large external field is applied to a sample, the states are split into strong field levels labelled by $|M_S\rangle$. The interaction $\mathcal{H}_{SS}$ predominantly induces transitions $\Delta M_{1S}=\pm 1$ and $\Delta M_{2S}=\mp 1$. Since the six levels are equally spaced by $g\beta H$, there are number of ways a neighbour can flip to induce a $\Delta M_{1S}=+1$ transition: $|\left|M_{2S} = \frac{5}{2}\right\rangle \rightarrow \left|\frac{3}{2}\right\rangle$ or $\left|\frac{3}{2}\right\rangle \rightarrow \left|\frac{1}{2}\right\rangle$, etc. This situation is common in iron.

4.1.3.1.3 *Cross Relaxation*

In systems where more than one type of spin species is present, relaxation by so-called cross relaxation may occur. The simplest case is when two spin systems, one having a fast, the other a slower relaxation time and a contact can be established between the two distinct systems, by application of external magnetic field, for instance, so that their resonances overlap, mutual spin flips can be combined, which nearly conserves energy. The cross relaxation often occurs because of dipolar broadening of the levels (and is concentration dependent), which causes them to overlap.

4.1.3.2 Relaxation Models

4.1.3.2.1 *Mössbauer Relaxation Spectra*

Ignoring for the present all relaxation processes except for those of electronic origin (affecting only the magnetic interactions), one can assume that the operators describing the relaxation are diagonal with respect to the nuclear levels. The lifetime of an electronic level, τ, or correlation time is related to the matrix element for relaxation. When $\frac{\Gamma}{\omega_N} < 1$ and $\frac{\tau^{-2}}{\omega_N} << 1$, where ω_N is a frequency parameter, $\omega_N \sim A/\hbar$. In the effective hyperfine field approximation (HFA) ω_N is the nuclear Larmor precession frequency, so $\omega_L = |A|/2\hbar$.

Mössbauer Spectroscopy is a powerful tool to study systems displaying paramagnetic spin relaxation, because it is sensitive to slight changes in the ligand sphere of the iron ion. In addition to the "basic" hyperfine parameters, which are characteristic of each individual iron species, the paramagnetic spin relaxation also has significance in such a system. High spin ferric species show paramagnetic spin relaxation the frequency of which, among other parameters, is a function of the distance between the different iron ions: the farther these ions from each other in the solution, the weaker is the coupling between their spins and the slower is the fluctuation of the magnetic field as sensed by the Mössbauer nucleus (spin-spin relaxation). At one extreme, when the iron ions form dimers they are so close to each other that the fluctuation of the hyperfine magnetic field becomes fast, the magnetic interaction cannot develop and the Mössbauer spectrum displays a doublet (or a singlet). At the

other extreme, when the ions are farther away from each other (monomeric species in a dilute solution), the frequency of the fluctuation is low and the Mössbauer spectrum displays a magnetic sextet (quasi-static field). At intermediate frequencies, the spectral line shape shows complicated spectrum deformations (see Fig. 4.1.5).

In a quantitative way, magnetic splitting may be observed if the average time of the paramagnetic spin relaxation (τ_{SPR}) is longer than the average time of Larmor precession of the magnetic moment of the atomic nucleus (τ_L). If the concentration of iron(III) species in the solution as well as the temperature are low enough both the spin-spin and the spin-lattice interactions are weak and the average times of spin-spin (τ_{SSR}) and spin-lattice (τ_{SLR}) relaxations will be long. (These concentration and temperature threshold values are also dependent on the electronic structure of the ligand sphere.) Consequently, the effective spin relaxation time, $\tau_{PSR} = \left(\frac{1}{\tau_{SSR}} + \frac{1}{\tau_{SLR}}\right)^{-1}$ will be longer than τ_L. In this work, for fitting such relaxation spectra, the Blume-Tjon model has been used (when the axis of the fluctuation of the hyperfine magnetic field is perpendicular to the Electric Field Gradient (**EFG**)), as it was developed especially for compounds of iron formed with organic ligands. However, because of the strong correlation of hyperfine parameters (and also because of the large number of the eventually free parameters), one has to carefully handle the data obtained by the line assumption. The best way to analyse a relaxing system is by studying its temperature dependence. However, in certain cases, the temperature dependence cannot provide enough information for fitting the resultant spectra either (relaxation spectra can be obtained in a large range of temperature; even at very low temperature not enough resolution of the spectrum can be observed). In these cases, utilisation of an external magnetic field is indispensable. Further details about general theories and the effects of an applied external magnetic field on the Mössbauer spectra are discussed in Appendix 1.

4.1.3.2.2 *The Blume-Tjon Model*

The ^{57}Fe Blume-Tjon two state magnetic relaxation model describes the physical model for a powdered sample, in which ^{57}Fe nuclei are experiencing fluctuating hyperfine magnetic field. It is assumed that the nuclei experience a magnetic field that relaxes between two values: H_1=–h and H_2=+h. Thus, the magnetic field can either point ”upwards” (+h) or “downwards” (–h). The direction of the magnetic field is

assumed to be along one of the principal axes of the **EFG**, as an approximation. The relaxation between the states $-h$ and $+h$ is described çby the two transition rates W_1 and W_2, which can be thought of as transition probabilities from one state from the other. Thus, the transition probability is described as follows[2]:

$$W(k) = \left(\frac{2}{\Gamma}\right) \mathrm{Re} \frac{1}{4} \sum_{m_0 m_1} \left|\langle I_0 m_0 | \mathcal{H}^{(+)} | I_1 m_1 \rangle\right|^2 \times \sum_{ij} pi \left(j \left| \tilde{A}(p) \left[1 + 3Q^2 \eta^{2\tilde{B}}(p) \tilde{A}(p) \right]^{-1} \right| i \right) \quad [3]$$

(4.1.22)

4.2 Data Analysis

All Mössbauer spectral line assumptions were done using the MossWinn3.0 software package. Fitting simple lines, such as singlets, quadrupole doublets or magnetic sextets, Lorentzian lines assumptions were used. In the case of line distortions caused by relaxation effects, the transversal case (when the direction of the fluctuation of the hyperfine magnetic field is perpendicular to the Electric Field Gradient) Blume-Tjon model has been used, as implemented in the software package (Eq. 4.1.22).

4.3 Experimental Techniques

In this paragraph, the basic Mössbauer constant acceleration type spectrometer is discussed. Figure 4.3.1 shows a schematic diagram of a simple Mössbauer spectrometer. The source velocity is controlled by a transducer which is oscillated with constant acceleration. A waveform generator sends a reference waveform to the drive amplifier, via a Digital to Analogue Converter. This signal is sent to the vibrator where is converted to a mechanical oscillation of the drive shaft and source. A small coil within the vibrator provides a feedback signal to correct any deviations from the reference waveform.

[2] Note that the Equation 10.14 is similar to this (Eq. 4.1.22) but the transition probability is denoted by *P*.
[3] Development of this formula to $I(\omega)$ was done in F. Hartmann-Boutron *Ann. Phys*. **1975**, *9*, 285-356.

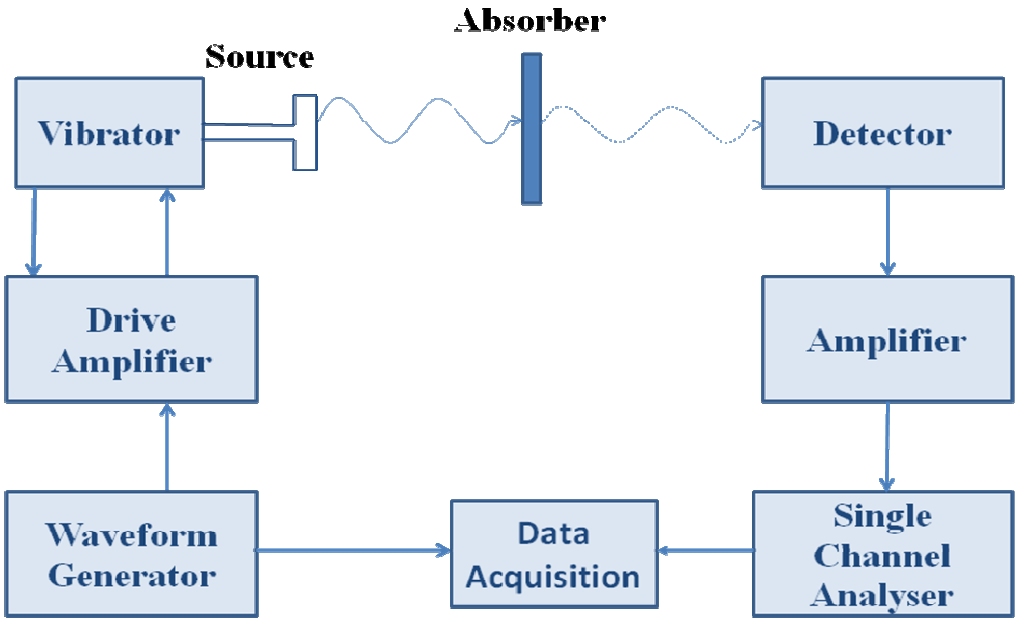

Figure 4.3.1 Schematic Diagram of a simple Mössbauer Spectrometer.

For ^{57}Fe-Mössbauer spectroscopy, the γ-rays are provided by a ^{57}Co source (for its decay scheme, see Figure 4.1.2), as mentioned above. Different types of detectors can be used. The set-ups that were used for recording spectra had been equipped with a scintillation-crystal detector (NaI/Tl).

The detector counts and source velocity are synchronised by a microprocessor system. The counts accumulate in 512 channels for one complete cycle, which contain two complete spectra: one for positive acceleration and for negative acceleration of the source. As the acceleration is constant the time interval is equal for all velocity intervals, hence each channel records for the same amount of time. During analysis the full spectrum is folded around a centre point to produce a single spectrum. This increases the number of counts (and hence gives better statistics) and flattens the background profile produced by the difference in intensity of the source radiation as the source moves relative to the absorber and the detector.

4.4 Study of Solution Samples Using Mössbauer Spectroscopy

The condition of the Mössbauer effect is the recoilless emission and absorption of the γ-rays. It requires a solid state, which means that Mössbauer spectroscopy can serve as a structural investigation technique for solid materials. Thus, the application of the Mössbauer spectroscopy for solution chemistry needs an adequate freezing (quenching) of the liquid solution. Several publications demonstrate that the coordination environment, the chemical bonding conditions, and the oxidation states in solutions are reflected in the Mössbauer spectra recorded after rapid freezing.

Solution samples for Mössbauer spectroscopy were all prepared in the way described below:

For the Mössbauer measurements, the solution samples obtained were quenched on an aluminium slab almost completely immersed in liquid nitrogen, with small holes drilled in its surface. The frozen beads obtained from liquid droplets were collected from these holes and transferred into the Mössbauer sample holder which was inserted then into a bath type cryostat in order to keep the sample solid.

This freezing technique provides a cooling rate which is safely over the critical cooling rate necessary to preserve the original structure of the solution and the iron species in the liquid state. There is only one way which provides a higher freezing rate, namely when the solution is adsorbed on filtering paper and the soaked filtering paper is placed in liquid nitrogen, this method provides a freezing rate over 60 K/s, but the amount of the solution adsorbed on the paper, *i.e.* that we can use for Mössbauer runs, is much less than in the previous case, and this latter one is much less suitable for studying reactions. Therefore, for every measurement described in the followings, the first method was used.

4.5 Bibliography

N. N. Greenwood and T. C. Gibb *Mössbauer Spectroscopy*, Chapman and Hall Ltd., *London*, **1971**.

H. H. Wickman and G. K. Wertheim *Spin Relaxation in Solids and Aftereffects of Nuclear Transformations*, in *Chemical Applications of Mössbauer Spectroscopy*, edited by V. I. Goldanskii, R. H. Herber, Academic Press, *New York and London*, **1968**.

A.Vértes and D. L. Nagy *Mössbauer Spectroscopy of Frozen Solutions*, Akadémiai Kiadó, *Budapest*, **1990**.

A.Vértes, L. Korecz, and K. Burger *Mössbauer Spectroscopy*, Elsevier Scientific Publishing Co., *Amsterdam-Oxford-New York*, **1979**.

Z. Klencsár, E. Kuzmann, A. Vértes *Hyperfine Interactions* **1998**, *112*, 269–274.

M. Blume, J. A. Tjon *Phys. Rev.* **1968**, *165*, 446-461.

A. Vértes, F. Parak *J. C. S. Dalton Trans.* **1972**, 2062-2068.

F. Hartmann-Boutron *Ann. Phys*. **1975**, *9*, 285-356.

K. Boukheddaden, F. Varret *Hyperfine Interactions* **1992**, *72*, 349-356.

J. C. Gressier, G. Levesque, H. Patin, F. Varret *Macromolecules* **1983**, *16*, 1577-1581.

5 Study of the Structure of the Fe^{III}EDTA, Fe^{III}CDTA and Fe^{III}EDDA Complexes in Aqueous Medium as a Function of pH

5.1 Introduction

Iron is one of the most important micronutrients of phytoplankton in natural waters [1]. The importance of iron speciation and its redox reactions involving Fe^{II} and Fe^{III} affect many processes [2-5]. Organic ligands like ethylenediaminetetraacetate (EDTA), which is a strong chelating agent for numerous metal ions may serve to solubilise and stabilise dissolved iron [3,6]. The Fe^{III}EDTA complex has also been used as a model compound for complicated biological systems, as oxygen transfer catalyst, and in wastewater treatment. [2-5,7-11]

Sodium ferric monoaqua-ethylenediaminetetraacetate dihydrate, $NaFeEDTA(H_2O)\cdot 2H_2O$, is one of the relatively rare examples of heptacoordinate ferric complexes. $[Fe^{III}(CDTA)(H_2O)]^-$ [12,13] is like $[Fe^{III}(EDTA)(H_2O)]^-$ [14] hepta-coordinate in the crystalline state, where the ligand is hexadentate and the seventh coordination site is occupied by a water molecule. In principle, this type of seven-coordinate iron complexes can adopt two different geometrical structures, *i.e.* pentagonal bipyramidal and monocapped trigonal-prismatic. It is often found that this type of complexes adopts an intermediate geometry, since the two structures are very close in energy. $Na[Fe(CDTA)(H_2O)]$ is a monocapped twisted trigonal prism (and the cyclohexyl ring in $[Fe^{III}(CDTA)(H_2O)]^-$ adopts a chair-like conformation), [12,13] and in contrast, $Na[Fe(EDTA)(H_2O)]$ adopts an approximate pentagonal bipyramidal structure.[14,15] Numerous scientific groups targeted to determine the structure of these complexes in solution phase, but their results are contradictory, since no direct structural information can be obtained in solutions: Neese *et al.* claimed that in solid state all four carboxylate arms, the two amine nitrogen atoms as well as one water molecule are coordinated to the Fe^{3+} centre, but after dissolution in aqueous medium one carboxylate arm gets detached and a six coordinate ligand structure is stabilised even at higher pH [16]. However, other studies suggested a heptacoordinated environment around the ferric ion, *i.e.* the complex keeps its structure in solution phase as well [17]. There exists another

explanation given by Stein *et al.* claiming that there is an equilibrium in solutions between hexa- and heptacoordinated ferric ethylenediaminetetraacetate species.[18] However, their explanation is erroneous because in the interpretation of the Mössbauer spectra they have not taken into account the effect of the paramagnetic spin relaxation phenomenon. Such studies have not been carried out for the ferric-EDDA complex; its structure is ignored even in solid state because of the lack of crystalline sample. However, it can be expected that the N-,N'-ethylenediaminediacetate chelating agent binds as a tetradentate ligand to the ferric centre, and possibly water molecule(s) complete its ligand environment.

These complexes may undergo protolytic reactions when varying the pH of the solution. To understand these possible reactions, potentiometric titrations were carried out as a function of pH for the Fe^{III}/EDTA system [19-29], but the results obtained are rather contradictory. For illustration, here are some hypotheses for the possible proton exchange reactions with their pK values:

pH(Fe^{III}EDTA+H)= 0.52 [26]/1.2 [20]/1.49 [25];
pK(Fe^{III}EDTA(OH)+H)= 3.88 [20]/7.49 [24]/7.58 [22];
pK(Fe^{III}EDTA+OH)=6.50 [20]/7.1 [21];
pK(Fe^{III}EDTA(OH)+H_2O)=4.0 [19];
pK(Fe^{III}EDTAOH+OH)=4.53 [23];
pK(Fe^{III}EDTA$(OH)_2$+H)=7.61 [28]/9.41 [24].

However, a more consistent theory has been established by Hutchenson and Cheng [30], which deals with two distinct species below pH=3, namely, with $Fe^{III}(H_2O)$EDTA and the $Fe^{III}(H_2O)$HEDTA. Only the $Fe^{III}(H_2O)$EDTA complex is present in the solution between pH=3-5. At pH=5, the Fe^{III}(OH)EDTA complex appears. The $Fe^{III}(H_2O)$EDTA complex disappears at pH=9.5. Furthermore, at pH=7.3 the $Fe(OH)_2$EDTA complex shows up in the solution.

For the CDTA complex, the studies have not shown such a complicated set of reactions. Following Seibig's studies two different complexes are present in the aqueous solution of the ferric-CDTA below pH=3, namely, the $Fe^{III}(H_2O)$HCDTA and the $Fe^{III}(H_2O)$CDTA, and this latter starts to get deprotonated at pH=4.2. Above pH=8.5 only the Fe^{III}(OH)CDTA appears in the solution.[12]

Such studies have not been carried out for the EDDA complex of iron(III).

Another interesting reaction of such complexes is their dimerisation. This is a pH independent reaction, which only depends on the concentration of the ferric species, however the appearance of the $[Fe^{III}LOH]^{2-}$ species is not independent on the pH, which means that once this latter species has been formed, the alteration of the pH does not vary the ratio of the dimeric species, but only above a pH value where the initial complex is formed. This reaction results in a very interesting and spectroscopically well characterised μ-oxo bridged complex as follows: [22,31,32]

$$2\ [Fe^{III}LOH]^{2-} \rightleftarrows [LFe^{III}–O–Fe^{III}L]^{4-} + H_2O \qquad \text{Eq. 5.1.1}$$

L=EDTA or CDTA.

This reaction is followed by the very characteristic change in the colour of the solution, which turns to red from the original light yellow. This red colour is due to the highly distorted electronic structure. It has been proposed, that the [Fe–O–Fe] moiety has a closely linear structure. [31,32] However, a remarkable difference occurs in the pK_a values of the two complexes: 7.5 for $[Fe^{III}(EDTA)H_2O]^-$ and 9.3 for $[Fe^{III}(CDTA)H_2O]^-$.

Fe^{III}EDTA can react with hydrogen peroxide which is a common transient compound in the aquatic environment at concentrations near 10^{-7} mol/dm^3 [33]. This reaction is important because it has a crucial contribution to the mechanism of how iron can catalyse the degradation of organic pollutants [34]. The complex ion $[Fe^{III}(EDTA)(\eta^2\text{-}O_2)]^{3-}$ of a very characteristic purple colour, which forms in the reaction of $[Fe^{III}(EDTA)]^-$ with hydrogen peroxide, is well known and properly characterised [35,36]. However, the solution phase reactions, which result in the formation of this complex, remained mostly unexplored. Several measurements on the Fe^{III}-EDTA-H_2O_2 system using the frozen solution Mössbauer technique were carried out and rather complicated sets of reactions with dependence on pH, concentration and possibly lighting conditions were found [37]. The iron(II) complexes produced by the photodegradation of Fe^{III}EDTA change the redox properties of the system after addition of H_2O_2 as well. Analysis of the Mössbauer spectra revealed new mono- and binuclear species with delicate acid-base properties therefore reproduction of the individual experiments is a crucial part of the investigation of this system. For a better understanding of the conditions of the photodegradation process there is a clear necessity to study first the Fe^{III}EDTA system without exposing it to light, to detect the

distinct species that may form and to identify them eventually. Carrying out the same studies for the CDTA and EDDA analogues is reasonable, since they can also contribute to the understanding of such reaction systems.

5.2 Results and Discussion

5.2.1 Study of the Structure of the Fe^{III}EDTA Complex in Aqueous Solutions as a Function of pH

5.2.1.1 Mössbauer measurements

5.2.1.1.1 *Mössbauer measurements without applied magnetic field*

A stock solution of c=0.1 mol/dm^3 $Fe(NO_3)_3$ solution has been prepared by dissolving ^{57}Fe enriched iron metal in pH=1 nitric acid, then Na_2H_2EDTA was added to the system in a Fe:EDTA=1:1.3 ratio. The stock solution was then divided into four parts and the pH of these solutions was adjusted to the following values by addition of KOH or nitric acid: pH=0.2, 0.6, 4.1, 6.3. The final iron concentration was c=0.05 mol/dm^3 for each sample. The samples were measured by different techniques. First their Mössbauer spectra were recorded at T=80 K (spectra displayed in Figure 5.2.1.1).

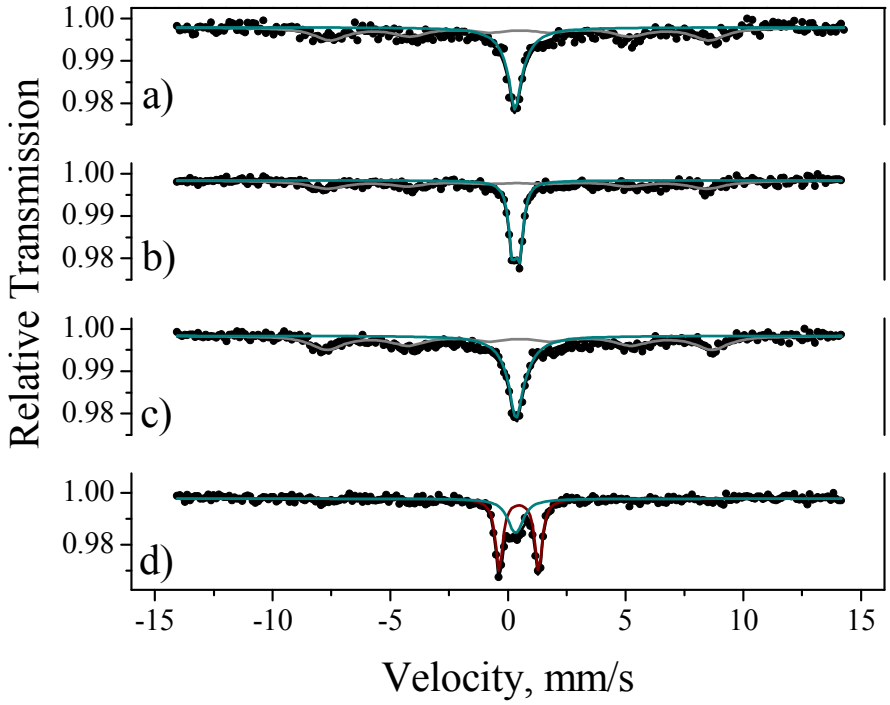

Figure 5.2.1.1 Mössbauer spectra of the $Fe^{III}EDTA$ complex at a) pH=0.2, b) pH=0.6, c) pH=4.1 and d) pH=6.3. Spectra recorded at 80 K.

The main difference between the spectra is the appearance of a doublet in spectrum d), which can be attributed to the well-known dimeric μ-O($Fe^{III}EDTA)_2$ complex [38]. Its presence is due to the pH higher than in the other samples. However, all the spectra display complicated relaxation lines (due to paramagnetic spin relaxation), the spectrum evaluation of which is complicated and not really reliable[4]. For this reason, the spectrum parameters obtained by spectrum evaluations are not displayed.

Previously, Mössbauer experiments were carried out at low temperature on $Fe^{III}EDTA$-containing (Fe:EDTA ratio was about 1:1.3) solutions (c~0.05 mol/dm^3) at different pH values (pH<1 and pH=6.3). See spectra in Figure 5.2.1.2.

[4] For explanation, see Chapter 4, paramagnetic spin relaxation.

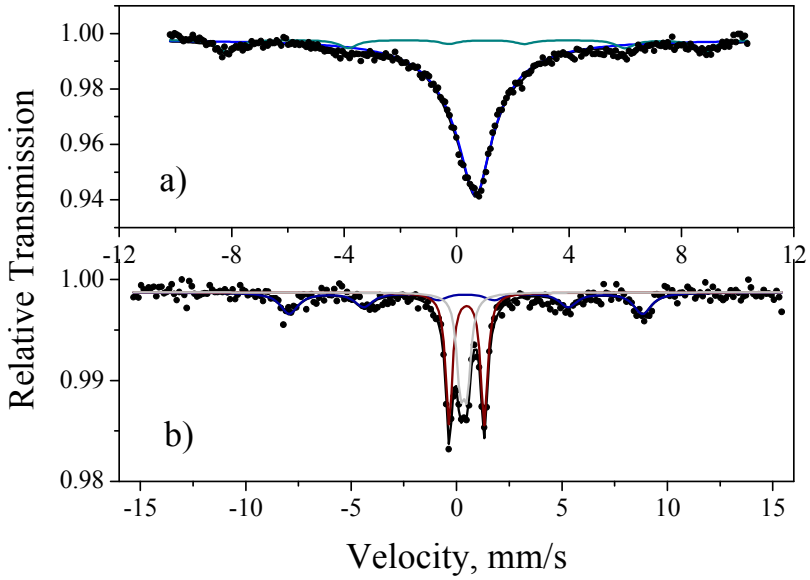

Figure 5.2.1.2 Mössbauer spectra of the Fe^{III}/EDTA system at low (a); <1) and high (b); 6.3) pH. Spectra recorded at 4.2 K.

The first spectrum could be evaluated as a superposition of two subspectra: a magnetic sextet and a subspectrum showing relaxation broadening, the second spectrum is composed of three subspectra: in addition to the two subspectra present in Figure 5.2.1.2a) already, a third component, a quadrupole doublet is displayed in spectrum 5.2.1.2b). Comparing the two spectra to those recorded at 80 K, it has to be noted here that although the paramagnetic spin relaxation slowed down (presence of a magnetic sextet in spectrum displayed in Figure 5.2.1.2b)), the spectra are still not well resolved and also display broadened lines due to paramagnetic spin relaxation. The quadrupole doublet in Figure 5.2.1.2b) refers to the dimeric μ-O(Fe^{III}EDTA)$_2$ complex (δ=0.476(5) mm/s and Δ=1.67(1) mm/s). Since the relaxation models used for spectrum evaluations are based on numerous approximations and the resultant spectrum parameters are in strong correlation, the data obtained are not reliable. Therefore spectrum parameters are not discussed in details.

As the spectra recorded at T=4.2 K still displayed relaxation lineshapes, the only way to stop the fluctuation of the hyperfine magnetic field caused by paramagnetic spin relaxation was applying an external magnetic field.

5.2.1.1.2 *Mössbauer measurements in applied magnetic field*

Experiments were carried out in an applied external magnetic field. The spectra obtained are displayed in Figure 5.2.1.3. (For the effect of an applied external magnetic field on the Mössbauer spectra see Appendix 1.)

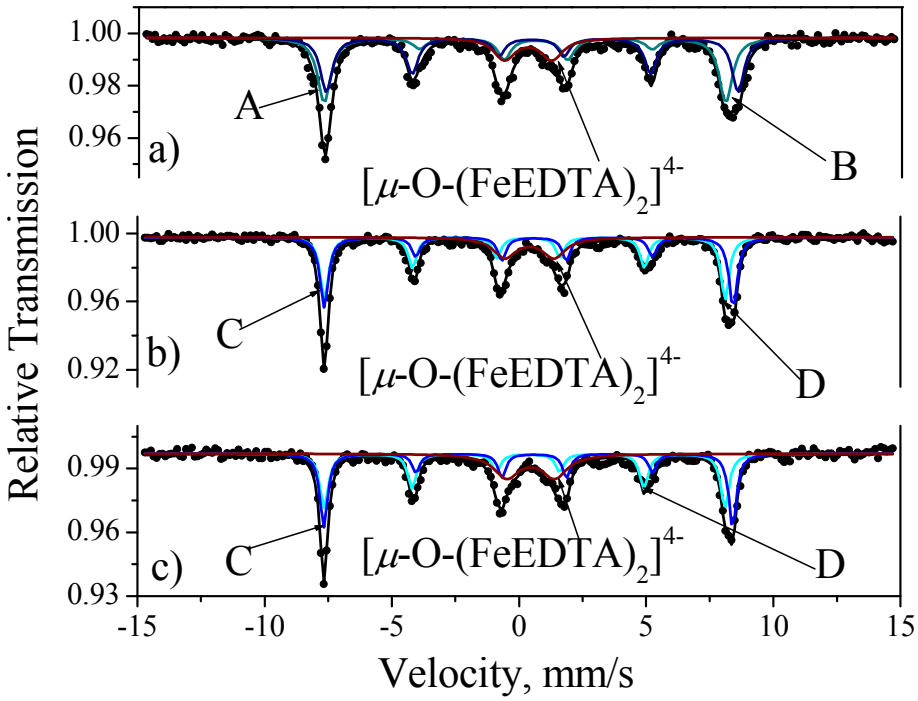

Figure 5.2.1.3 Mössbauer spectra of the solutions of $Fe^{III}EDTA$ at a) pH=0.2, b) pH=4.1 and c) pH=6.3. Spectra recorded at T=8 K and in a B=6 T applied external magnetic field.

As can be seen, all spectra are composed by three subspectra: two magnetic sextets with quadrupole interactions[5] and one quadrupole doublet is present in all spectra. The doublet corresponds obviously to the μ-O($Fe^{III}EDTA$)$_2$ complex. The fact that it appeared in all spectra and not only in spectrum 5.2.1.3c), as expected following the information obtained from the Mössbauer spectra recorded at 80 K, is certainly due to the other quenching technique used. In fact, the sample holder designed for the in-field measurements was different from the one used to the measurements without applied field, so the solution could not be frozen drop by drop. Therefore it was frozen in a bulk, and thus the speed of freezing decreased, and this allowed room for the dimerisation of the $Fe^{III}EDTA$ complex. The solution was being frozen possibly in the following way: It

[5] This results in the shift of all the lines in a way that the 1st and 6th lines move in one way while the others in the opposite way and the lines shifting in the same way do not change their positions relative to each other.

is known that the higher the concentration of a solution the lower its melting point is. Since the freezing process was relatively slow (it took a few seconds), the less concentrated parts of the solution could get frozen first and thus the other parts of it were enriched in the ferric ethylenediaminetetraacetate complex, which further decreased its melting point. It is also known that the yield of the dimerisation does not depend on the actual pH but it only depends on the concentration of the monomeric and dimeric species (see Eq.5.1.1). Probably this concentration range of c=0.05 mol/dm^3 is very delicate and high enough to produce dimeric species when it is raised a little.[6]

Although applied magnetic field was parallel to the γ-ray propagation direction, each sextet is built up of six lines. From the appearance of the 2nd and 5th lines of the magnetic sextets, it is obvious that the systems display ferrimagnetic behaviour (for explanation, see Appendix 1). For spectrum evaluations two ways are reasonable (some restrictions are needed to be imposed to reduce the number of free variables): i, when the relative amount of the two magnetic sextets is identical, and ii, when the linewidths of the two magnetic subspectra are equal (this latter is only valid for very low temperatures, but in a first approximation this can be used as well). Spectrum parameters are listed in Table 5.2.1.1.

As, during the measurement, the source and the absorber were at the same temperature a temperature correction has to be applied (+0.17 mm/s) to compare the in-field isomer shifts to the ones without an external magnetic field. During the latter experiments the source was at room temperature, while in the case of in-field experiments the absorber was placed into the cryostat.

[6] Since several trials were made to change the freezing rate and hyperfine parameters of the two sextets did not change, we can be assured that the slow freezing had no other effect on the system than the dimerisation.

Table 5.2.1.1. Hyperfine parameters for tentative spectrum evaluations for spectra of the solutions of $Fe^{III}EDTA$ at a) pH=0.2, b) pH=4.1 and c) pH=6.3. Spectra recorded at T=8 K and in a B=6 T applied external magnetic field. Θ refers to the angle between the effective magnetic fields and the γ-ray propagation direction for each magnetic moment.

pH/Species		Rel %		δ (mm/s)		B (T)		eQV_{zz} (mm/s)		Θ (deg)		Γ (mm/s)		Dimer %	
Parameters		1	2	1	2	1	2	1	2	1	2	1	2	1	2
pH=0.2	A	42.4	36.4	0.39	0.39	49.0	48.9	-0.86	-0.90	27.9	23.9	0.63	0.59	15.2	
	B		48.3	0.45	0.44	50.2	50.2	0.06	0.01	54.3	54.1	0.56			
pH=4.1	C	40.2	40.3	0.30	0.30	48.9	48.9	-0.29	-0.29	47.2	47.1	0.39	0.39	19.5	
	D		40.2	0.49	0.49	49.8	49.8	-0.42	-0.42	36.0	35.9	0.39			
pH=6.3	C	37.7	35.1	0.29	0.28	48.9	48.9	-0.27	-0.28	53.7	53.9	0.40	0.38	24.7	
	D		40.2	0.48	0.48	49.8	49.8	-0.47	-0.47	34.7	35.6	0.36			

1 and 2 correspond to the two different ways of spectrum evaluation, 1) when the relative ratios of the two magnetic subspectra are identical and 2) when the linewidths belonging to the magnetic sextets are equal.

Comparing the two spectrum evaluation models, only one difference within the parameters is remarkable. This difference consists of the decrease of the relative amount of the species represented by magnetic sextets in the Mössbauer spectra. In case of model 1) there is a monotonous change in these values, while in the case of model 2) there is a tendency, but there are discrepancies. Nevertheless, as there is no difference in the hyperfine parameters using model 1) or 2), a spectrum evaluation without such restrictions is possible, which results in the following hyperfine parameters, listed in Table 5.2.1.2.

Table 5.2.1.2. Hyperfine parameters and their errors resulting from the evaluation for spectra of the solutions of $Fe^{III}EDTA$ at a) pH=0.2, b) pH=4.1 and c) pH=6.3. Spectrum evaluations were made without any mathematical restriction. Spectra were recorded at T=8 K and in a B=6 T applied external magnetic field. Θ refers to the angle between the effective magnetic fields and direction of the propagation of γ-rays for each magnetic moment.

Species/ Parameters		Rel.%	δ (mm/s)	Δ/eQV_{zz} (mm/s)	B (T)	Θ (deg)	Γ (mm/s)
pH=0.2	A	37.0	0.39(2)	−0.90(1)	48.9(1)	24(7)	0.60(5)
	B	47.7	0.44(1)	0.02(1)	50.2(1)	54(3)	0.59(5)
	Dimer	15.3	0.31(4)	1.89(8)	–		1.01(1)
pH=4.1	C	44.6	0.31(1)	−0.29(3)	48.9(1)	46(2)	0.42(2)
	D	35.9	0.49(1)	−0.42(3)	49.9(1)	35(2)	0.37(2)
	Dimer	19.5	0.42(3)	1.92(5)	–		1.09(8)
pH=6.3	C	40.0	0.30(1)	−0.27(3)	48.9(1)	53(2)	0.4(2)
	D	35.4	0.49(1)	−0.48(3)	49.9(1)	34(2)	0.35(2)
	Dimer	24.6	0.46(3)	1.88(5)	–		1.20(8)

Using Mössbauer spectroscopy only, we cannot decide which one of these three possible spectrum evaluations (Tables 5.2.1.1, 5.2.1.2) is the most realistic. However, some general remarks can be made. The first remark consists of the relative amount of the dimeric species, which increases with increasing pH. The two possible ways of dimer formation are the following:

$$2\ [Fe^{III}EDTAOH]^{2-} \rightleftarrows [EDTAFe^{III}–O–Fe^{III}EDTA]^{4-} + H_2O \qquad \text{Eq. 5.2.1}$$

$$2\ [Fe^{III}EDTAH_2O]^{-} + H_2O \rightleftarrows [EDTAFe^{III}–O–Fe^{III}EDTA]^{4-} + 2H_3O^{+} \qquad \text{Eq. 5.2.2}$$

The reaction described with Eq. 5.2.1 is not pH dependent, but the formation of the original ferric complex Eq. 5.2.2 ($[Fe^{III}EDTAH_2O]^{-} + OH^{-} \rightleftarrows [Fe^{III}EDTAOH]^{2-}$ Eq. 5.2.3), clearly depends on the pH of the solution, so this finding is not really surprising. In literature, one can find several publications claiming the antiferromagnetic behaviour of the μ-oxo dimeric $Fe^{III}EDTA$ complex, which was first reported by Schugar *et al.* [39]. However, in the in-field Mössbauer spectra of the dimer-containing system, there is only one subspectrum, the quadrupole doublet, which refers to this dimeric species and no antiferromagnetic behaviour has been observed. If there had been any antiferromagnetic interaction, it should have been detected by Mössbauer spectroscopy

since the Néel temperature of this complex is above 8 K according to Schugar *et al*. [39] This lack of antiferromagnetic interaction is probably due to the fact that Schugar *et al.* studied it in solid state, and the complex logically does not preserve long range magnetic order in solution phase. This re-affirms that although the cooling rate was rather slow in our experiment, the dimerised fraction is not a precipitate.

In the case of solution samples, the above mentioned ferrimagnetic behaviour is even more obvious than the same property observed for the solid $NaFeEDTA \cdot 3H_2O$[7]. The angles of the magnetic moments have a dependence on pH. For one of them, a remarkable increase with increasing pH can be observed (23.9°/27.9° at pH=0.2 → 53.9°/53° for pH=6.3), while the angle between the other effective and the applied magnetic field displays a smaller decrease with increasing pH (54.3°/54° at pH=0.2 → 34°/35.6° for pH=6.3, depending on the spectrum evaluation model). The occurrence of this phenomenon raising the pH from 0.2 to 4.1 could be explained by the assumption that the ferrimagnetic system is composed of different species at pH=0.2 and at pH=4.1 (see below), but it also occurs when species are the same at pH=4.1 and at pH=6.3.

Having a careful look on the hyperfine parameters on the distinct magnetic sextets, one has to realise that species A and B are not the same as species C and D. This change is probably due to a proton exchange reaction that takes place between these pH values. This latter finding was confirmed by our potentiometric titration data (see in Appendix 2), since a proton exchange reaction could be observed below pH=3. The hyperfine parameters of subspectra resulting from the solutions of pH=4.1 and pH=6.3 are identical except for the higher amount of the dimeric ferric EDTA in the latter case. The presence of two different subspectra at all pH values can be explained by the existence of two different species at each pH value, the coordination numbers of which are different. This hypothesis has been already proposed by Stein *et al*. [18] but it is also supported by these results, mostly by the differences in the isomer shift values: δ_A=0.39 mm/s and δ_B=0.44-0.45 mm/s and δ_C=0.28-0.31 mm/s, while δ_D=0.48-0.49 mm/s (depending on the model of spectrum evaluation). Such a big difference between the distinct isomer shift values (~0.05 mm/s for the pH=0.2 system and nearly 0.2 mm/s for the pH=4.1-6.3 systems) can be explained by the change of the coordination number, where the lower coordination number refers to the lower isomer shift value. In this case

[7] For further details see Chapter 8.

species A and C must be six-coordinated, while species B and D must be seven-coordinated. Therefore, species A has to be a protonated form of species C, while species B has to be a protonated form of species D. Taking into account the former hypotheses for the structure of the $Fe^{III}EDTA$ species in the solution, species A has to refer to a complex, which is the [$Fe^{III}HEDTA$] neutral complex, with a six-fold coordinated ligand sphere around the ferric centre and all the ligands are provided by the EDTA; species B is a neutral complex as well, but it is seven-fold coordinated and the seventh ligand is a water molecule [$Fe^{III}HEDTA(H_2O)$]. Species C refers then to the [$Fe^{III}EDTA$]$^-$ sixfold coordinated complex and species D to the seven-fold coordinated [$Fe^{III}EDTA(H_2O)$]$^-$. In addition to Eq. 5.2.2, probably the following reaction can produce the dimeric ethylenediaminetetraacetate species as well:

$$2\,[Fe^{III}HEDTA(H_2O)] + 3H_2O \rightleftarrows [EDTAFe^{III}–O–Fe^{III}EDTA]^{4-} + 4H_3O^+ \quad \text{Eq. 5.2.4}$$

Subsequently, the dimeric species can be formed at lower pH values as well, if the concentration is high enough.

The relative amounts of species A to B and species C to D display the biggest uncertainty when comparing the results of different fitting models. The relative amount of the dimeric species does not vary as a function of the spectrum evaluation model (15.2%-15.3% at pH=0.2, 19.5% at pH=4.1 and 24.6%-24.7% at pH=6.3). This is not true for the other species, depending on the model chosen for spectrum evaluation, the relative amount of species A can vary from 36.4% to 42.4%, the amount of species B from 42.4% to 48.3%. In the pH=4.1 solution the different fitted relative amounts range from 40.2% to 44.6% for species C and for species D from 35.9% to 40.2%; in solution pH=6.3, these ranges are 35.1%-40.0% for species C and 35.4%-40.2% for species D, respectively. These differences are acceptable; they still remain in a ± 3% error interval, which is normal for the errors of the Mössbauer line areas, but make the origin of the change of the angle in the magnetic moments unpredictable, because one cannot decide whether it is due to the change of the relative amount of the two components or to other effects. To understand this latter problem, other techniques have been used in the investigation of the Fe^{III}/EDTA system.

5.2.1.2 ESR measurements

In order to further investigate the Fe^{III}/EDTA aqueous solutions as a function of pH, ESR experiments have been carried out at 110 K and at 4 K (see spectra in Figure 5.3.1)

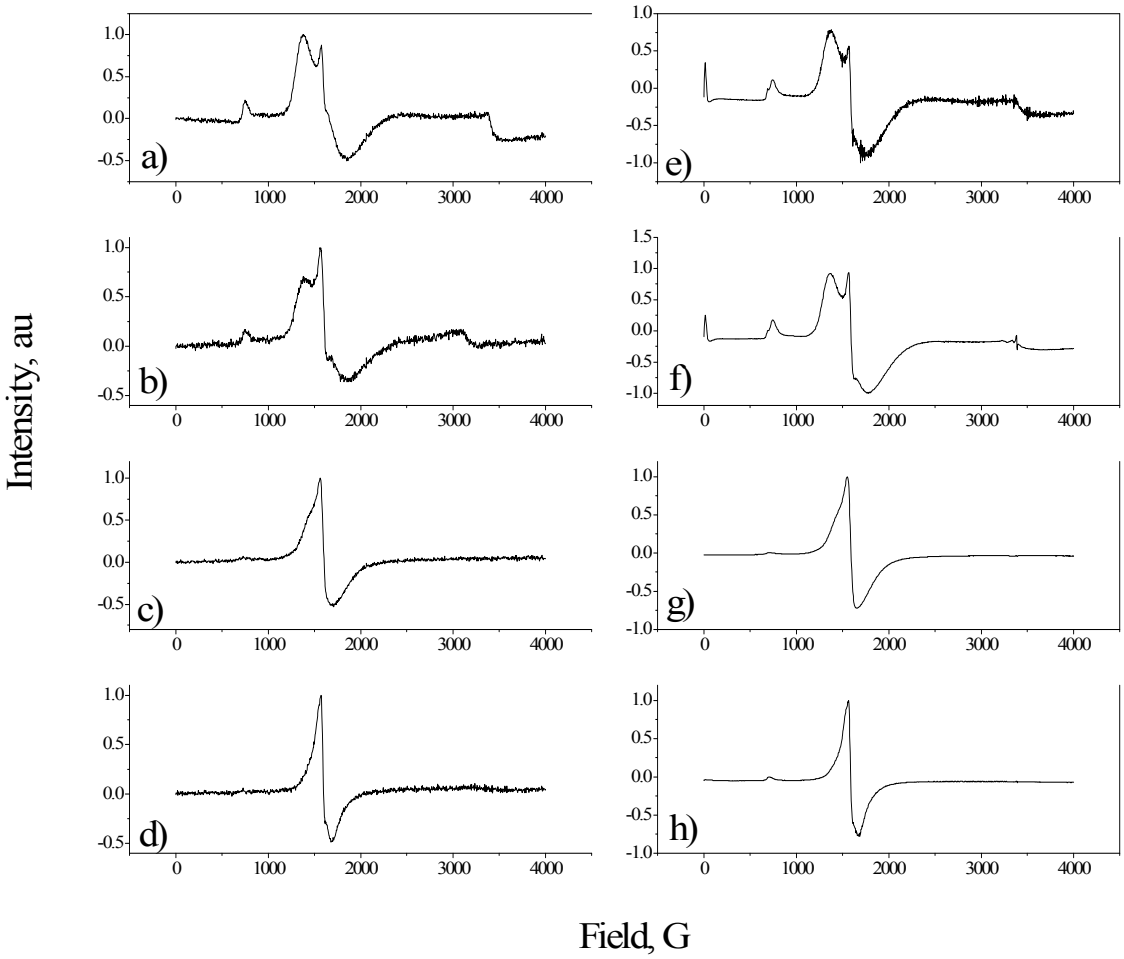

Figure 5.2.1.4 ESR spectra of the aqueous solution of Fe^{III}EDTA at pH=0.2 (spectra a) and e)), at pH=0.6 (spectra b) and f)), at pH=4.1 (spectra c) and g)) and at pH=6.3 (spectra d) and h)). Spectra a), b), c) and d) were recorded at T=110 K, while spectra e), f), g), and h) were recorded at T=4 K).

The peak at about 1550 G corresponds to the μ-oxo dimer Fe^{III}EDTA.[39] The fact that dimeric Fe^{III}EDTA can be present in very acidic solutions as well has been discussed earlier, unfortunately, there were no means to achieve a higher speed of freezing when preparing the samples for the ESR measurements and therefore the same phenomenon occurred as in the case of preparing samples for the in-field Mössbauer

runs. At 1360-1370 G, a peak can be observed, which obviously belongs to one of the monomeric species, but unfortunately, the intensity of the peak corresponding to the dimeric species is so high that one cannot further examine the location of this peak as a function of pH, since it appears as a shoulder for the peak of the dimer, and raising the pH, as the intensity of the line of the Fe^{III}EDTA dimer grows, no good resolution can be obtained for the 1360-1370 peak. Despite these problems, a quite well resolved peak at about 700-750 G is present in the spectra, which can serve for further investigation. A slight change in its location can be observed as a function of pH (for parameters see Table 5.2.1.3).

Table 5.2.1.3 Peak maxima (G) at different pH values and at different temperatures.

pH/Temperature	110 K	4 K
0.2	750.7	742.9
0.6	746.8	746.8
4.1	727.3	711.6
6.3	727.3	707.7

As can be seen, at both temperature values, the location of the peak maximum is the same for solutions pH=0.2 and 0.6 and for solutions pH=4.1 and 6.3, but that of the low pH solutions differs considerably from that of the higher pH solutions. This observation reinforces the hypothesis based on Mössbauer results *i.e.* that there is two different systems at low (0.2/0.6) and at high (4.1/6.3) pH, *i.e.* a proton exchange reaction occurs within the pH range of 0.6-4.1.

Unfortunately further conclusions cannot be drawn from the analysis of ESR spectra because of the very high intensity of the peak referring to the dimeric ferric ethylenediaminetetraacetate, which increases with increasing pH.

5.2.1.3 Magnetic susceptibility measurements

In order to determine the relative amount of the monomeric species and to further study their magnetic properties, magnetic susceptibility measurements have been carried out as a function of applied magnetic field and as a function of temperature (see in Figure 5.2.1.5).

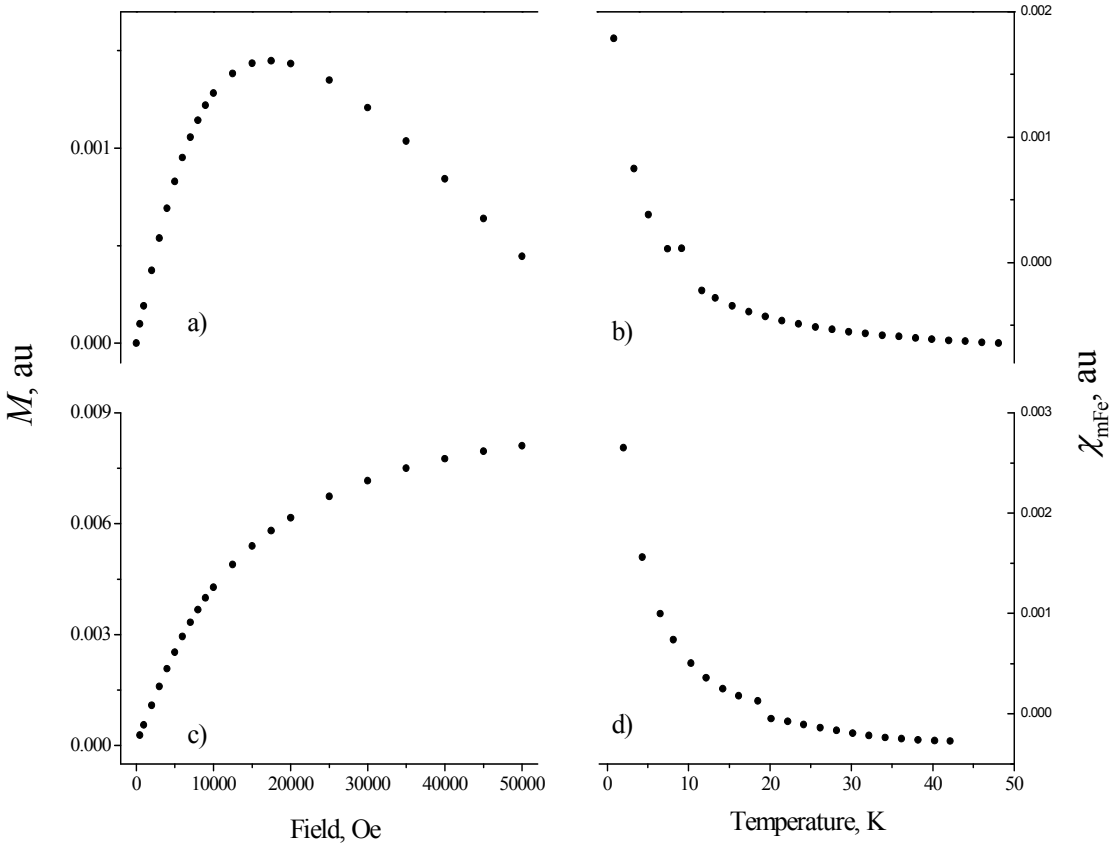

Figure 5.2.1.5 Magnetic susceptibility measurements as a function of applied magnetic field (spectra a) and c)) at T=2 K and as a function of temperature (spectra b) and d)) at H=1000 Oe of aqueous Fe^{III}EDTA solutions samples at pH=0.2 (spectra a) and b)) and at pH=4.1 (spectra c) and d)).

The ferrimagnetic behaviour of the solutions was confirmed using magnetic susceptibility measurements. It is rather surprising that such a greater ferrimagnetic ordering can occur in frozen solution phase than in a crystalline state[8].

However, the reason of the change of the angle of the magnetic moments, whether it is due to the change of the relative amounts of its constituents, could not be discovered

[8] See Chapter 8.

using magnetic susceptibility measurements either, since this macroscopic method is not sensitive enough for such little changes. Since only qualitative conclusions could be drawn from the magnetic susceptibility measurements, because of the variety of dissolved species in the solutions, the Néel temperature of the systems could not be determined precisely, however, it must be around 10-20 K, following the magnetic susceptibility curves.

5.2.2 Study of the Structure of the $Fe^{III}CDTA$[9] Complex in Aqueous Solutions as a Function of pH

In order to study the speciation of iron as a function of pH in the Fe-CDTA system, 0.27 g (7.3 mmol) CDTA monohydrate was suspended in 5 cm^3 distilled water and a concentrated sodium hydroxide solution was added drop-wise until a clear solution was obtained. 0.0139 g (0.2 mmol) ^{57}Fe (95.95 % enriched) dissolved in 5cm^3 HNO_3 (*ca.* 12%) was added drop-wise to the CDTA solution. A yellow solution was obtained and the pH was adjusted with a concentrated NaOH solution to 5. The total concentration of iron(III) was about 0.021 mol/dm^3. The stock solution was divided into two parts and subsequently the pH of samples was adjusted to the values of pH=8.1 and pH=10.4 (in order to study the proton exchange reaction taking place at about pH=9.5, see in the introduction).

The frozen solution Mössbauer spectra (recorded at 83±2 K) of the Fe^{III}/CDTA system at pH=8.1 and pH=10.4 can be seen in Fig. 5.2.2.1. At pH=8.1, the dominance of the $[Fe^{III}(CDTA)H_2O]^-$ is expected, while at pH=10.4 deprotonation can take place resulting in $[Fe^{III}(CDTA)OH]^{2-}$. At pH=8.1, the spectrum is a combination of a sextet and a distorted subspectrum because of paramagnetic spin relaxation. This latter was evaluated by the Blume-Tjon model as an approximation; the parameters are not discussed in detail of strong correlation of the parameters, which can be eventually misleading. The sextet is well resolved and its high isomer shift (0.56 mm/s) indicates 7-fold coordination. The connection between the isomer shift and the coordination number in similar systems has been studied by Takeda [40]. The parameters of all species

[9] This work has been carried out in collaboration with Ariane Brausam (from Rudi van Eldik's research group). My contribution was to evaluate and to interpret the spectra recorded.

identified in these experiments are listed in Table 5.2.2.1. It is straightforward to assign this sextet to the $[Fe^{III}(CDTA)H_2O]^-$ species.

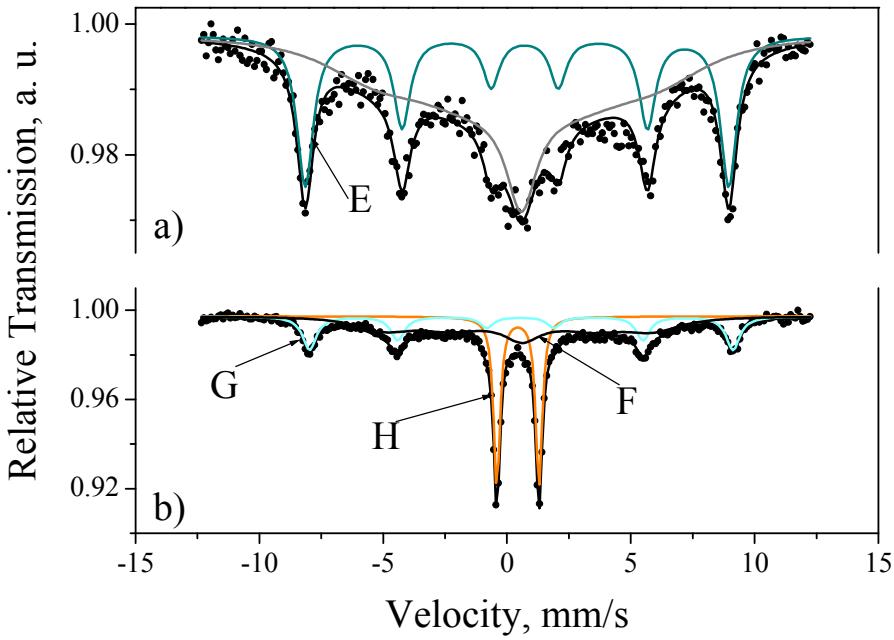

Figure 5.2.2.1. Frozen solution Mössbauer spectra recorded at 83±2 K of the Fe^{III}-CDTA system at pH=8.1 (a) and pH= 10.4 (b).

At pH=10.4, the spectrum is very different; in addition to a relaxation component, a sextet and a doublet appeared. The isomer shift and the hyperfine magnetic field of the sextet are the same as those observed for $[Fe^{III}(CDTA)H_2O]^-$, but the quadrupole shift (eQV_{zz}) is markedly different (see Table 5.2.1). This difference is consistent with the assumption that this species is the deprotonated form of $[Fe^{III}(CDTA)H_2O]^-$, namely $[Fe^{III}(CDTA)OH]^{2-}$. The fact that only the quadrupole interaction differs upon deprotonation shows that the protonation/deprotonation does not alter the 3*d* electron density on the Fe^{3+} centre appreciably, but the electric charge of the OH^- ion causes slight distortion of the ligand sphere.

The sharp doublet with parameters δ=0.44 mm/s and Δ=1.69 mm/s almost perfectly matches the parameters of the $[\{Fe(EDTA)\}_2(\mu\text{-}O)]^{4-}$ dimeric species; only the quadrupole splitting is higher by about 0.09 mm/s and is therefore assigned to the dimeric Fe^{III}CDTA. The isomer shift obviously indicates six-fold coordination, thus one carboxylate arm of the CDTA chelating agent must be detached from the iron centre on each side of the dimer analogously to the EDTA complex.

It is noteworthy that only a fraction of iron species was found in dimeric form while in the analogous Fe^{III}EDTA system only the dimer was found at pH~7 already (in the same concentration range).

Also note that in the EDTA system, there is no chance to observe monomeric species in frozen solution with well resolved magnetic structure, *i.e.* a sextet, which means that in the Fe^{III}CDTA containing samples the paramagnetic spin-spin relaxation slowed down in comparison with the Fe^{III}EDTA system, which is probably due to the more rigid structure of the complex. Monomeric species with EDTA in acidic solutions where they exist (in the 0.02-0.05 mol/dm^3 range [37]) are always displayed as badly relaxed spectra.

It is very important to emphasise that it is the concentration of iron species which basically defines the chances for spin-spin relaxation. These experiments were carried out in the ~0.02 mol/dm^3 concentration range for iron, while Stein and Marinsky [18] carried out similar experiments in the Fe^{III}CDTA system but in 0.5 mol/dm^3 solutions. At pH=8.0, these authors reported two doublets. One with Δ=1.70 mm/s is identical with our doublet representing the dimer $[\{Fe(CDTA)\}_2(\mu\text{-}O)]^{4-}$, while the other doublet with Δ=0.65 mm/s was assigned to the monomer $[Fe^{III}(CDTA)H_2O]^-$. If this assignment is correct, this species must have appeared in the "fast relaxation limit" due to the 25 times higher concentration.

The relaxation subspectra can also represent another species. A similar case to the Fe^{III}/EDTA system, where two monomeric components are present in this pH range cannot be excluded.

Table 5.2.2.1. Mössbauer parameters of the Fe^{III} species observed in the Fe^{III}-CDTA system at T=83(2) K.

Species / Parameters	δ (mm/s)	Δ (mm/s)	eQV_{zz} (mm/s)	B (T)
$[Fe^{III}(CDTA)H_2O]^-$	0.56-0.59	–	–(0.19-	52.9-53.1
$[Fe^{III}(CDTA)OH]^{2-}$	0.54-0.56	–	+(0.04-0.08)	52.4-53.3
$[\{Fe^{III}(CDTA)\}_2(\mu\text{-}O)]^{4-}$	0.44-0.45	1.68-1.70	–	0

5.2.3 Study of the Structure of the Fe^{III}EDDA Complex in Aqueous Solutions as a Function of pH

The dimerisation of the Fe^{III}EDDA complex has also been studied using Mössbauer spectroscopy. A c=0.05 mol/dm^3 Fe^{III}EDDA solution was prepared by the addition of 30% excess of H_2EDDA, the pH of the solution was adjusted to 1.6 and the Mössbauer spectrum recorded. Then the pH of the solution was further raised to 10.1, but in the meantime precipitation occurred at rather low pH (even below pH=1), so the concentration of the solution decreased considerably. The colour of the solution faded and did not turn to red, but remained yellow. A Mössbauer spectrum of this latter sample was recorded as well, the spectra obtained are displayed in Figure 5.2.3.1, and the spectrum parameters are listed in Table 5.2.3.1.

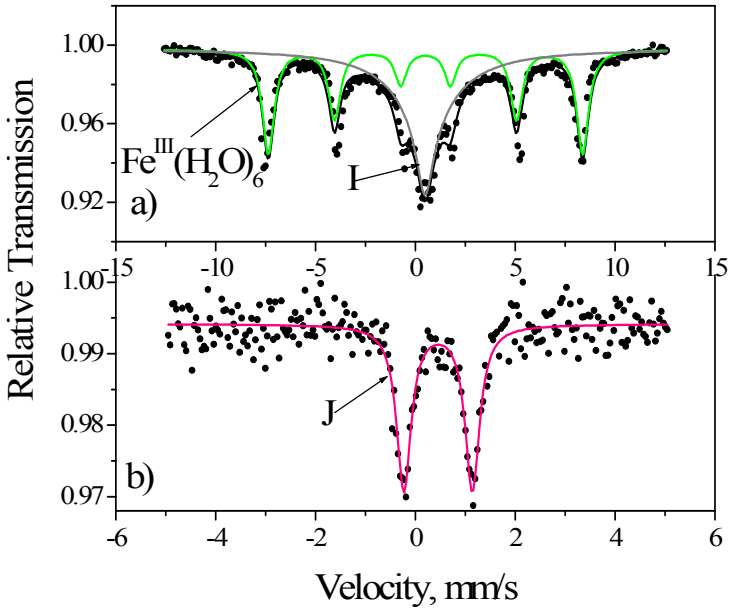

Figure 5.2.3.1 Mössbauer spectra of frozen solutions at 80 K, a) Fe^{III}EDDA at pH=1.6 and b) Fe^{III}EDDA at pH=10.1.

Spectrum a) displays two subspectra, a well resolved magnetic sextet and a broadened relaxation line which refer to monomeric species, similarly to the two previous cases, but this sextet is identified as the ferric hexaaqua complex on the basis of its hyperfine parameters [41]. Spectrum b), at higher pH displays a quadrupole doublet that corresponds to a dimeric species, as in the case of EDTA. The highly broadened relaxation line will not be discussed because of strong correlation of the parameters,

which can be misleading eventually. However, it is evident that subspectrum I refers to a high spin ferric species.

Table 5.2.3.1 Mössbauer parameters and their errors of the Fe^{III} species observed in the Fe^{III}-EDDA system at T=83(2) K.

Species / Parameters	δ (mm/s)	Δ (mm/s)	B (T)	Γ (mm/s)
J	0.45(1)	1.37(1)	–	0.35(2)

Unlike EDTA and CDTA, the EDDA ligand is only tetradentate, which is the main reason of the differences in its Mössbauer spectra; while the hyperfine parameters for the ferric EDTA and CDTA complexes were very close, the parameters for the EDDA complexes display a great difference. Species I is obviously a monomeric complex, Fe^{III}EDDA, its isomer shift (about 0.54 mm/s) corresponds to a sixfold coordination environment, which probably means that the chelating agent is coordinated as tetradentate and two water molecules complete the coordination sphere of the ferric ion. Species J must be a dimeric high spin ferric complex. However, its quadrupole splitting is considerably lower than that of the EDTA and CDTA complexes, which means that it is not the well known μ-oxo dimer with the Fe–O–Fe angle being close to 180°. This hypothesis is reinforced by the lack of red colouration of the dimer containing solution. The low isomer shift and the relatively high quadrupole splitting are probably due to a 6-fold coordination environment around the ferric ion, *i.e.* the ligand sphere of the ferric ion is probably built up of the following ligands: the EDDA ligand is coordinated as a tetradentate ligand, a water molecule and a bridging oxygen binds the two ferric entities together.

5.3 Conclusions

Aqueous solutions of the ferric EDTA, CDTA and EDDA systems have been investigated as a function of the pH of the solutions. Structures of species present in the systems have been suggested.

For the EDTA containing system, a protolytic reaction has been found between pH=0.6 and 4.1. This system also displays ferrimagnetic behaviour, with a Néel temperature within around 10-20 K. The angles of the magnetic moments in this latter

system displayed a pH dependence, but the origin of this phenomenon could not be determined using Mössbauer spectroscopy. The two species building up the ferrimagnetic system differ probably in their coordination number at all pH values, *i.e.* when the coordination number is six, there must be no water molecule attached to the ferric ligand sphere, while in the case of coordination number of seven, there is a water molecule coordinating in addition to the hexadentate EDTA. The well-known dimeric ferric ethylenediaminetetraacetate has also been detected at higher pH and concentration values.

Dimerisation and one protolytic exchange reaction within the pH range of 8.1-10.5 have also been observed in the CDTA containing system. The monomeric species has been found to be more stable relative to the μ-oxo dimeric species in this case than in the case of EDTA, that is why at pH=10.5 there still has been a large amount of monomeric species, which is not the case for the EDTA system, since the spectra of this latter one at such pH and concentration values only display a quadrupole doublet.

Dimerisation of the ferric EDDA complex has also been studied and the formation of another type of dimer species was found, due to the different number of possible coordinating atoms in the EDDA chelating agent. The resultant complex was found to be a μ-oxo dimer as well, but because of the difference in the structure of the chelating agent, there would be more room for the bridging oxygen atom, therefore the Fe–O–Fe angle should be less than in the EDTA or in the CDTA cases. This should be responsible for the lack of the typical red colouration of such dimeric species. Due to the fact that the EDDA chelate is only a tetradentate chelating agent, its ferric complex is less stable than the analogous EDTA or CDTA complexes, thus ferric hexaaqua complex remained in the pH=1.6 solution and considerable precipitation has already been observed at low pH values.

5.4 References

[1] M. L. Wells, N. M. Price, K.W. Bruland *Mar. Chem*. **1995**, *48*, 157-182.

[2] F. J. Millero *Geochem. Trans*., **2001**, *2*, 57-65.

[3] E. L. Rue, K. W. Bruland *Mar. Chem*. **1995**, *50*, 117-138.

[4] H. J. W. de Baar, J. T. M. de Jong, D. C. E. Bakker, B. M. Löscher, C. Veth, U. Bathmann, V. Smetacek, *Nature* **1995**, *373*, 412-415.

[5] M. Gledhill, C. M. G. van de Berg, R. F. Nolting, K.R. Timmermans, *Mar. Chem*. **1998**, *59*, 283-300.

[6] D. A. Hutchins, A. Witter, A. Butler, G. W. Luther III *Nature* **1999**, *400*, 858-861.

[7] J. T. Groves *Proc. Natl. Acad. Sci. USA* **2003**, *100*, 3569-3574.

[8] K. Chen, M. Costas, L. Que Jr. *J. Chem. Soc. Dalton Trans.* **2002**, 672-679.

[9] A. Wada, S. Ogo, S. Nagamoto, T. Kitagawa, Y. Watanabe, K. Jitsukawa, H. Masuda, *Inorg. Chem*. **2002**, *41*, 616-618.

[10] A. J. Simaan, F. Banse, J.-J. Girerd, K. Wieghardt, E. Bill, *Inorg. Chem.* **2001**, *40*, 6538-6540.

[11] R. E. M. Diederix, M. Fittipaldi, J. A. R. Worrall, N. Huber, M. Ubbink, G. W. Canters *Inorg. Chem.* **2003**, *42*, 7249-7257.

[12] S. Seibig and R. van Eldik *Inorg. Chim. Acta* **1998,** *279*, 37-43.

[13] G. H. Cohen, J. L. Hoard *J. Am. Chem. Soc.* **1966,** *88*, 3228-3234.

[14] M. D. Lind, M. J. Hamor, T. A. Hamor, J. L. Hoard *Inorg. Chem.* **1964,** *3*, 34-43.

[15] J. L. Hoard, M. Lind, J. V. Silverton *J. Am. Chem. Soc.* **1961,** 83, 2770-2771.

[16] F. Neese, E. I. Solomon, *J. Am. Chem. Soc.* **1998**, *120*, 12829-12848.

[17] K. Kanamori, H. Dohniwa, N. Ukita, I. Kanesaka, K. Kawai *Bull. Chem.. Soc. Jpn.* **1990**, *63*, 1447-1454.

[18] G. E. Stein, J. A. Marinsky *J. Inorg. Nucl. Chem*. **1975**, *37*, 2421-2428.

[19] A. Babko, N. Loriya *Zhur. Neorg. Khim.* **1968**, *13*, 506.

[20] E. Bottari, G. Anderegg *Helv. Chim. Acta* **1967**, *50*, 2349-2356.

[21] T. Bhat, D. Radhamma *Indian J. Chem.* **1965**, *3*, 151.

[22] R. Gustafson, A. Martell *J. Phys. Chem.* **1963**, *67*, 576-582.

[23] R. Skochdopole, S. Chaberek *J. Inorg. Nucl. Chem.* **1959**, *11*, 222-233.

[24] G. Schwarzenbach, J. Heller *Helv. Chim. Acta* **1951**, *34*, 576-591.

[25] E. Clarke, A. Martell *Inorg. Chim. Acta*, **1991**, *186*, 103-111.

[26] J. Ahmad, W. Higginson *J. Chem. Soc. Dalton Trans.* **1983**, 1449-1459.

[27] N. Zhirnova, K. Astakhov, S. Barkov *Zhur. Phys. Khim.* **1967**, *41*, 366.

[28] G. Anderegg, G. Schwarzenbach Helv. Chim. Acta, **1940**, *38*.

[29] M. Beck, S. Görög *Analyst*, **1959**, *48*, 90.

[30] R. Hutchenson and F. I. Cheng *Personal Communication*, **2004**.

[31] H. J. Schugar, A. T. Hubbard, F. C. Anson, H. B. Gray, *J. Amer. Chem. Soc.* **1969**, *91*, 71–77.

[32] G. McLendon, R. J. Motekaitis, A. E. Martell, *Inorg. Chem.* **1976**, *15*, 2306–2308.

[33] W. J. Cooper, D. R. S. Lean, J. Carey *Can. J. Fish. Aquat. Sci.* **1989**, *46*, 1227-1231.

[34] A. Y. Sychev, V. G. Isak *Russ. Chem. Rev.* **1995**, *64*, 1105-1129.

[35] A. Brausam, R. van Eldik *Inorg. Chem.* **2004**, *43*, 5351-5359.

[36] O. Horner, C. Jeandey, J.-L. Oddou, P. Bonville, J.-M. Latour *Eur. J. Inorg. Chem.* **2002**, *5*, 1186-1189.

[37] V. K. Sharma, P. Á. Szilágyi, Z. Homonnay, E. Kuzmann, A. Vértes *Eur. J. Inorg. Chem.* **2005**, *21*, 4393-4400.

[38] H. J. Schugar, G. R. Rossman, C. G. Barraclough and H. B. Gray *J. Am. Chem. Soc.* **1972**, *94*, 2683-2690.

[39] A. Márton, N. Sükösd-Rozlosnik, A. Vértes, I. Nagy-Czakó and K. Burger *Inorg. Chim. Acta*, **1987**, *137*, 173-176.

[40] M. Takeda, *Hyperfine Interactions* **1986**, *28*, 737–740.

[41] A. Vértes, D. L. Nagy *Mössbauer Spectroscopy of Frozen Solutions*, Akadémiai Kiadó, *Budapest*, **1990**.

6 Tuning the oxidation state: Study of the Photodegadaration of the Fe^{III}EDTA Complex Study of the Autoxidation of the Fe^{II}/EDTA System in Solid State and in Solution Phase

6.1 Study of the Photodegadaration of the Fe^{III}EDTA Complex

6.1.1 Introduction

Uptake of metals in plants is known to be driven by the concentration of the free ionic species, which is described by the Free-Ionic Activity Model (FIAM) [1], which predicts that adding ethylenediaminetetraacetic acid (EDTA) to a metal ion-bearing system will decrease the proportion of trace metal available for uptake, since the metal-EDTA complexes are not available for uptake. The Fe^{III}EDTA complex is the only environmentally relevant EDTA complex that is susceptible to photodegradation by sunlight [2]. Furthermore, photochemical reactions seem to be the only way to remove EDTA from surface waters [3]. Thus, the photodegradation of the Fe^{III}EDTA complex has been extensively studied during the past three decades. [4-28] Furthermore, it is not only the uptake of iron, which is affected by the photodegradation of ferric-ethylenediaminetetraacetate. Weltje *et al.* carrying out experiments with duckweed plants, suggested that the observed uptake of europium(III) was governed by the photodegradation of iron(III)-EDTA as well [16]. Several authors found the reaction quantum yield to be pH dependent [3,7,13]. Others found that, although the pH does not exert any influence on the photochemical reaction of Fe^{III}EDTA at low concentrations, it changes the molar extinction coefficient of the complex along the pH scale and thus, has some consequences for the photolysis rates via the light absorption rates of Fe^{III}EDTA [4]. The quantum yield is clearly dependent on wavelength, and light of wavelengths <400 nm are mainly responsible for photodegradation [2], even if UV light is not indispensable to degrade iron(III)-EDTA [11].

Laan *et al.* presented the reaction scheme for the iron(III)/EDTA system (see Fig. 6.1.1) [6].

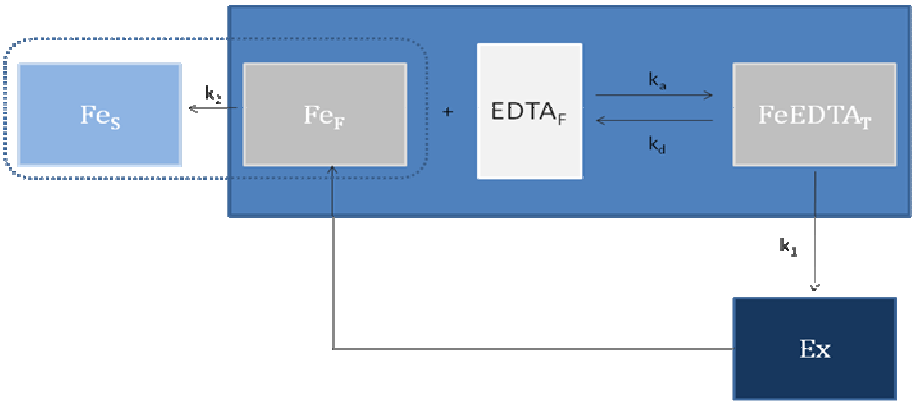

Figure 6.1.1 Scheme for reactions taking place in the iron(III)/EDTA system. See explanation in the text.

Processes taking place without irradiation are presented in the dark rectangle; processes requiring light are displayed in the outer part of the scheme. Fe_S signifies the solid ferric particles settled down from a saturated solution, Fe_F, $EDTA_F$ and FeEDTA signify the total amount of free ferric species, EDTA and $Fe^{III}EDTA$ complex, respectively. Ex signifies the species produced from the reaction $[FeEDTA_T] \xrightarrow{k_1} [Fe_F] + [Ex]$ (ferrous species for instance). If enough EDTA is provided, virtually all iron binds to EDTA, therefore no photodegradation of $FeEDTA_T$ occurs and the solubility threshold for $[Fe_F]$ will not be reached. In illuminated media, however, the photodegradation of $FeEDTA_T$ will lower the EDTA pool and as the Fe_F solubility threshold will be reached, iron will leave the system (as Fe_S). The photodegradation pathway was further studied and degradation products have been identified as CO_2, CH_2O, ED3A, EDDA (N,N'- and N,N- as well), EDMA, IMDA, glycine by GC-MS but no NTA has been found [13]. The proposed reaction schemes at different pH values are displayed in Figure 6.1.2 and 6.1.3.

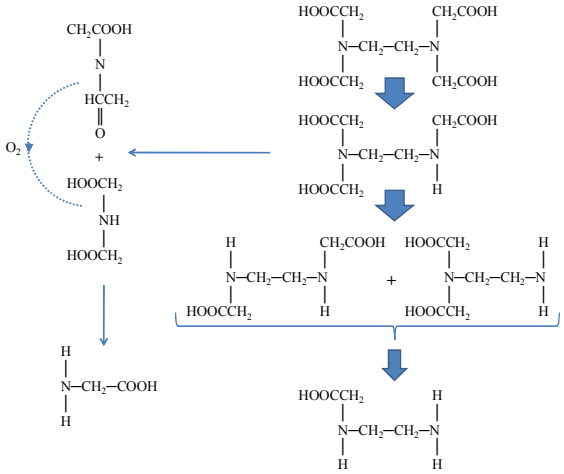

Figure 6.1.2 Proposed aerobic $Fe^{III}EDTA$ photodegradation scheme at pH=4.5

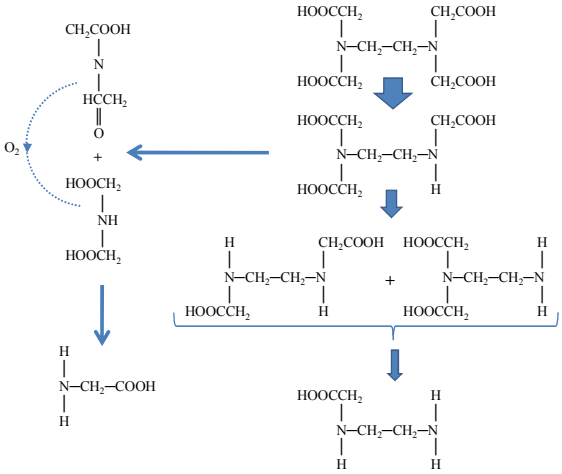

Figure 6.1.3 Proposed aerobic $Fe^{III}EDTA$ photodegradation scheme at pH=6.9-8.5.

Kari *et al.* carried out measurements in order to determine the main processes taking place and the reactants of the photodegradation process [12]. The most important process was found to be the direct photolysis, but chemical processes may be important for the long-term behaviour of EDTA. Mätserinne *et al*. studied the effect of the presence of molecular oxygen on the photodegradation. In their proposed reaction pathway they count with the production of an intermediate dimeric species in the course of the process. In the presence of molecular oxygen, the intermediate dimer quickly decomposes, yielding $[Fe^{III}EDTA]^-$, $[Fe^{III}ED3A]$ and EDTA oxidation products. The formation of this intermediate dimer was reported by Carey *et al*. as well. They also claimed the dimeric $Fe^{III}EDTA$ not to be photoreactive [7]. Karametaxas *et al*. described a conceptual model (for its scheme see Fig. 6.1.4) for the photodegradation of initially uncomplexed EDTA in the presence of γ-FeOOH (lepidocrocite), which is the following [8].

A, The free EDTA becomes adsorbed at the surface of γ-FeOOH and is initially photooxidised as a surface species.

B, γ-FeOOH is reductively dissolved; the photooxidation of adsorbed EDTA, coupled to reductive dissolution of γ-FeOOH, occurs through photolysis of the $Fe^{III}EDTA$ surface complex. The photochemically formed Fe^{II} catalyses the thermal dissolution of the solid phase in the presence of EDTA then. The initially uncomplexed EDTA is photooxidised via two pathways:

i, photooxidation at the surface of γ-FeOOH and

ii, photolysis of dissolved $Fe^{III}EDTA$.

The predominating pathway depends on the relative rates of Fe(II) oxidation and of Fe(II)-catalysed formation of dissolved $Fe^{III}EDTA$ (at pH=3, photolysis of dissolved $Fe^{III}EDTA$ was found to be more important, while at pH=7, photooxidation of adsorbed EDTA was). Main products were the CH_2O and dissolved Fe(II), the initial concentration of EDTA was 10^{-4} mol/dm^3. The formation of CH_2O at pH=7 was not accompanied by the formation of appreciable concentrations of dissolved Fe(II).

C, Iron acts as a catalyst in the thermal dissolution of γ-FeOOH, which becomes then an additional or even the dominant pathway (dearated system at pH=3).

D, Formation of dissolved $Fe^{III}EDTA$, which undergoes subsequent photolysis:

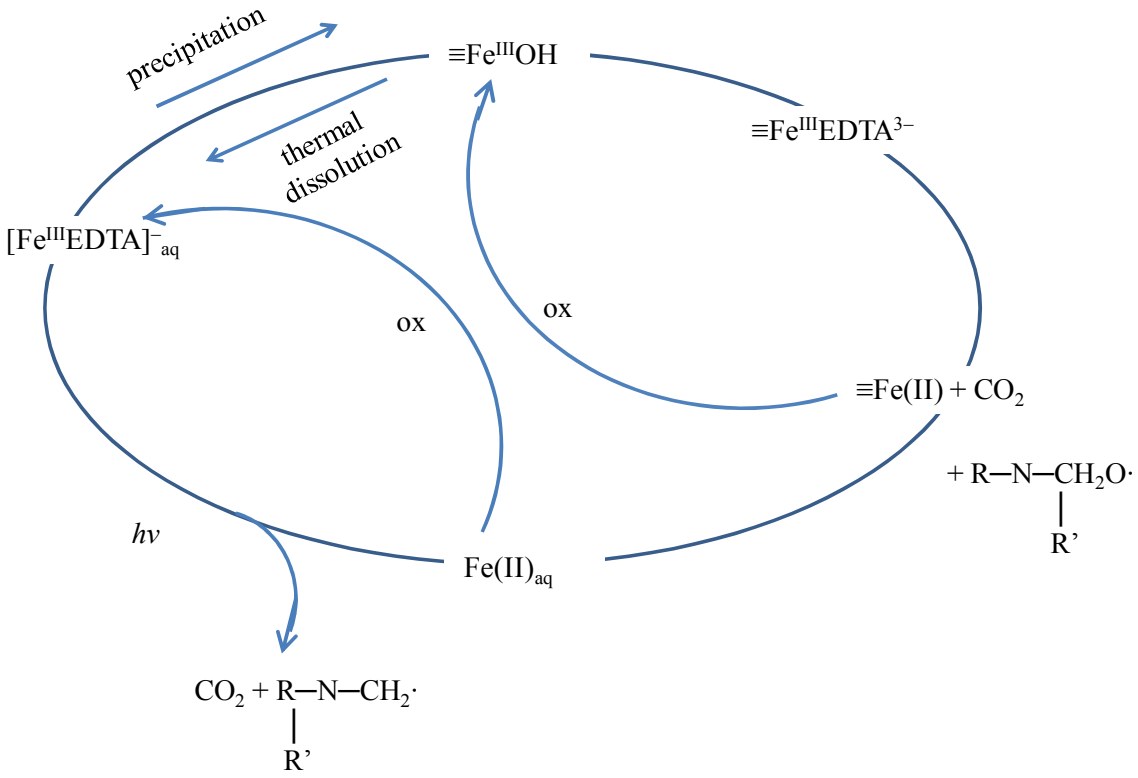

Figure 6.1.4 Conceptual model for the photodegradation of initially uncomplexed EDTA in the presence of γ-FeOOH. Where, R=—$(CH_2)_2$—$N(CH_2COO^-)_2$ and R'=—CH_2COO^-.

6.1.2 Results and Discussion

In order to study the $Fe^{III}EDTA$ photodegradation mechanism, Mössbauer experiments were carried out. In a first experiment, in order to avoid paramagnetic spin relaxation subspectra in the Mössbauer spectrum (which result in broadened lines and consequently in large linewidths and make the spectrum evaluations difficult) high concentration and pH values were applied, which enable the formation of the dimeric ferric-ethylenediaminetetraacetic species. Therefore, a $c_{Fe^{3+}}$=0.01 mol/dm^3 stock solution, containing a 1.3-fold excess of Na_2H_2EDTA, was prepared. After the mixing of the reactants, the pH of the solution was adjusted to pH~10.0. When raising the pH precipitation occurred and the solution was then filtered. The solution was prepared in darkness, only a low energy IR lamp (red) was used before its exposition to white light (3 min long by an integrated system of a FiberOptic light source, FOT 150, purchased from LOT Oriel, equipped with an OSRAM 15 V/150 W, No. 64634 halogen-lamp). Mössbauer spectra were recorded before and after the irradiation (see figures in Fig. 6.1.5 a) and b), respectively), at 80 K.

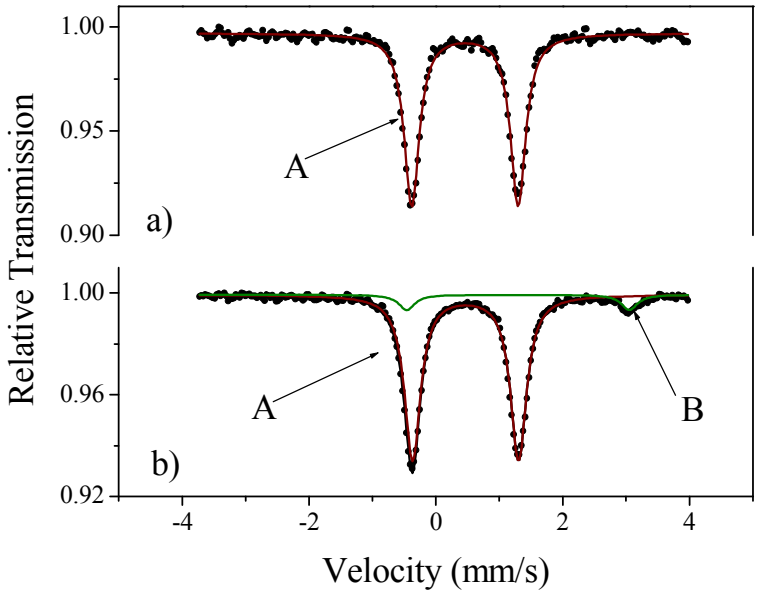

Figure 6.1.5 Mössbauer spectra of the aqueous solution of $Fe^{III}EDTA$ at pH~10.0 before (a)) and after (b)) irradiation by white light, at 80 K.

Table 6.1.1 Mössbauer parameters (at 80 K) and their errors for spectra of the aqueous solution of $Fe^{III}EDTA$ at pH~10.0 before (a)) and after (b)) irradiation by white light.

Spectrum/ Species / Parameters		Proportion (%)	δ (mm/s)	Δ (mm/s)	Γ (mm/s)
6.1.5a)	A	100	0.46(1)	1.68(2)	0.30(1)
6.1.5b)	A	91.5	0.47(1)	1.67(2)	0.30(1)
	B	8.5	1.30(1)	3.51(2)	0.30(1)

During the preparation of the solution, no photodegradation has occurred, as was expected when using only a low energy IR lamp. Spectrum in Fig. 6.1.5a) displays only one quadrupole doublet, A corresponds to the well known μ-oxo bridged dimeric species $[\mu\text{-O(FeEDTA)}_2]^{4-}$. As clearly visible after irradiating the system, photoreduction of the ferric species into a ferrous species has occurred. This fact is rather surprising after the hypothesis of Kari *et al.* [7] who claimed the dimeric species not to be photoreactive, but the appearance of the quadrupole doublet in Fig. 6.1.5b) displaying a ferrous species induced by photochemical reaction is obvious. Mätserinne *et al.* [11] suggested the formation of intermediate ferrous-ethylenediamineetraacetate species (see Eqs. 6.1.1-6.1.4), which were not detected using Mössbauer spectroscopy.

The reaction pathway proposed by Mätserinne *et al.* [11] is the following: The reduction is initiated by the photoinduced electron transfer (PET):

$$[Fe^{III}EDTA(H_2O)]^- \xrightarrow{h\upsilon\ (\mathrm{LMCT})} [Fe^{II}EDTA^{\bullet}\cdot(H_2O)]^- \text{ at pH=4} \qquad (6.1.1)$$

$$[Fe^{III}EDTA(OH)]^{2-} \xrightarrow{h\upsilon\ (\mathrm{LMCT})} [Fe^{II}EDTA^{\bullet}\cdot(OH)]^{2-} \text{ at pH=9} \qquad (6.1.2)$$

and followed by the back electron transfer:

$$[Fe^{II}EDTA^{\bullet}\cdot(H_2O)]^- \rightarrow [Fe^{III}EDTA(H_2O)]^- \qquad (6.1.3)$$

$$[Fe^{II}EDTA^{\bullet}\cdot(OH)]^{2-} \rightarrow [Fe^{III}EDTA(OH)]^{2-}. \qquad (6.1.4)$$

On the contrary, only the ferrous hexaaqua complex formed, since the hyperfine parameters for species B (in Figure 6.1.5b)) are identical to the parameters of the $[Fe(H_2O)_6]^{2+}$ [29]. This phenomenon reinforces the mechanism proposed by Karametaxas *et al.* (Eqs. 6.1.5-6.1.12) [8]. Although no precipitate was present in macroscopic amount in the sample (the solution was filtered when raising the pH precipitation appeared) and

no additional subspectrum due to solid particles is present in the resultant Mössbauer spectrum. Since the filtering paper was not designed to filter off fine colloidal particles some precipitate could remain in the solution (in a lower amount than the minimum that can be detected, <5 rel%) and might have served as a catalyst for the photodegradation.

The mechanism proposed by Karametaxas *et al.* [8] is the following

i, adsorption of EDTA at the surface of γ-FeOOH

$$\equiv Fe^{III}OH + HEDTA^{3-} \leftrightarrows \equiv Fe^{III}EDTA^{3-} + H_2O \quad (6.1.5)$$

ii, absorption of light by the primary chromophore

iii, oxidation of adsorbed EDTA

ii, and iii, together: $\equiv Fe^{III}EDTA^{3-} \leftrightarrows \equiv Fe^{II}EDTA\bullet^{3-*}$ (6.1.6)

iv, dissociation and decarboxilation of oxidised EDTA

$$\equiv Fe^{II}EDTA\bullet^{3-*} \rightarrow \equiv Fe(II) + CO2 + R{-}\underset{\displaystyle R'}{\overset{\displaystyle |}{N}}{-}CH_2O\bullet \quad (6.1.7)$$

v, detachment of reduced surface iron from the crystal lattice and reconstitution of the surface site.

$$\equiv Fe(II) + 2H^{+} \rightarrow Fe^{2+} + \equiv_{rec} \quad (6.1.8)$$

(where $\equiv_{rec}$ is a new $\equiv Fe^{III}OH$ site)

The primary chromophore is either the surface complex (a) or the γ-FeOOH itself (b). In case of (a), the electron transfer occurs through a ligand-to-metal charge transfer transition within the surface complex. In case of (b), a semiconductor mechanism has to be invoked where a photoelectron-photohole pair is formed.

Eventually $\equiv Fe(II) + ox \rightarrow \equiv Fe(III)^{+} + ox^{-}$ may occur, as well.

Fe^{2+} becomes readsorbed at the surface sites that are coordinated with EDTA, forming a ternary surface complex with EDTA acting as a bridging ligand ($\equiv Fe^{III}EDTAFe^{II-}$):

$$Fe^{2+} + \equiv FeEDTA^{3-} \leftrightarrows \equiv Fe^{III}EDTAFe^{II-} \quad (6.1.9)$$

$$\equiv Fe^{III}EDTAFe^{II-} \xrightarrow{\text{Electron Transfer}} \equiv Fe^{II}EDTAFe^{III-} \quad (6.1.10)$$

$$\equiv Fe^{II}EDTAFe^{III-} \rightarrow Fe^{III}EDTA^{-}{}_{aq} + \equiv Fe(II) \quad (6.1.11)$$

$$\equiv Fe(II) + 2H^{+} \rightarrow Fe^{2+} + \equiv_{rec} \quad (6.1.12)$$

To demonstrate the necessity of the surface of a precipitate for the photodegradation reaction, experiments were carried out with and without the occurrence of precipitation in the solution. A series of solutions, with pH ranging from 1

to 10, was prepared in a way that no precipitation occurred at higher pH values either. Each of these samples was exposed to white light (same light source as in the previous case) and then Mössbauer spectra were recorded. None of these spectra displayed any trace of ferrous component, consequently no photodegradation occurs in systems that do not contain any precipitate.

The experiment described in page 58 was repeated and the spectrum of the wet precipitate filtered off from the solution and exposed to white light was recorded as well, in order to identify the precipitate, it was also prepared without its exposition to light, the resultant spectra and the spectrum parameters are shown in Figure 6.1.6 and in Table 6.1.2, respectively.

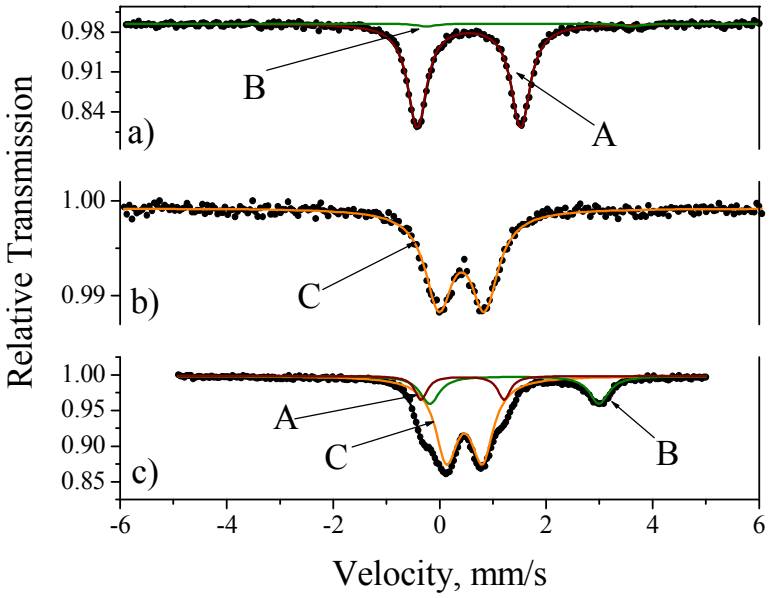

Figure 6.1.6 Mössbauer spectra of the aqueous solution of $Fe^{III}EDTA$ at pH~10.0 and at c<0.01 mol/dm^3 (a)) after illumination by white light, at 80 K (precipitate was filtered off before the illumination); of the precipitate (b)) prepared in a separate experiment, with the exclusion of light, at room temperature; and of the wet, illuminated precipitate (c)), filtered off of the solution, displayed in spectrum a), at 80 K.

Table 6.1.2 Mössbauer parameters and their errors for spectra of the aqueous solution of $Fe^{III}EDTA$ at pH~10.0 and at c<0.01 mol/dm^3 (a)) after illumination by white light, at 80 K (precipitate was filtered off before the illumination); of the precipitate (b)) prepared in a separate experiment, with the exclusion of light, at room temperature; and of the wet, illuminated precipitate (c)), filtered off of the solution, displayed in spectrum a), at 80 K.

Spectrum/Species / Parameters		Proportion (%)	δ (mm/s)	Δ (mm/s)	Γ (mm/s)
6.1.6a), (80 K)	A	97.3	0.46(1)	1.62(2)	0.36(3)
	B	2.7	1.36(4)	3.42(8)	0.36(3)
6.1.6b), (RT)	C	100	0.34(3)*	0.71(4)	0.52(1)
6.1.6c), (80 K)	A	11.4	0.43(2)	1.56(1)	0.30(1)
	B	20.7	1.40(1)	3.2(1)	0.44(1)
	C	67.9	0.46(1)*	0.67(1)	0.51(1)

*The difference in isomer shifts is due to the Second Order Doppler Shift.

RT-room temperature (~298K)

As can be seen, photodegradation has occurred in both solution and solid phases, but on the surface of the precipitate its effect was much more important (11.4% of the total iron species converted into ferrous ion in the case of the illumination in solid, while only 2.7% of the ferric species has been reduced in the case of the irradiation in solution phase). This supports the theory of Karametaxas *et al.* [8], that iron oxyhydroxides catalyse the photoreduction of ferric-ethylenediaminetetraacetate. The resultant ferrous species was found to be the hexaaqua complex again, as in the previous case.

6.1.3 Conclusions

It was found that in the aqueous solutions of $Fe^{III}EDTA$ complex the photodegradation reaction also takes place at high pH and concentration values, *i.e.* when the ferric species is in a dimeric form, which is contradictory to the previous hypotheses established. It was also found that the presence of the smallest amount of precipitate is not only favourable to the reaction but it is also a necessary condition, since no photodegradation was detected when no precipitation has occurred in the course of the experiments. This suggests that the surface of some ferric oxyhyroxide is needed to the photoreduction of the ferric species and this reinforces the hypothesis of Karamatexas *et al.* [8] who proposed a reaction pathway, in which the resultant ferrous species is the ferrous hexaaqua complex. This is the only ferrous species that could be detected with Mössbauer technique but this is not in contradiction with the fact that Karametaxas *et al.* suggested the presence of another ferrous complex, a surface related complex with very short lifetime. In contrast, the validity of the pathway proposed by Mätserinne *et al.* [11] can be questioned, because they did not consider the possible formation of the $[Fe(H_2O)_6]^{2+}$ complex at all.

6.2 Study of the Autoxidation of the Fe^{II}/EDTA System in Solid State and in Solution Phase

6.2.1 Introduction

There are several protein systems that catalyse the superoxide dismutation:

$$2\ O_2^- + 2\ H^+ \rightarrow O_2 + H_2O_2 \qquad (6.2.1)$$

and some of these require Fe ions as co-factors [30]. Enzyme mimic complexes, such as ferrous ethylenediaminetetraacetate (Fe^{II}EDTA) [31] may serve as useful models for understanding the protein catalysts, since they catalyse superoxide dismutation as well. That is the reason why there has been great interest in the oxidation of ferrous polyamino carboxylate complexes by molecular oxygen and hydrogen peroxide as well in the past 50 years. [32-48] The main interest in such reactions has resulted from their fundamental importance in biochemical processes, such as the cleavage of DNA, the decomposition of H_2O_2, and the dismutation of superoxide, as mentioned above [49-55]. The most investigated complexes are the Fe^{II}EDTA, Fe^{II}NTA, Fe^{II}HEDTA (ferric hydroxyethylethylenediaminetriacetate), Fe^{II}MIDA, Fe^{II}CDTA, Fe^{II}EDDA and the Fe^{II}DPTA, however, several studies concern their analogues and the autoxidation of the ferrous-hexaaqua complex. Concerning the further investigation of the complexes of EDTA, the question that arises is how the autoxidation of Fe^{II}EDTA into Fe^{III}EDTA takes place. To answer this question, first, we have to recall the stability of these complexes: the literature survey on the vast coordination chemistry of iron [56-60] reveals that both oxidation states can be stabilised by choosing a suitable ligand: ligands with carboxylate [61,62] groups exhibit preference toward Fe^{III} centres. However, despite its stability, synthesis of Fe^{III}EDTA species (either the monomeric $[Fe(EDTA)]^-$ or the μ-oxo dimer $O[Fe(EDTA)]_2^{4-}$ depending on the actual pH) is often hampered by kinetic effects. Raising the pH of a solution already containing Fe^{3+} and EDTA frequently results in precipitation of $Fe(OH)_3$ or FeOOH of various forms. This shows that the formation and precipitation of iron hydroxides or oxyhydroxides may be much faster than chelation of Fe^{3+}. There are several laboratory techniques which are supposed to

avoid this precipitation.[10] For example, it is known that the presence of Fe^{II} in a solution containing Fe^{III} and EDTA helps redissolve precipitated iron oxides or oxyhydroxides [63,64] by its oxidation. In the present work, Mössbauer study of the mechanism of the autoxidation of Fe^{II}EDTA in aqueous solution and in solid state is reported.

6.2.2 Results and Discussion

Autoxidation chemistry consists of the study of the transformation of transition metal complexes into oxidising species, or their reaction with oxidisable substrates. Regarding the mechanism of these reactions, the question arose whether the mediating species contain higher-valent iron (like ferryl or perferryl radicals) or the OH radical is generated in the course of Fenton-like reactions [65-68]. Oxygenated Fe^{II}EDTA undergoes autoxidation until all the Fe^{II} is converted to Fe^{III}. The proposed reaction pathway for this process was given by Seibig *et al.* [44]. Their hypothesis consisted of the following reaction steps (the investigated pH range was pH=3-7):

$$[Fe^{II}EDTA(H_2O)]^{2-} + O_2 \leftrightarrow [Fe^{II}EDTA(O_2)]^{2-} + H_2O \quad (6.2.2)$$

$$[Fe^{II}EDTA(O_2)]^{2-} \leftrightarrow [Fe^{III}EDTA(O_2^{-})]^{2-} \quad (6.2.3)$$

$$[Fe^{II}EDTA(H_2O)]^{2-} + [Fe^{III}EDTA(O_2^{-})]^{2-} \rightarrow [EDTAFe^{III}(O_2^{2-})Fe^{III}EDTA]^{4-} + H_2O \xrightarrow{2H^+} 2\,[Fe^{III}EDTA(H_2O)]^{-} + H_2O_2 \quad (6.2.4)$$

$$2\,[Fe^{II}EDTA(H_2O)]^{2-} + H_2O_2 \xrightarrow{2H^+} 2\,[Fe^{III}EDTA(H_2O)]^{-} + 2\,H_2O \quad (6.2.5)$$

(reaction pathway proposed for pH=6)

They also assumed that when oxygen was used in excess, only one reaction step was observed between pH=4 and pH=6 since a peroxo-bridged complex could not be formed under these conditions.

We followed the Fe^{II} autoxidation in a solution of which the initial pH was 7.06[11] containing Na_2H_2EDTA (Fe:EDTA ratio was 1:1.3), by aerial oxygen until the

[10] On the other hand, sometimes it is exactly this effect of which one can take advantage of in order to study interesting phenomena related to this system, such as the photodegradation of the Fe^{III}EDTA complex, for instance, see above.

[11] The relaxation line broadening causes serious problems in Mössbauer spectroscopy without any applied external magnetic field (see Chapter 4), thus, to avoid the presence of broadened spectral lineshapes in the Mössbauer spectrum, no monomeric ferric species are desired in the solutions; therefore, a pH and concentration range was chosen where the ratio of monomeric ferric species is not important anymore.

complete conversion of Fe^{II} to Fe^{III}. The samples were prepared in the following way: 5 cm^3 of deoxygenated $c_{Fe^{2+}}$=0.025 mol/dm^3 $FeCl_2$ solution was prepared by dissolving solid iron, enriched in ^{57}Fe to ~90%, in a deoxygenated hydrochloride solution, then solid Na_2H_2EDTA was added to the solution. The pH of the reaction mixture was 7.06 after the addition of Na_2H_2EDTA. The system was allowed to stand in an open flask in order to be oxidised by aerial oxygen. 0.5 cm^3 samples were taken from this solution 15, 30, 45, 60, 90, 120 and 150 min after the mixing of the reactants, and quenched immediately to 83±2 K for the Mössbauer measurement. The Mössbauer spectra presented in Figure 6.2.1 display only two subspectra except for the last spectrum recorded 150 min after the mixing of the reactants, where one subspectrum is left. The parameters of the fitted spectra are listed, in Table 6.2.1.

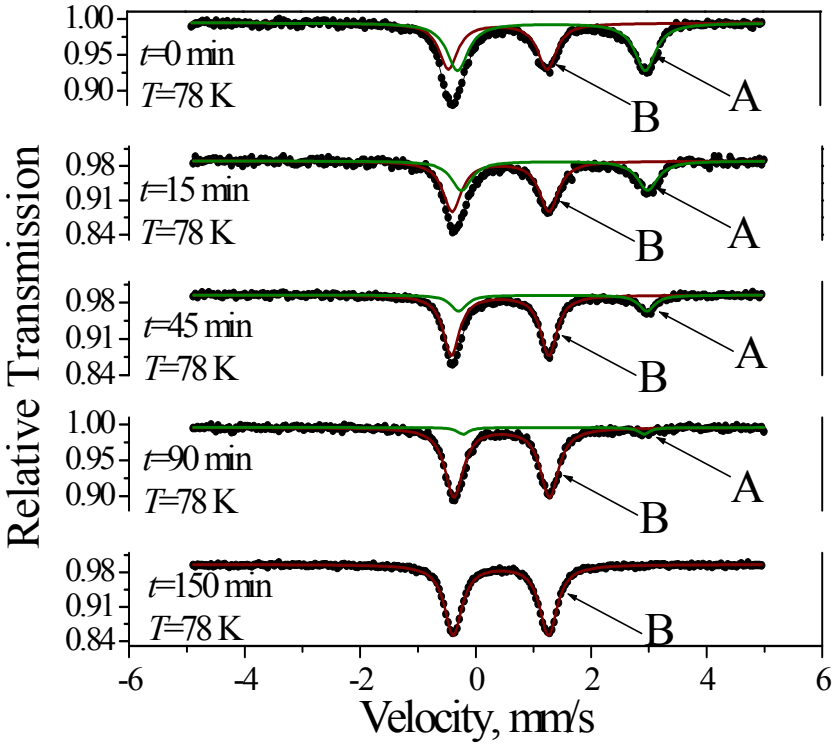

Figure 6.2.1. Frozen solution Mössbauer spectra of the aqueous 0.025 molar $FeCl_2$-EDTA system at pH~7 after aerial oxidations at room temperature for various durations indicated, spectra were recorded at 83±2 K.

Table 6.2.1. Mössbauer parameters (at 83±2 K) and their errors for spectra of the aqueous 0.025 molar $FeCl_2$-EDTA system at pH~7 after aerial oxidations at room temperature for various durations indicated, spectra were recorded at 83±2 K.

Species/Parameters	δ (mm/s)	Δ (mm/s)	Γ (mm/s)
A	1.35(2)	3.20(6)	0.38(5)
B	0.44(2)	1.67(3)	0.36(3)

Doublets A and B correspond to the original Fe^{II} species and the product of the oxidation process, respectively. Undoubtedly, the autoxidation of the Fe^{II} species took place immediately after mixing the reactants, which is proven by the presence of the doublet B in the first spectrum already. This shows that during the few seconds that passed between the addition of the Na_2H_2EDTA and freezing the system, almost 50% of the Fe^{2+} ions were oxidised. However, the reaction slowed down afterwards and even 90 min after the addition of Na_2H_2EDTA 6% Fe^{2+} remained in the sample. The ratio of the concentration of the ferrous and ferric species as a function of the time passed after the mixing of the reactants is displayed in Figure 6.2.2.

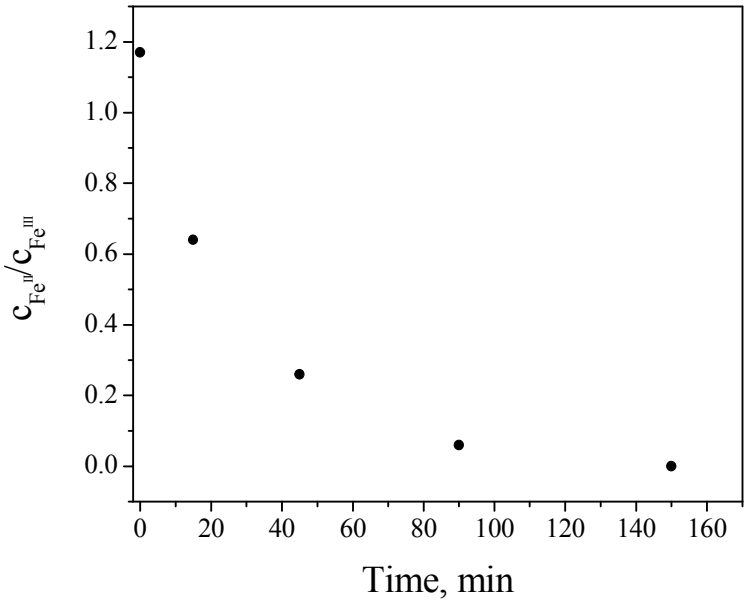

Figure 6.2.2 Variation of the concentration ratio of ferrous and ferric species in time.

Surprisingly, the hyperfine parameters of species A are identical to those, of the $[Fe(H_2O)_6]^{2+}$ species [29], which means that no complexation took place in the solution at such a pH and concentration value. This finding is rather surprising since, so far, the existence and stability of the Fe^{II}EDTA have been treated as evidence. The fact, that the

subspectrum of $Fe^{II}EDTA$ could not be seen in the Mössbauer spectra is contradictory to the results of Handshow Clark and Martell [69], who investigated the system using potentiometric titration, but the conditions under which the system was studied were different from the conditions discussed here (concentration of the initial ferrous salt was twenty five times higher and ionic strength was not controlled in this case). However, these changes should not affect the presence of the $Fe^{II}EDTA$ complex in the solution. Nevertheless, in ref. [69], the authors did not give spectroscopic evidence for the existence of the complex, nor did they prove their results by publishing their titration curves obtained for the EDTA complex. The hyperfine parameters of species A being identical with those of the ferrous hexaaqua complex leave no doubt about the argument that under these conditions no $Fe^{II}EDTA$ complex forms in detectable amounts (>5 rel. %).

Despite the numerous intermediate species suggested, only one subspectrum representing an iron(III) species appeared in the spectra, which is the final product of the autoxidation process, the μ-oxo dimer $\{O[Fe(EDTA)]_2\}^{4-}$. Thus, no intermediate species like the peroxo bridged $[EDTAFe^{III}(O_2^{2-})Fe^{III}EDTA]^{4-}$, which would have had to appear as a third doublet [70], could be detected in the spectra. The presence of monomeric species is also excluded on the basis of their very characteristic relaxation line shape in this concentration range [29]. The absence of new subspectra, however, may not contradict the hypothesis established by Seibig *et al.* [44] on the mechanism because it is possible that the intermediate species cannot be detected using Mössbauer spectroscopy due to their possibly short lifetimes resulting in or combined with very low stationary or equilibrium concentration. The fast dimerisation in this work is most probably due to the somewhat higher pH (7 instead of 6) and the higher concentration of the ferrous species (0.025 mol/dm^3 instead of the range 0.00003-0.0025 mol/dm^3) used in this experiment. Considering these differences and the fact that the initial ferrous species was the ferrous hexaaqua complex, two other reaction pathways have to be considered, namely when

i) the first reaction step is the oxidation of the hexaaqua complex by dissolved molecular oxygen into the ferric hexaaqua complex, which has to be followed by the rapid coordination of the EDTA to the ligand sphere of the ferric ion, followed by the immediate dimerisation, or, when

ii) the formation of the $Fe^{II}EDTA$ complex takes place first, and is followed by the oxidation and the dimerisation.

In both cases, there are several intermediate species, which could be detected using Mössbauer spectroscopy; in case i), the ferric hexaaqua complex, and the monomeric $Fe^{III}EDTA$ could be detected, while in case ii), the ferrous and the monomeric ferric ethylenediaminetetraacetate could appear in the resultant Mössbauer spectrum. As none of the subspectra assigned to these three species appeared in the spectra, we cannot predict which reaction pathway is more probable. However, we suggest that case i) is less credible since at this pH and concentration value, the ferric hexaaqua complex should undergo hydrolysis and precipitation as ferrihydrate which was not observed. We also have to admit that a low amount of ferrous ethylenediaminetetraacetate can be present in the reaction mixture (therefore the reaction pathway proposed by Seibig *et al.* [44] cannot be excluded), thus pathway ii) seems to be more favourable to the system. In addition, Xue *et al.* [5] have studied the speciation of ferric-ethylenediaminetetraacetate in natural waters, and they found that under typical freshwater conditions (pH~6-8) iron(III) is in equilibrium with $Fe(OH)_3$, therefore the formation of the $Fe^{III}EDTA$ complex is not straightforward, which supports the hypothesis that pathway ii) is more probable.

Since the mechanism of the autoxidation reaction may differ in solid state from the one in solution phase, the experiment was repeated under different conditions. The complex $(NH_4)_2[FeEDTA(H_2O)]$ was prepared in solid state as follows: The preparation of the compound took place in inert atmosphere during the whole process. 10 cm^3 oxygen free concentrated aqueous ammonia solution was mixed with 0.6690 g of Mohr salt, which resulted in a brownish-yellow solution without precipitation. After dissolving the Mohr salt, 0.5016 g of H_4EDTA was immediately added to the system which was stirred and heated afterwards for a half an hour. When the H_4EDTA was dissolved completely, the colour of the solution turned to beige. The pH of the solution was higher than 8. Finally, the solution was evaporated to dryness and the light pink powder obtained was used for Mössbauer investigation. Exposing to air during the Mössbauer measurements, the colour of the sample gradually turned to red as an indication of oxidation. The sample was not perfectly sealed (it was placed in between plastic foils and, only partially, sealed by scotch tapes) so that aerial oxidation could take place. This solid sample was measured at room temperature; its Mössbauer

spectrum (see in Figure 6.2.3) was saved and evaluated 1, 2 and 4 days after the beginning of the measurement. For the evaluated hyperfine parameters see Table 6.2.2.

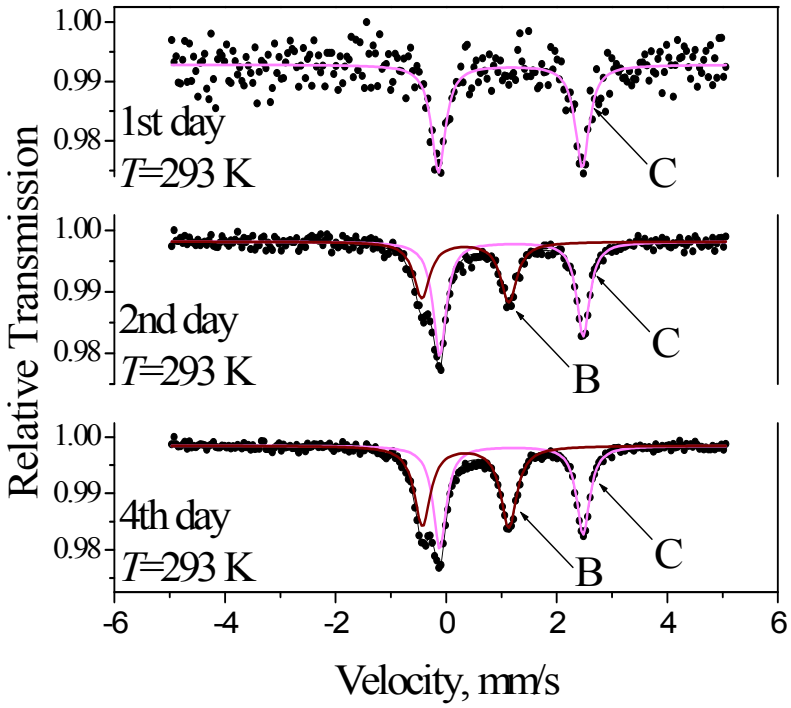

Figure 6.2.3. Mössbauer spectra of the solid $(NH_4)_2[FeEDTA(H_2O)]$ at room temperature after aerial oxidations for different durations. (Note that the relative doublet intensities should be considered as time integrals from the beginning to the 1st, 2nd and 4th days of the measurement as indicated.)

Table 6.2.2. Mössbauer parameters (at room temperature) and their errors for spectra of the solid $(NH_4)_2[FeEDTA(H_2O)]$ at room temperature after aerial oxidations for different durations. (Note that the relative doublet intensities should be considered as time integrals from the beginning to the 1st, 2nd and 4th days of the measurement as indicated.)

Species/Parameters	δ (mm/s)	Δ (mm/s)	Γ (mm/s)
B	0.35(1)	1.56(3)	0.35(2)
C	1.17(1)	2.59(2)	0.29(1)

In this case, the hyperfine parameters of the initial doublet, C, are markedly different from those of the hexaaqua iron(II)-complex (even if the expected temperature dependence is taken into account). Therefore this doublet can be assigned to the $[Fe^{II}EDTA(H_2O)]^{2-}$ complex ion. We assume here that this complex corresponds neither to $[Fe(H_2O)_4][Fe(HEDTA)(H_2O)]_2 \cdot 4H_2O$ (I) nor to $[Fe(H_2EDTA)(H_2O)] \cdot 2H_2O$ (II),

synthesised and characterised by Mizuta *et al.* [71], since complex I should display two quadrupole doublets in its Mössbauer spectrum representing the two different iron(II) microenvironments and complex II was prepared at a much lower pH (pH=2). However, no Mössbauer spectra have been recorded of these compounds. We can assume that compound C is the iron(II) complex formed with totally deprotonated ethylenediaminetetraacetic acid. This is also reinforced by its hyperfine parameters being close to those ones measured by Epstein (δ=1.45 mm/s and Δ=2.80 mm/s, at 80 K, calibration was done against stainless steel absorber). [72]

The product of the autoxidation in this case is obviously the μ-oxo dimer species $\{O[Fe(EDTA)]_2\}^{4-}$ again. The difference in the isomer shift (compare Table 6.2.1 and Table 6.2.2) is due to the expected temperature shift, and the slightly lower quadrupole splitting at room temperature is also reasonable. Thus the following oxidation took place:

$$2\ [Fe^{II}EDTA(H_2O)]^{2-} + 1/2\ O_2 \rightarrow \{O[Fe^{III}(EDTA)]_2\}^{4-} + H_2O. \qquad (6.2.6)$$

This indicates that despite the solid-state reaction, the dimer formation takes place without any transitional state of appreciable lifetime, and thus, since dimerisation in the solid state would certainly require rather slow diffusion steps, the hypothesis for the Fe^{II} complex, being in dimeric state already in $(NH_4)_2[FeEDTA(H_2O)]$, itself, cannot be excluded. There is an other possibility to explain the immediate formation of the μ-oxo bridged dimer upon oxidation of the ferrous species, which is discussed in Chapter 8 as well; namely, when an oxygen molecule oxidises the ferrous species, it binds to it, forming a short-lived intermediate species, then, an other ferric species gets oxidised by this adduct, forming the dimeric species and ejecting an oxygen atom, which can oxidise further ferrous entities (Eqs. 6.2.7-6.2.16).

$$Fe^{II}(H_2O)_6 + EDTA \xrightarrow{-6\,H_2O} \{[Fe^{II}EDTA]^{2-}\} \qquad 6.2.7$$

$$\{[Fe^{II}EDTA]^{2-}\} \xrightarrow{O_2} \{O_2[Fe^{II}EDTA]^{2-}\} \qquad 6.2.8$$

$$\{O_2[Fe^{II}EDTA]^{2-}\} \xrightarrow{ET} \{O_2[Fe^{III}EDTA]^{2-}\} \qquad 6.2.9$$

$$\{O_2[Fe^{III}EDTA]^{2-}\} \xrightarrow{\{[Fe^{II}EDTA]^{2-}\}} \{[EDTAFe^{II}(O_2)Fe^{III}EDTA]^{4-}\} \qquad 6.2.10$$

$$\{[EDTAFe^{II}(O_2)Fe^{III}EDTA]^{4-}\} \xrightarrow{ET} \{[EDTAFe^{III}(O_2)Fe^{III}EDTA]^{4-}\} \qquad 6.2.11$$

$$\{[EDTAFe^{III}(O_2)Fe^{III}EDTA]^{4-}\} \xrightarrow{-O:} [EDTAFe^{III}–O–Fe^{III}EDTA]^{4-} \qquad 6.2.12$$

$$\{[Fe^{II}EDTA]^{2-}\} \xrightarrow{O:} \{\cdot O[Fe^{II}EDTA]^{2-}\} \quad 6.2.13$$

$$\{\cdot O[Fe^{II}EDTA]^{2-}\} \xrightarrow{ET} \{:O[Fe^{III}EDTA]^{2-}\} \quad 6.2.14$$

$$\{:O[Fe^{III}EDTA]^{2-}\} \xrightarrow{\{[Fe^{II}EDTA]^{2-}\}} \{[EDTAFe^{II}–O–Fe^{III}EDTA]^{4-}\} \quad 6.2.15$$

$$\{[EDTAFe^{II}–O–Fe^{III}EDTA]^{4-}\} \xrightarrow{ET} [EDTAFe^{III}–O–Fe^{III}EDTA]^{4-} \quad 6.2.16$$

6.2.3 Conclusions

For the autoxidation reaction of Fe^{II}/EDTA system, it has been demonstrated that in a pH=7.06, c=0.025 mol/dm^3 solution no intermediate species may be observed using Mössbauer spectroscopy in frozen solutions. The initial Fe^{II} species did not seem to be chelated in any form, only the $[Fe(H_2O)_6]^{2+}$ species could be identified as Fe^{II} component in the Mössbauer spectra, and the $\{O[Fe^{III}(EDTA)]_2\}^{4-}$ complex was readily produced in the solution when it was allowed to get oxidised by aerial oxygen. The same type of oxidation was observed in solid state; however, the doublet representing the initial Fe^{II} state was recognised as the Mössbauer spectrum of the $[Fe^{II}EDTA]^{2-}$ complex. As the $O[Fe^{III}(EDTA)]_2^{4-}$ μ-oxo dimer was the direct product of the autoxidation reaction, and the formation of no other Fe^{III} compound was observable, we can assume that the $[Fe^{II}EDTA]^{2-}$ complex existed in the solid state in a dimeric form already.

It is remarkable that such a direct dimer-formation took place when, in the presence of 0.001 mol/dm^3 borate and 0.005 mol/dm^3 phosphate at pH~10, a c=0.1 mol/dm^3 ferrate(VI) solution was reacted with EDTA [73]. This hints that redox steps involving the contribution of O_2^{2-} (should it come from aerial oxygen photochemically [45] or possibly produced by decomposing FeO_4^{2-}) are crucial for the formation of μ-oxo dimer Fe^{III}EDTA species.

6.3 References

[1] F. M. M. Morel, *Principles of Aquatic Chemistry*, John Wiley & Sons: *New York*, **1983**.

[2] F. G. Kari *PhD Thesis*, **1994**, ETH *Zürich*.

[3] R. Frank and H. Rau *Ecoxicol. Environ. Saf.* **1990**, *19*, 55-63.

[4] F. G. Kari, S. Hilger, and S. Canonica *Environ. Sci. Technol.* **1995**, *29*, 1008-1017.

[5] H. Xue, L. Sigg and F. G. Kari *Environ. Sci. Technol*. **1995**, *29*, 59-68.

[6] R. G. W. Laan, T. Verburg, H. Th. Wolterbeek and J. M. de Goeij *Environ. Chem.* **2004**, *I.* 107-115.

[7] J. H. Carey and C. H. Langford *Can. J. Chem*. **1973**, *51*, 3665-3670.

[8] G. Karametaxas, S. J. Hug and B. Sulzberger *Environ. Sci. Technol*. **1995**, *29*, 2992-3000.

[9] B. Nowack and U. Baumann *Acta Hydrochim. Hydrobiol.* **1998**, *26*, 104-108.

[10] P. Kocot, A. Karocki and Z. Stasicka *J. Photochem. Photobiol*. **2006**, *179*, 176-183.

[11] S. Mätserinne, T. Tuhkanen and R. Aksela *Chemosphere* **2001**, *45*, 949.

[12] F. G. Kari and W. Giger *Environ. Sci. Technol*. **1995**, *29*, 2814-2827.

[13] H. B. Lockhart, R. V. Blakeley *Environ. Sci. Technol*. **1975**, *9*, 1035-1038.

[14] P. Natarajan and J. F. Endicott *J. Phys. Chem*. **1973**, *77*, 2049-2054.

[15] F. G. Kari and W. Giger, *Wat. Res*. **1996**, *30*, 122-134.

[16] L. Weltje, J. J. H. Haftka, T. G. Verbug, T. Th. Wolterbeek *Environ. Sci. Pollut. Res.* **2000**, *1*, 29.

[17] A. R. Bowers, C. P. Huang *J. Colloid Interface Sci.* **1986**, *110*, 575-590.

[18] R. Buitenhuis, C. M. N. Bakker, F. R. Stock, P. W. F. Louwrier *Radiochim. Acta* **1977**, *24*, 189-192.

[19] B. C. Faust, J. Hoigné *Environ. Sci. Technol*. **1987**, *21*, 957-964.

[20] R. G. Zepp, J. Hoigné, H. Bader *Environ. Sci. Technol*. **1987**, *21*, 443-450.

[21] R. G. Zepp, B. C. Faust, J. Hoigné Environ. Sci. Technol. 1992, 26, 313-319.

[22] R. C. Barry, J. L. Schnoor, B. Sulzberger, L. Sigg, W. Stumm *Water Res.* **1994**, *28*, 323-342.

[23] B. Sulzberger, J. L. Schnoor, R. Giovanoli, J. G. Hering, J. Zobrist *Aquat. Sci.* **1990**, *52*, 56-74.

[24] C. Siffert, B. Sulzberger *Langmuir*, **1991**, *7*, 1627-1634.

[25] M. I. Litter, E. C. Baumgartner, G. A. Urrutla, M. A. Blesa *Environ. Sci. Technol*. **1991**, *7*, 1907-1913.

[26] B. C. Faust, J. Hoigné *Atmos. Environ*. **1990**, *24A*, 79-89.

[27] M. Unger, E. Mainka and W. König *Fresenius' J. Anal. Chem*. **1987**, *329*, 50-54.

[28] R. Torres, M. A. Blesa and E. Matijević *J. Colloid Interface Sci*. **1989**, *131*, 567-579.

[29] A. Vértes, D. L. Nagy *Mössbauer Spectroscopy of Frozen Solutions*, Akadémiai Kiadó, *Budapest*, **1990**.

[30] I. Fridovich *Annu. Rev. Biochem*. **1975**, *44*, 147-159.

[31] B. Halliwell *FEBS LETT*. **1976**, *56*, 34-38.

[32] M. Cher and N. Davidson *J. Am. Chem. Soc*. **1955**, *77*, 793-798.

[33] R. E. Huffman, N. Davidson *J. Am. Chem. Soc*. **1956**, *78*, 4836-4842.

[34] T. Kaden, S. Fallab *Chelate Catalysed Autoxidation of Iron(II) Complexes*: Macmillan: *New York*, **1961**.

[35] Y. Kurimura, R. Ochiai, N. Matsuura *Bull. Chem. Soc. Jpn*. **1968**, *41*, 2234-2239.

[36] A. P. Purmal, Y. I. Skurlatov, S. O. Travin *Bull. Acad. Sci. USSR, Div. Chem. Sci.* (Engl. Transl.) **1980**, *29*, 315-320.

[37] E. Sada, H. Kumazawa, H. Machida *Ind. Eng. Chem. Res*. **1987**, *26*, 1468-1472.

[38] E. R. Brown, J. R. Mazzarella *J. Electroanal. Chem. Interfacial Electrochem*. **1987**, *222*, 173-192.

[39] M. Ranhal, H. W. Richter *J. Chem. Soc*. **1988**, *110*, 3126-3133.

[40] J. D. Rush, W. H. Koppenol *J. Am. Chem. Soc*. **1988**, *110*, 4957-4963.

[41] H. J. Wubs and A. A. C. M. Beenackers *Ind. Eng. Chem. Res*. **1993**, *32*, 2580-2594.

[42] L. Liang, J. A. McNabb, J. M. Paulk, B. Gu, J. F. McCarthy *Environ. Sci. Technol.* **1993**, *27*, 1864-1870.

[43] D. W. King, H. A. Lounsbury, F. J. Millero *Environ. Sci. Technol*. **1995**, *29*, 818-824.

[44] S. Seibig, R. van Eldik *Inorg. Chem*. **1997**, *36*, 4115-4120.

[45] I. L. Yurkova, H. P. Schuchmann, C. J. von Sonntag *Chem. Soc. Perkin Trans*. **1999**, *2*, 2049-2052.

[46] T. Schneppensieper, S. Finkler, A. Czap, R. van Eldik, M. Heus, P. Nieuwenhuizen C. Wreesmann, W. Abma *Eur. J. Inorg. Chem*. **2001**, *17*, 491-501.

[47] K. D. Welch, T. Z. Davis, S. D. Aust *Archives of Biochemistry and Biophysics*, **2002**, *397*, 360-369.

[48] F. Gambardella, I. J. Ganzeveld, J. G. M. Winkelman, E. J. Heeres *Ind. Eng. Chem. Res.* **2005**, *44*, 8190-8198.

[49] W. Krapp Pogozelski, T. J. McNeese, T. D. Tullius *J. Am. Chem. Soc*. **1995**, *117*, 6428-6433.

[50] M. Fontecave, J. L. Pierre *Bull. Soc. Chim. Fr*. **1993**, *130*, 77-85.

[51] G. J. McClune, J. A. Fee, G. McCluskey, J. T. Groves *J. Am. Chem. Soc*. **1977**, *99*, 5220-5222.

[52] C. Bull, G. J. McClune J. A. Fee *J. Am. Chem. Soc*. **1983**, *105*, 5290-5300.

[53] R. P. Hertzberg, P. B. Dervan *Biochemistry* **1984**, *23*, 3934-3945.

[54] R. S. Youngquist, P. B. Dervan J. *Am. Chem. Soc*. **1985**, *107*, 5528-5529.

[55] P. D. Dervan *Science* **1986**, *232*, 464-471.

[56] E. Nordlander, A. M. Whalen *Coord. Chem. Rev*. **1995**, *142*, 43-99.

[57] E. Nordlander, A. M. Whalen, F. Prestopino *Coord. Chem. Rev*. **1995**, *146*, 225-306.

[58] A. K. Powell *Coord. Chem. Rev*. **1994**, *134*, 91-169.

[59] P. Thornton *Coord. Chem. Rev*. **1992**, *113*, 131-288.

[60] S. A. Cotton *Coord. Chem. Rev*. **1972**, *8*, 185-223.

[61] T. J. Mizoguchi, J. Kuzelka, B. Spingler, J. Dubois, R. M. Davydov, B. Hedman, K. O. Hodgson, S. J. Lippard *Inorg. Chem*. **2001**, *40*, 4662-4673.

[62] J. Dubois, T. J. Mizoguchi, S. J. Lippard *Coord. Chem. Rev*. **2000**, *200-202*, 443-485.

[63] E. Baumgartner, M. A. Blesa, H. A. Marinovich, A. J. G. Maroto *Inorg. Chem*. **1983**, *22*, 2224-2226.

[64] M. A. Blesa, H. A. Marinovich, E. C. Baumgartner, A. J. G. Maroto *Inorg. Chem*. **1987**, *26*, 3713-3717.

[65] S. Croft, B. C. Gilbert, J. R. Lindsay Smith, A. C. Withwood *Free Radical Res. Commun*. **1992**, *17*, 21-39.

[66] A. Y. Sychev, V. G. Isak *Russ. Chem. Rev*. **1995**, *64*, 1105-1129.

[67] C. Walling *Acc. Chem. Res*. **1998**, *31*, 155-157.

[68] P. A. McFaul, D. D. A. Wayner, K. U. Ingold *Acc. Chem. Res*. **1998**, *31*, 159-162.

[69] C. N. Handshaw and A. E. Martell *Inorg. Chem*. **1988**, *27*, 1297-1298.

[70] V. K. Sharma, P. Á. Szilágyi, Z. Homonnay, E. Kuzmann and A. Vértes Eur. J. *Inorg. Chem.* **2005**, *21*, 4393-4400.

[71] T. Mizuta, J. Wang, K. Miyoshi *Inorg. Chim. Acta* **1995**, *230*, 119-125.

[72] L. M. Epstein *J. Chem. Phys*. **1962**, *36*, 2731-2737.

[73] Z. Homonnay, N. Smith, V. K. Sharma, P. Á. Szilágyi and E. Kuzmann, In: *ACS Symposium Series: Ferrates: Synthesis, Properties, and Applications in Water and Wastewater Treatment*, in press, **2007**.

7 Study of the reaction of Fe^{III}EDTA, Fe^{III}CDTA and Fe^{III}EDDA with H_2O_2

7.1 Introduction

Fe^{III} complexes are widely used as catalysts in oxidation reactions. Especially their reactions with hydrogen peroxide as a cheap oxidising agent have received much attention. Key complexes formed during these processes are iron-peroxo species. These peroxo intermediates have been spectroscopically characterised for various heme and non-heme Fe complexes and play important role in the oxygen activation and transfer reactions mediated by heme and non-heme iron proteins.[1,2] The iron-peroxo complexes have also been shown to catalyse the polymerisation of styrene and organic substrates.[3,4] The formation of iron-peroxo complex in the decomposition of hydrogen peroxide by Fe^{III} in aqueous solution is relevant in the chemistry of natural waters and atmospheric water droplets.[5–7]

One well understood peroxo complex is the purple $[Fe^{III}(EDTA)(\eta^2\text{-}O)]^{3-}$, which is formed upon addition of hydrogen peroxide to $Na[Fe^{III}(EDTA)]$ (first studied in 1956[8]) and was proven to be a high spin[9] (S=5/2) Fe^{III} side-on peroxo[12] complex by a variety of techniques such as Raman spectroscopy,[10,11] Mössbauer spectroscopy,[12,13] low temperature absorption spectroscopy, variable temperature – variable magnetic field circular dichroism (VTVH MCD) and electron spin resonance spectroscopy (ESR).[14] In addition, kinetic information on the activation of H_2O_2 by EDTA is available.[9,15-17]

[12] Two sorts of peroxo complexes can be distinguished by the position of the metal containing moiety: one is the *end-on* position: M-OO-
and the other one is the *side-on* position:

Brausam and van Eldik[18] have performed a detailed study on the reaction between $[Fe^{III}(EDTA)(H_2O)]^-$ and hydrogen peroxide with the aid of stopped-flow technique. They investigated the effect of the pH, temperature and pressure on the reaction of hydrogen peroxide with $[Fe^{III}(EDTA)(H_2O)]^-$. The reaction consists of two steps and the second one is independent of the hydrogen peroxide concentration. The first involves the reversible end-on coordination of H_2O_2 to give an intermediate, $[Fe^{III}(EDTA)OOH]^{2-}$, which goes through intramolecular rearrangement to give high-spin Fe^{III} side-on bound peroxo complex, $Fe^{III}(EDTA)(\eta^2\text{-}O_2)]^{3-}$. Both steps are affected by general acid catalysis. The reaction only takes place at pH values above the pK_a value of $[Fe^{III}(EDTA)(H_2O)]^-$ (pK_a=7.5).

In recent years, there has been tremendous interest in the diiron complexes due to their role in biological systems.[1,2,19] Metalloproteins consist of carboxylate bridged diiron centre, which perform a variety of functions.[20,21] This has prompted many workers to develop small molecule synthetic model compounds for non-heme dinuclear iron-base metalloproteins.[20–23] Studies of such compounds with hydrogen peroxide help understand the function of an enzyme that catalyses an important chemical transformation. Furthermore, characterising the diiron(III) peroxo intermediates in the reactions will eventually enhance understanding in the biological environment.[20,24]

In order to obtain more information on the reactivity of ferric complexes with polyaminecarboxylate ligands towards hydrogen peroxide, $[Fe^{III}(CDTA)(H_2O)]^-$ another representative of this ligand family for the present study has been selected. The reaction taking place between Fe^{III}CDTA and H_2O_2 has been studied only in the presence of albumin, in order to study of its DNA cleavage properties. [25] It has been demonstrated that as a consequence of the difference in the stability of the different ferric polyaminecarboxylate complexes, different reaction rate, reaction yield and catalytic behaviours were displayed.

The reaction of ferric (N,N')-ethylenediaminediacetate with hydrogen peroxide has not been studied so far, however, the reaction taking place between its ferrous complex with H_2O_2 is known to be similar to the reaction between the ferric ethylenediaminetetraacetate and hydrogen peroxide.[26]

7.2 Results and Discussion

7.2.1 Reaction of iron(III)-EDTA with H_2O_2

A stock solution of $Fe(NO_3)_3$ (0.05 mol/dm^3) was prepared by dissolving metallic iron (enriched in ^{57}Fe to ~90%) in nitric acid. The final pH of this stock solution was ~1.0. The Mössbauer measurements were performed by mixing the ferric solution (0.05 cm^3, 0.05 mol/dm^3) with solid EDTA. The amount of EDTA in the mixture was in excess and final molar ratio of EDTA to Fe^{III} was 1.3:1.0. The pH of the solution, measured with a digital pH-meter (Radelkis), was adjusted by using KOH (0.5 mol/dm^3). At alkaline pH, some precipitation in the Fe^{III}EDTA solution was observed. The precipitate was filtered off using 5 μm filter. The filtrate was diluted with distilled water to achieve 1.0 cm^3 total volume. No further precipitation of the solution was noticed.

The reaction of Fe^{III}EDTA with hydrogen peroxide was studied by adding H_2O_2 (0.05 cm^3, 30%) to the solution. The concentration of H_2O_2 in the final solution was in large excess. The Mössbauer study of the reaction of iron(III)-EDTA with H_2O_2 was conducted in alkaline medium. Addition of H_2O_2 to the Fe^{III}-EDTA system at pH~10.4 gave a purple colouration to the solution, which can be attributed to the formation of an $[Fe^{III}(EDTA)(\eta^2\text{-}O_2)]^{3-}$ species (F).[11,12,14] The Mössbauer spectrum of the purple species showed a sextet (Fig. 7.1b)), indicating that the dimer species (B) was converted to a monomer (F) by hydrogen peroxide[13]. This is due to the side-on coordination of the peroxide ion, which saturates the coordination environment of the Fe centre and steric hindrance does not allow the coordination of another Fe. The observed large isomer shift (Table 7.1) is consistent with an increased coordination number of the iron centres. Brausam and van Eldik[18] suggested that iron is 7-coordinate in this complex which means dechelation of one carboxylate arm (pentadentate EDTA), although they cited theoretical calculations in the literature that were in favour of six-fold coordination[14]. XAS measurements on peroxoiron(III) complexes with pentadentate N-donor ligands by Koehntop *et al.*[27] were not always conclusive either regarding the exact coordination number of iron (side-on or end-on bonding of O_2^{2-}). Our Mössbauer data support minimum 7-fold coordination on the basis of the large isomer shift. Horner *et al.*[12] who

[13] For explanation see Chapter 5.

prepared $[Fe^{III}(EDTA)(\eta^2\text{-}O_2)]^{3-}$ in a very pure form in solution, also found a large isomer shift but these authors did not discuss possible implications with the coordination number.

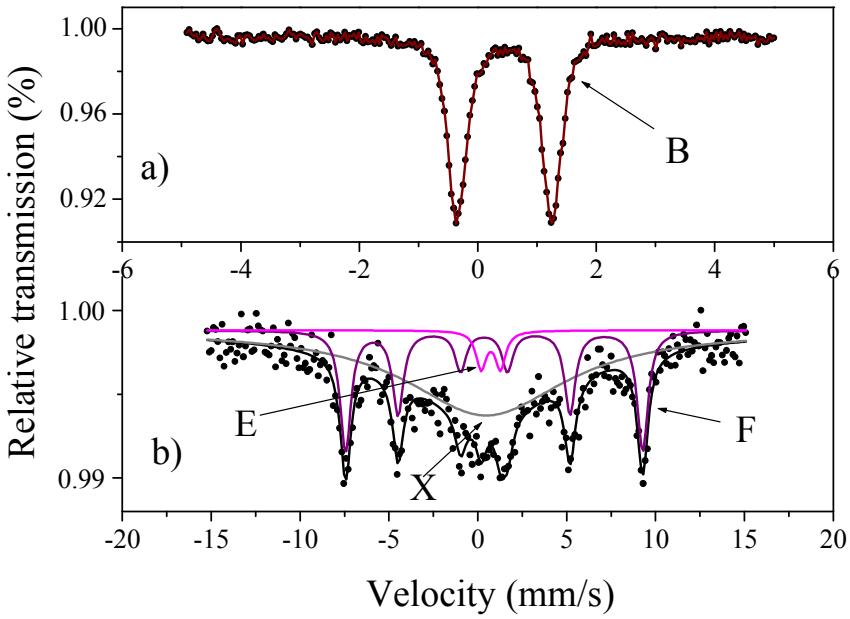

Figure 7.1 The Mössbauer spectrum of the frozen solution of the Fe^{III}-EDTA system at pH~10.4 (a)) and the spectrum after addition of excess H_2O_2 (b)). Spectra recorded at 80 K.

Beside species F, two other species, E and X, were also observed (Fig. 7.1b)). A small doublet (species E) appeared with the sextet (Species F), with isomer shift δ=0.46 mm/s (see Fig. 7.1b)). This species was found to be formed from the species represented by the sextet (See Scheme 7.2). Doublet E had no magnetic splitting; therefore, it was assigned to a dimer species (Table 7.1). It is worth mentioning that peroxo diiron(III) coordination compounds with other ligands have very similar Mössbauer parameters[19]. Species X showed up with extreme line broadening, which is due to relaxation.

In a separate experiment, the further reactions of the purple complex were studied. In this experimental set-up, Fe^{III}EDTA and H_2O_2 solutions were mixed in darkness[14] and the Mössbauer spectrum of the frozen purple solution was recorded (Fig. 7.2a)). The formation of species F, E, and X occurred, similarly to the observations made in the previous experiment (Fig. 7.1b)). The frozen solution was then allowed to melt for 5 minutes at room temperature in the dark and a Mössbauer spectrum was recorded again

[14] In order to avoid the eventual effect of the photodegradation of the ferric ethylenediaminetetraacetate, experiments were carried out in the light of a low energy IR lamp (red).

after freezing the solution (Fig. 7.2b)). The fraction of doublet E slightly increased at the expense of X. Species X can thus be an intermediate in the conversion of species F to E. After further aging at room temperature (RT) for 10 min under daylight conditions, an abrupt change in Mössbauer spectra was observed. Species F, E, and X all disappeared, and a new species having a doublet with isomer shift δ=0.57 mm/s (D) formed in addition to the already known μ-oxo-bridged species, [(EDTA)Fe^{III}–O–Fe^{III}(EDTA)]$^{4-}$ (B) (Fig. 7.2c)).

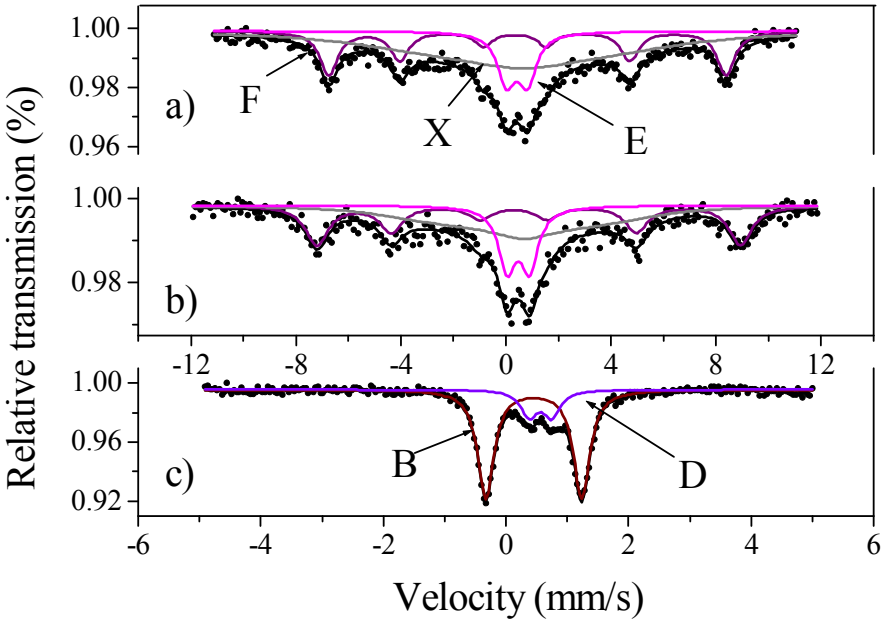

Figure 7.2 Mössbauer spectra of the Fe^{III}-EDTA-H_2O_2 system at pH~10.4. a): initial state, b): after 5 min aging at room temperature (RT) in dark, c): after further 10 min aging at RT in daylight. Spectra were recorded at 80 K.

The formation of species B from species D was confirmed by conducting the reaction between Fe^{III}EDTA and H_2O_2 at room temperature in daylight, where formation and decay of the purple species could be fast. The Mössbauer spectra of the reaction are given in Fig. 7.3. Species X and E were not observed. This further suggests intermediate nature of these species. Initial spectra showed traces of the sextet of species F together with doublets of species B and D (Fig. 7.3a)). Species D quickly decayed to the original Fe^{III}EDTA species, B (Fig. 7.3bc)).

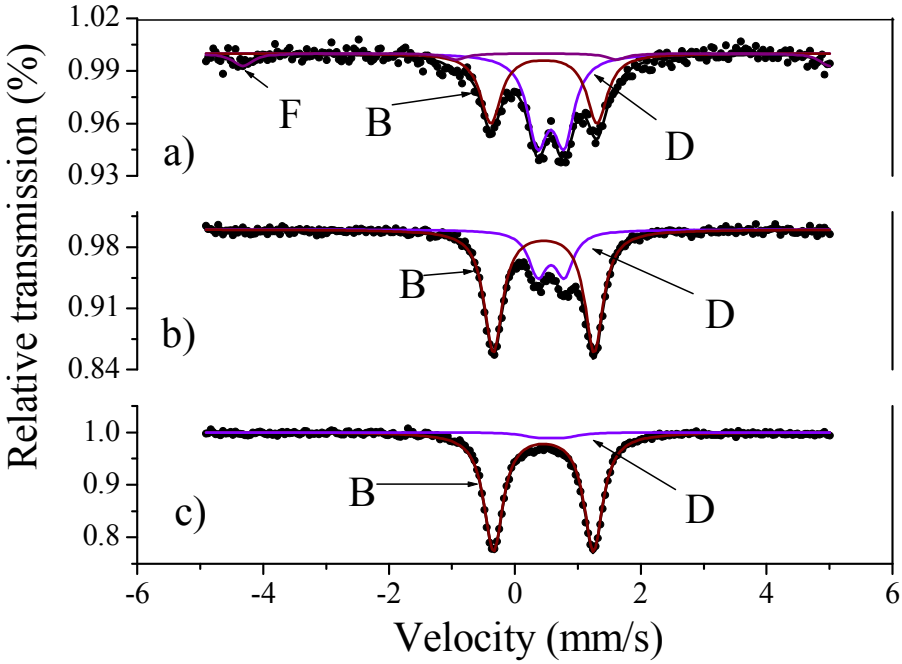

Figure 7.3 Evolution of Fe-containing species in the Fe^{III}-EDTA-H_2O_2 system at pH~10.4 in daylight: initial state (a)), after 4 min aging at RT (b)), and after 10 min aging at RT (c)).

To further understand the conversions of species in the purple solution, another study was conducted at low temperature in darkness in order to slow down the reactions. The Fe^{III}EDTA and H_2O_2 were mixed in an ice bath (~0 ^oC) and the spectra were recorded after aging the mixture in consecutive 3 minute steps (Fig. 7.4). All aging were carried out at ~0 ^oC. The slow evolution of the various species from B to F and X to E at low temperature was observed. The formation and decomposition of species X is pronounced (Fig. 7.4cd)). Since species X shows up together with F and/or E, it is confirmed that it should represent a very short lived transitional state between F and E. (It should be noted here that in spectra c) and d) of Fig. 7.4 and b) of Fig. 7.1, the assignment of the very small doublets (3–4%) to species E is rather tentative due to its relatively small amount; this doublet fully develops only in spectra Fig. 7.4e) and Figs. 7.2a) and b.)

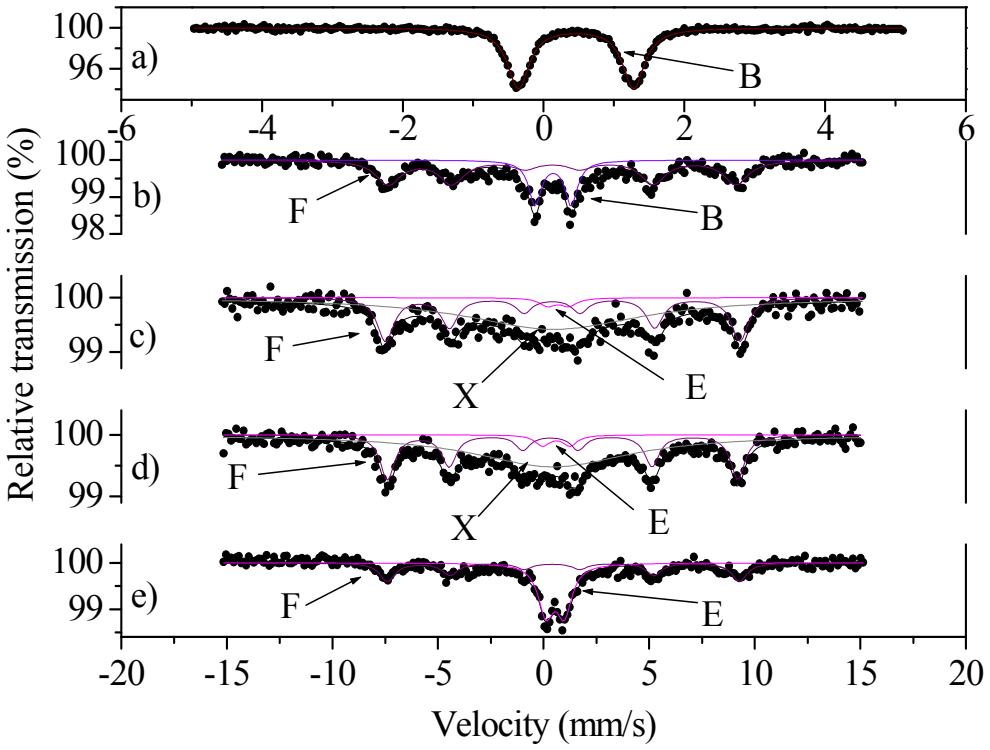

Figure 7.4 Evolution of Fe-containing species in the Fe^{III}-EDTA-H_2O_2 system at pH~10.4 (initial value before adding H_2O_2) at around 0 ^oC. a): before addition of H_2O_2, b): immediately after addition of H_2O_2, c): after 3 min aging at 0 ^oC, d): after additional 3 min aging at 0 ^oC, e): after second additional 3 min aging at 0 ^oC.

The formation and the decomposition of species F may be summarised as shown in Scheme 7.1 and Scheme 7.2, respectively.

Scheme 7.1.

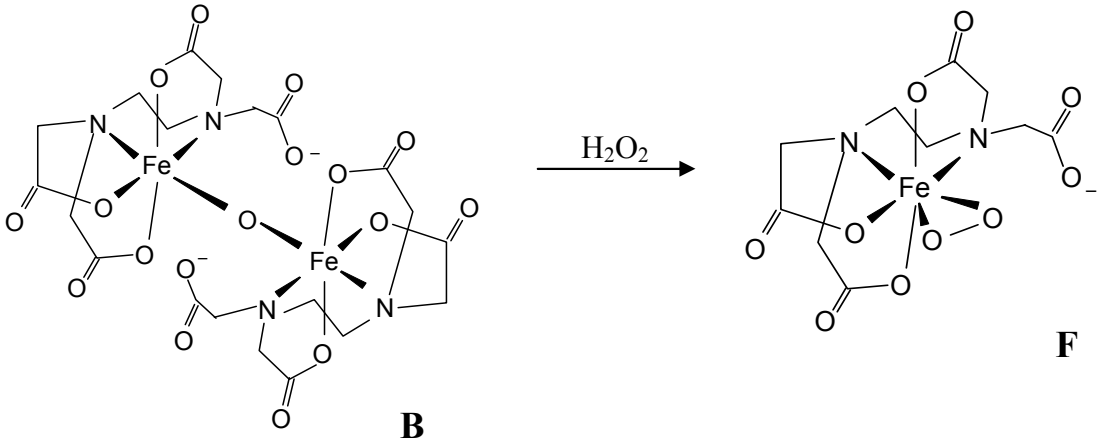

In Scheme 7.1, the dimer species B is converted to monomeric species F with the addition of hydrogen peroxide.

Only the much more stable dimer (E) clearly showed up in the Mössbauer spectra. The isomer shift of species E is practically the same as that of species B and formally corresponds to a 6-fold coordinated monomeric species. This indicates that the dechelation of one carboxylate arm at each iron centre occurs here, similar to the species B. At the same time, since the peroxo bridge allows larger separation of the Fe^{III}EDTA moieties as compared to the case of a regular oxo bridge, the repulsion between the two pentadentate EDTA, and, inherently, their spatial distortion is smaller, which results in only half of the quadrupole splitting found for species B. It is noteworthy that in this picture, the isomer shift does not differ for a μ-oxo and a μ-peroxo species. Probably the difference in the donicity of the oxo and peroxo oxygens (as a sixth ligand around the Fe^{3+} centre) is not substantial.

The driving force for the transformation of monomeric species F to dimeric species E can be the loss of H_2O_2 due to its decomposition. The decomposition of H_2O_2 results in decreasing pH since H_2O_2 is more acidic then H_2O. Therefore further decomposition of species E may occur through the addition of an OH^- ion, forming a double bridged species D. Double (also triple) bridged binuclear complexes of Fe^{III} with non-equivalent bridging ligands are known *i.e.*, (μ-oxo)(μ-carboxylato)-diiron(III) type compounds[28]. The isomer shift of species D is significantly higher than that of species E, which is in agreement with the increased coordination number (7). The decrease of the quadrupole splitting cannot be fully understood in this simple picture.

From this stage, decomposition (further loss) of H_2O_2 and the concomitant raise in pH logically drives us back to species B.

Scheme 7.2.

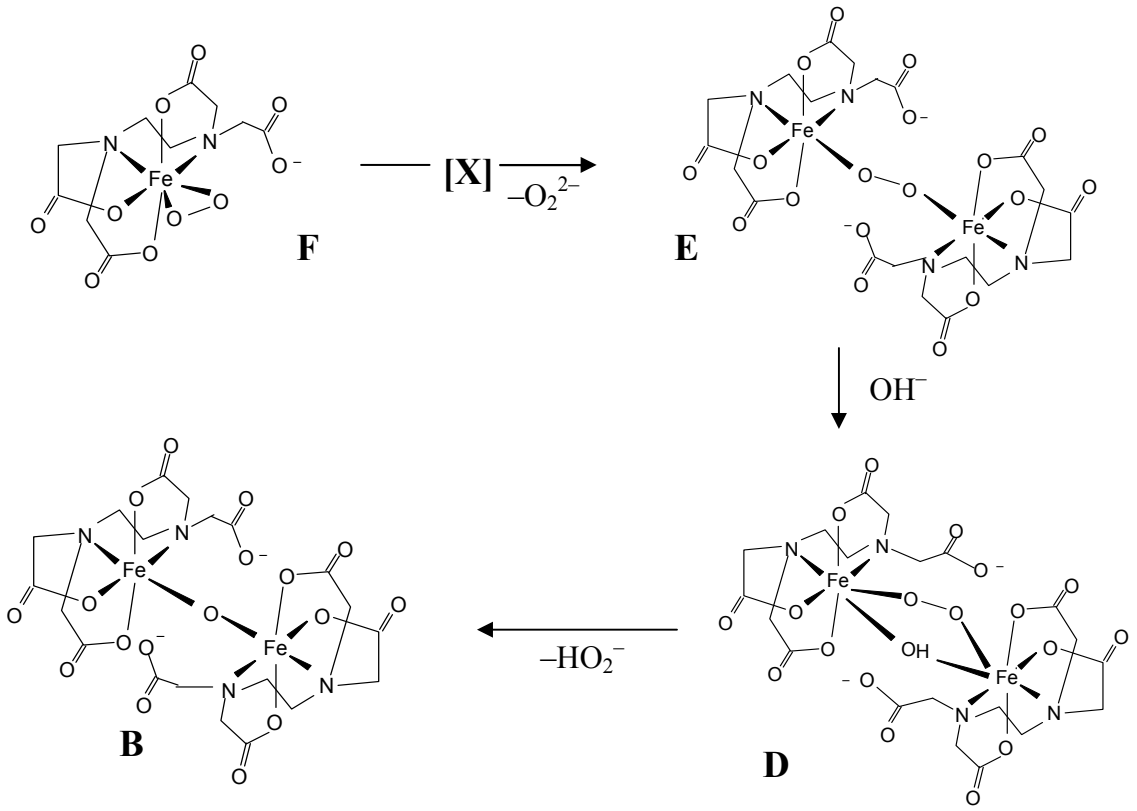

It has to be mentioned here that the proposed structures for species E and D, should be very logical, but may not be the unique possibilty. For example, partial protonation of the peroxo bridge may occur which would result in a species $[(EDTA)Fe^{III}–HOO–Fe^{III}(EDTA)]^{2-}$. However, such a species contains non-equivalent iron centres, and thus two doublets were always expected to be in pair in the Mössbauer spectrum. This is not observed. It is assumed that the position of the proton is not averaged out between the two oxygens in the Mössbauer time scale, and that the Mössbauer parameters of the two non-equivalent irons would be significantly different. Thus, since species D is a peroxo-type dimeric species, the increase of the isomer shift upon going from species E to D can be considered as a strong argument to support the formation of the double bridge.

The photodegradation of the ferric-ethylenediaminetetraacetate, discussed in detail in Chapter 6, affects the reaction as well. To study this effect, the Fe^{III}EDTA solution was allowed to be photodegraded and then hydrogen peroxide was added to it. The solution took the well known purple colouration immediately after the mixing of the reactants and this colour remained for more than 30 min, without cooling the reaction mixture. The pH of the reaction mixture was about 10.4. The spectra recorded immediately after

the mixing of the reactants and half an hour later are displayed in Fig. 7.5ab, respectively.

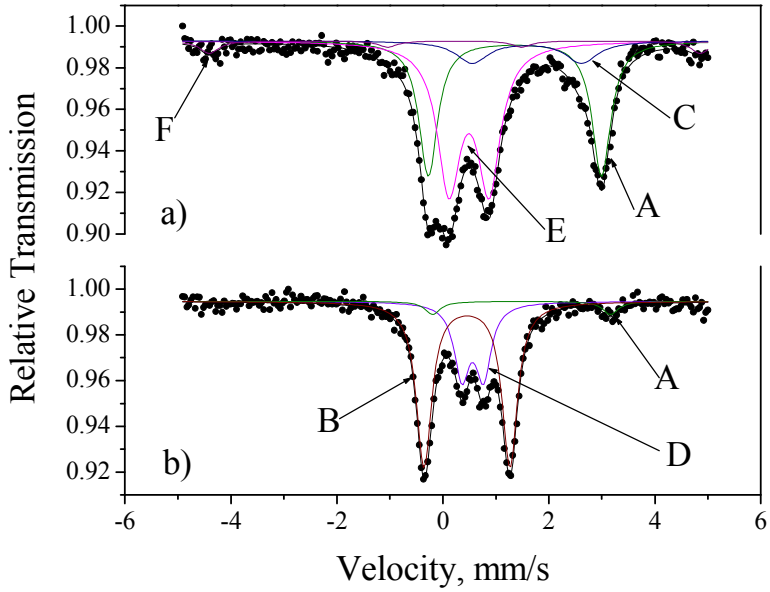

Figure 7.5 Evolution of Fe-containing species in the $[Fe(H_2O)_6]^{2+}$-containing Fe^{III}-EDTA-H_2O_2 system at pH~10.4 (initial value before adding H_2O_2) a): immediately after the addition of H_2O_2, b): after 30 min aging at room temperature.

It is remarkable that only a very little amount of monomeric species was produced in this reaction mixture. It seems that the ferrous ions inhibit in certain way the formation of the $[(EDTA)Fe(\eta^2\text{-}O_2)]^{3-}$ complex. This can be explained in the following way: it is the $[Fe(H_2O)_6]^{2+}$ (species A) ion that reacts primarily with the hydrogen peroxide, the reaction pathway can be the following: Species A reacts with the EDTA present in the solution, forming a complex. This metastable species is very likely to be oxidised, and then forms an intermediate adduct (species C) with the peroxo ion, where another iron centre gets oxidised by the peroxo moiety of the adduct which can be ejected from the ligand sphere of the iron, leaving a bridging oxygen behind and thus, forming the μ-oxo dimer (Eqs 7.1.1-7.1.6).[15]

$$Fe^{2+}(H_2O)_6 + EDTA \xrightarrow{-6H_2O} \{[Fe^{II}EDTA]^{2-}\} \quad (7.1.1)$$

$$\{[Fe^{II}EDTA]^{2-}\} \xrightarrow{+\,H_2O_2} \{H_2[O_2Fe^{II}EDTA]^{2-}\} \quad (7.1.2)$$

$$\{H_2[O_2Fe^{II}EDTA]^{2-}\} \xrightarrow{ET} \{H_2[O_2Fe^{III}EDTA]^{2-}\} \quad (7.1.3)$$

$$\{H_2[O_2Fe^{III}EDTA]^{2-}\} \xrightarrow{\{[Fe^{II}EDTA]^{2-}\}} \{H_2[EDTAFe^{II}(O_2)Fe^{III}EDTA]^{4-}\} \quad (7.1.4)$$

[15] Possible additional protolytic reactions can take place in the system.

$$\{H_2[EDTAFe^{II}(O_2)Fe^{III}EDTA]^{4-}\} \xrightarrow{ET} \{H_2[EDTAFe^{III}(O_2)Fe^{III}EDTA]^{4-}\} \quad (7.1.5)$$

$$\{H_2[EDTAFe^{III}(O_2)Fe^{III}EDTA]^{4-}\} \xrightarrow{-H_2O} [EDTAFe^{III}–O–Fe^{III}EDTA]^{4-} \quad (7.1.6)$$

It is worth mentioning that Horner *et al.* [12] could obtain species F in a very pure form, in fact, the only subspectrum present in their spectra recorded is that of species F. Since their experiments were carried out at T=4.2 K and in an applied external magnetic field, another explanation of the appearance of species X is possible. X might not be an independent species but the same complex as F and due to the non-uniform distribution intermolecular distances in a random solution, in a situation where the individual species are closer to each other. This proximity of species results in the acceleration of the paramagnetic spin-spin relaxation, consequently in a line broadening and partial collapse of the sextet in the Mössbauer spectrum (see Chapter 4).

Table 7.1. Mössbauer parameters and their errors of various $Fe^{III}EDTA$ species observed at 80 K; δ: isomer shift, Δ: quadrupole splitting, eQV_{zz}: quadrupole shift (in case of magnetic splitting), η: asymmetry parameter; B: internal magnetic field.

Species	Description	pH	Coord. number	Oxid. number	δ (mm/s)	Δ (mm/s)		B(T)
A	$[Fe^{II}(H_2O)_6]^{2+}$	~10.4	6	2	1.42(6)	3.31(4)		0
B	[(EDTA)Fe–O–Fe(EDTA)]$^{4-}$	~10.4	6	3	0.42(5)	1.64(8)		0
C	$[Fe^{II}(EDTA)O_2]^{4-}$	~10.4	6	2	1.61(3)	2.11(5)		0
D	[(EDTA)Fe–(OO)(OH)–]	~10.4	7	3	0.54(4)	0.49(8)		0
E	[(EDTA)Fe–(OO)–Fe(EDTA)]$^{4-}$	~10.4	6	3	0.50(5)	0.80(6)		0
F	[(EDTA)Fe(η^2-O_2)]$^{3-}$	~10.4	7	3	0.63(9)	+0.53(9)*		51.4(8)
X	[(EDTA)Fe–(OO)···Fe(EDTA)]$^{4-}$	~10.4	-	3	0.6*	eQV_{zz}* (mm/s)	η*	29(3)
						–0.33	*–3*	

*Parameters fixed for fit.

7.2.2 Reaction of iron(III)-CDTA with H_2O_2[16]

In order to study the reaction of ferric cyclohexanediaminetetraacetate (Fe^{III}CDTA) with H_2O_2, a 0.2 mmol/dm^3 $^{57}Fe^{III}$CDTA at pH=5 was prepared. To adjust the pH of the stock solution to a suitable value where the reaction takes place, the pH of this stock solution was raised by addition of cc NaOH.

At pH=11.6, addition of H_2O_2 resulted in intense purple colouration that immediately started fading but the sample could be quenched to liquid nitrogen temperature before it turned to yellow. The spectrum obtained is displayed in Fig. 7.6a. Repeating this experiment, the system was cooled in an ice bath before adding H_2O_2. The colouration was more intense and more stable and the resultant Mössbauer spectrum is shown in Fig. 7.6b. This latter spectrum is strikingly similar to the one obtained in the analogous experiment with EDTA[13], see Figures 7.1, 7.2 and 7.4. The isomer shift of the sextet (~0.61 mm/s) is the highest of all species found in the system and the quadrupole shift is very characteristically high positive (~+0.8 mm/s). Sextet I can be logically assigned to the heptacoordinate $[Fe^{III}(CDTA)(\eta^2\text{-}O_2)]^{4-}$ where CDTA is pentadentate with one carboxylate arm detached and O_2^{2-} is side-on bound, by analogy to the well known EDTA case, discussed earlier. Doublet J, with parameters δ=0.48 mm/s and Δ=0.79 mm/s can be tentatively assigned to a peroxo bridged species, $[\{Fe(EDTA\}_2(\mu\text{-}O_2)]^{4-}$, analogously to the case of the EDTA system, although it should be mentioned that unlike in the EDTA experiments, this species was not observed as a major component in any other spectra [13].

[16] This work has been carried out in collaboration with Ariane Brausam and Rudi van Eldik and the preparation of reaction mixtures and the recording of spectra were not carried out by me; I evaluated the spectra and interpreted them.

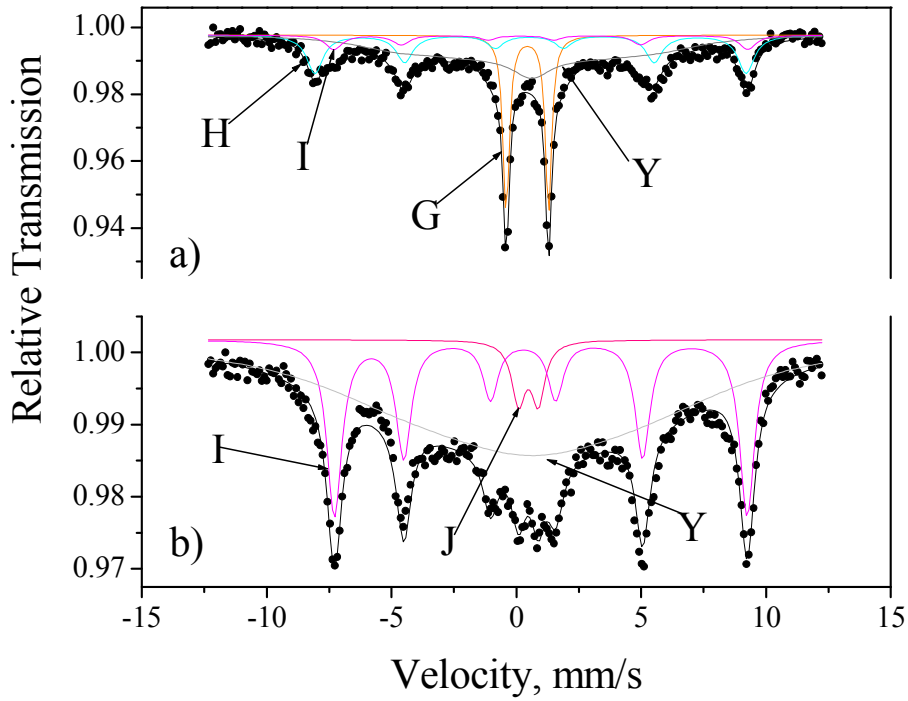

Figure 7.6 Frozen solution Mössbauer spectra of the Fe^{III}-CDTA system at pH=11.4-11.6 after the addition of H_2O_2. Spectra were recorded at 80 K.

The spectrum shown in Fig. 7.6a exhibits only a relatively weak relaxation background with two sextets and one doublet. The two sextets, I and H could be assigned to $[Fe^{III}(CDTA)(\eta^2\text{-}O_2)]^{4-}$ and $[Fe^{III}(CDTA)OH]^{2-}$, respectively, in agreement with the observed faint purple colour when the sample was quenched, while doublet G represents the dimer $[\{Fe(CDTA)\}_2(\mu\text{-}O)]^{4-}$, final product of the reaction, as in the case of EDTA.

The spectra shown in Fig. 7.7 were recorded on the same sample the Mössbauer spectrum of which is shown in Fig. 7.6b) However, for the spectrum displayed in Fig. 7.7a) the rapid freezing was carried out 3 minutes after the addition of H_2O_2, while for spectrum displayed in Fig. 7.7b) the sample was quenched several minutes later, when the yellow colour of the solution returned completely. The pH of this solution was measured again and found to be 10.4, *i.e.* one unit lower than before the addition of H_2O_2.

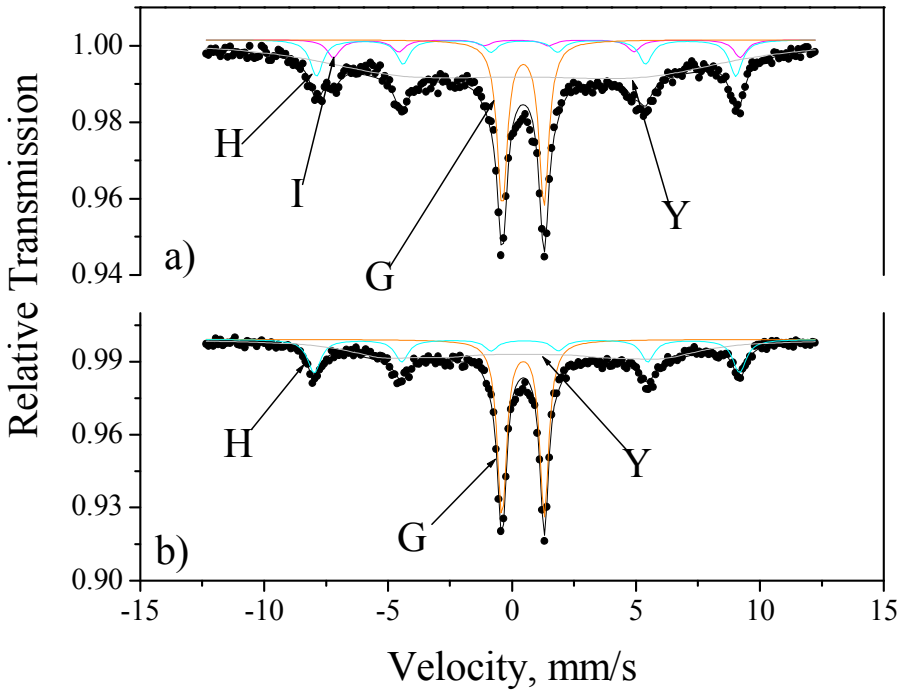

Figure 7.7 Frozen solution Mössbauer spectra of the Fe^{III}-CDTA system at pH=11.4-11.6 displayed in Fig. 7.6b); a) 3 min after the addition of H_2O_2; b) several minutes later.

In spectrum shown in Fig. 7.7a), the simultaneous presence of species I, H, and G is revealed, while in the spectrum displayed in Figure 7.7b), sextet I is absent. These observations are in agreement with the gradual decomposition of the purple peroxo species. After decomposition of the H_2O_2 (or a part of it), the system returned to its initial state, with somewhat lower pH, characterised by the equilibrium $[Fe^{III}(CDTA)OH]^{2-} \rightleftarrows [\{Fe(CDTA)\}_2(\mu\text{-}O)]^{4-}$.

Table 7.2. Mössbauer parameters and their errors of various Fe^{III}CDTA species observed at 80 K; δ: isomer shift, Δ: quadrupole splitting, eQV_{zz}: quadrupole shift (in case of magnetic splitting), η: asymmetry parameter, B: internal magnetic field.

Species	Description	pH	Coord. number	δ (mm/s)	Δ (mm/s)		B(T)
G	[(CDTA)Fe–O–Fe(CDTA)]$^{4-}$	11.4-11.6	6	0.44-0.45	1.68-1.70		0
H	[Fe(CDTA)OH]$^{2-}$	11.4-11.6	6	0.54-0.56	0.04-0.08		52.4-
I	[(CDTA)Fe(η^2-O_2)]$^{3-}$	11.4-11.6	7	0.59-0.63	+(0.71-0.92)		50.9-
J	[(CDTA)Fe–(OO)–Fe(CDTA)]$^{4-}$	11.4-11.6	6	0.48	0.79		0
Y	[(CDTA)Fe–(OO)···Fe(CDTA)]$^{4-}$	11.4-11.6	6	0.47-0.54	eQV_{zz} (mm/s)	η	34.5-43
					-0.27	*-3*	

7.2.3 Reaction of iron(III)-EDDA with H_2O_2

Another analogous chelating agent is the ethylenediaminediacetic acid (EDDA), which can form a complex only as a tetradentate ligand, where the two nitrogen atoms and two oxygen atoms from the carboxylate arms serve as coordinating agents. To study the reaction taking place between the ferric ethylenediaminediacetate and hydrogen peroxide, a stock solution of Fe^{III}EDDA was prepared at pH=10.1. Its concentration is lower than 0.05 mol/dm^3 due to the precipitation occurred when raising the pH, which is not surprising, since the EDDA cannot stabilise the complex in alkaline medium as much as the other chelating agents, EDTA and CDTA do. The alkaline solution was mixed with hydrogen peroxide but its colour changed only slightly and did not turn to purple as was expected after the experiments carried out using EDTA or CDTA. The solution was frozen immediately after the mixing of the reactants and the resulted spectrum is displayed in Figure 7.8a). The spectrum displays only one doublet, doublet K, which is different from the oxo-bridged dimer (discussed in Chapter 5). This spectrum component has a relatively high isomer shift (see in Table 7.3) and a low quadrupole splitting, which is probably due to a sixfold coordination around the ferric ion where four coordination sites are taken by EDDA and an oxide ion remaining from

the original dimer species and a peroxo ion complete the ligand sphere, donating a high electron density (*i.e.* an oxo-peroxo double bridged binuclear complex).

The reaction mixture was then melted and left relax for three days at room temperature, when another Mössbauer spectrum was recorded, which is shown in Figure 7.8b). This second spectrum also contains one quadrupole doublet only, species L, but, surprisingly, this doublet does not refer to that, describing the original μ-oxo dimer (see in Table 5.2.3.1), which means that the reaction mixture did not relax back to its initial state after the addition of hydrogen peroxide as it did in the previous cases.

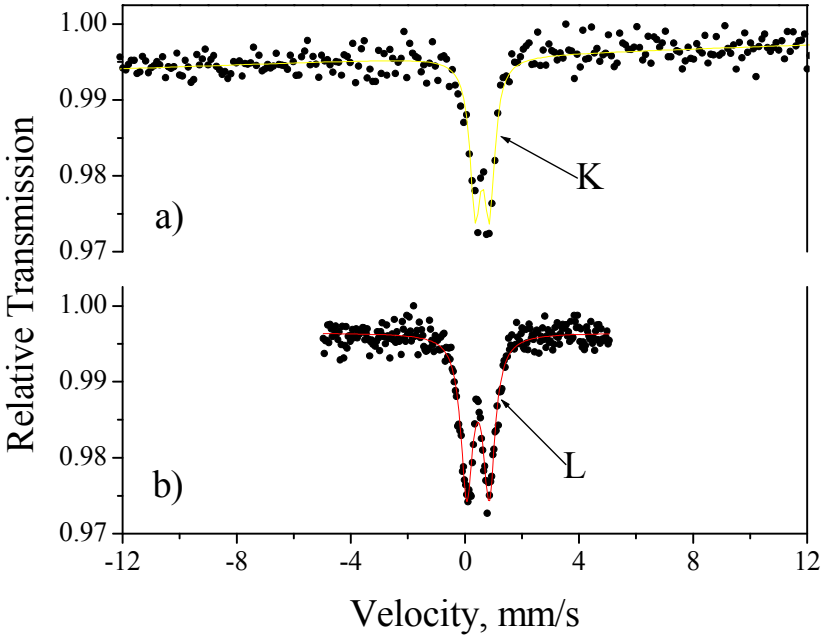

Figure 7.7 Frozen solution Mössbauer spectra of the Fe^{III}-EDDA system at pH=10.1 a) immediately after the addition of H_2O_2; b) three days later. Spectra were recorded at 80 K.

Table 7.3. Mössbauer parameters and their errors of various Fe^{III}EDDA species observed at pH=10.1 and at 80 K; δ: isomer shift, Δ: quadrupole splitting.

Species	δ (mm/s)	Δ (mm/s)
K	0.62(1)	0.49(2)
L	0.46(1)	0.79(1)

7.3 Conclusions

The chelating agents used for studying the reactions of different ferric aminocarboxylate complexes with hydrogen peroxide were EDTA, CDTA and EDDA. The main difference between the third and the first two is that while the EDTA and CDTA chelating agents are able to be bound to the ligand sphere of a ferric ion as a hexadentate ligand, the EDDA has only four possible atoms to bond.

Amongst these reactions most studied and understood is the one which takes place between the iron(III)-EDTA and the hydrogen peroxide. This reaction results in a purple colouration of the originally yellow solution. Two intermediate species have been discovered in the course of the reaction taking place between the $Fe^{III}EDTA$ and H_2O_2 and possible structures have been proposed. In the present work, a possible reaction pathway for the reaction of $Fe^{III}EDTA$ with H_2O_2 has also been proposed. The effect of the photodegradation of iron(III)-EDTA on its reaction with hydrogen peroxide was also studied and it was established that when ferrous ions are present in large amount in the solution they will be the primary reaction partner for the hydrogen peroxide and due to the change in the reaction pathway, mainly dimeric species will be produced in the reaction, which is a remarkable difference from the case where only ferric ions are present in the original reaction mixture.

After the complete decomposition of the species produced in the course of the reaction, the original state returned and the total amount of iron was in the oxidation state of +3.

Very similar observations were made when CDTA was used as a chelating agent. This reaction is less known and studied in the literature, although it results in almost the same reaction products and follows the same reaction pathway. However, this reaction does not result in as many intermediates detectable by Mössbauer spectroscopy as the one with EDTA.

As could be seen, the reaction of $Fe^{III}EDTA$ and $Fe^{III}CDTA$ with H_2O_2 are rather similar, unlike in the case of EDDA where no purple colouration appears in the course of the reaction and the resultant spectrum contains only one quadrupole doublet.

Another striking difference between this reaction and the two others is that the original state does not return after all reactions are completed.

It seems to be that the presence of the μ-oxo dimer of the ferric complex with a Fe-O-Fe bite angle being close to 180° is necessary for the formation of the $[(L)Fe(\eta^2\text{-}O_2)]^{1-x}$ complex, where L is the chelating agent and x is its electric charge.

7.4 References

[1] M. Costas, M. P. Mehn, M. P. Jehnsen, L. Que, Jr. *Chem. Rev.* **2004**, *104*, 939–986.

[2] E. I. Solomon, T. C. Brunold, M. I. Davis, J. N. Kemsley, S.-K. Lee, N. Lehnert, F. Neese, A. J. Skulan, Y.-S. Yang, J. Zhou *Chem. Rev.* **2000**, *100*, 235–350.

[3] C. Walling, *Acc. Chem. Res.* **1975**, *8*, 125–131.

[4] J. Bond, C. W. Brown, G. S. Rushton *J. Polymer Sci.* **1964**, *2*, 1015–1017.

[5] T. E. Graedel, M. L. Mandich, C. J. Weschler *J. Geophys. Res.* **1986**, *91(D4)*, 5205 5221.

[6] D. L. Sedlak, J. Hoigné *Environ. Sci. Technol.* **1994**, *28*, 1898–1906.

[7] J. D. de Laat, H. Gallard *Environ. Sci. Technol.* **1999**, *33*, 2726–2732.

[8] K. L. Cheng, P. F. Lott *Anal. Chem.* **1956,** *28*, 462-465.

[9] C. Walling, M. Kurz, H. J. Schugar *Inorg. Chem.* **1970,** *9*, 931-937.

[10] R. E. Hester, E. M. Nour *J. Raman Spectrosc.* **1981,** *11*, 49-58.

[11] S. Ahmad, J. D. McCallum, A. K. Shiemke, E. H. Appelman, T. M. Loehr, J. Sanders-Loehr *Inorg. Chem.* **1988,** *27*, 2230-2233.

[12] O. Horner, C. Jeandey, J.-L. Oddou, P. Bonville, J.-M. Latour *Eur. J. Inorg. Chem.* **2002**, *5*, 1186-1189.

[13] V. K. Sharma, P. Á. Szilágyi, Z. Homonnay, E. Kuzmann, A. Vértes *Eur. J. Inorg. Chem.* **2005**, *21*, 4393-4400.

[14] F. Neese, E. I. Solomon *J. Am. Chem. Soc.* **1998,** *120*, 12829-12848.

[15] V. K. Sharma, F. J. Millero, Z. Homonnay *Inorg. Chim. Acta* **2004,** *357*, 3583-3587.

[16] C. Bull, G. J. McClune, J. A. Fee *J. Am. Chem. Soc.* **1983,** *105)*, 5290-5300.

[17] K. C. Francis, D. Cummins, J. Oakes *J. Chem. Soc., Dalton Trans.* **1985**, *3*, 493 501.

[18] A. Brausam, R. van Eldik *Inorg. Chem.* **2004**, *43*, 5351–5359.

[19] E. Y. Tshuva, S. J. Lippard *Chem. Rev.* **2004**, *104*, 987–1012.

[20] D. M. Kurtz, Jr. *J. Biol. Inorg. Chem*. **1997**, *2*, 159–167.

[21] D. Lee, S. J. Lippard In *Comprehensive Coordination Chemistry II*: *From Biology to Nanotechnology*, Elsevier Ltd.: *Oxford*, **2004**, *8*, 309.

[22] M. Fontecave, S. Ménage, C. Duboc-Toia *Coord. Chem. Rev.* **1998**, *178–180*, 1555–1572.

[23] R. H. Holm, P. Kennepohl, E. I. Solomon *Chem. Rev.* **1996**, *96*, 2239–2314.

[24] J. B. Vincet, G. L. Oliver-Lilley, B. A. Averill *Chem. Rev.* **1990**, *90*, 1447–1467.

[25] S. Inoue, Sh. Kawanashi, *Cancer Research* **1987**, *47*, 6522-6527.

[26] J. D. Rush, W. H. Koppenol *J. Am. Chem. Soc.* **1988**, *110*, 4957-4963.

[27] K. D. Koehntop, J.-U. Rohde, M. Costas, L. Que Jr. *J. Chem. Soc. Dalton Trans.* **2004**, 3191-3198.

[28] D. M. Kurtz, Jr. *Chem. Rev.* **1990**, *90*, 585–606.

8 Solid State Study of the Fe^{III}EDTA Complex: Study of the Relaxation Properties of the Solid Fe^{III}EDTA Study of the Thermal Stability of the Fe^{III}EDTA Complex in its Monomeric Form

8.1 Study of the Relaxation Properties of the Solid Fe^{III}EDTA

8.1.1 Introduction

Sodium monoaqua-ethylenediaminetatraacetato ferrate(III) dihydrate, $NaFeEDTA(H_2O)\cdot 2H_2O$, is a relatively rare example of heptacoordinate Fe^{III} complexes which does not keep its coordination number in solution. While in solid state all four carboxylate arms, the two amine nitrogens as well as one water molecule are coordinated to the Fe^{3+} centre, after dissolution in aqueous medium one carboxylate arm can get detached and, for a certain amount of the complex, a six coordinate ligand structure is stabilised even at higher pH (see in Chapter 5). It is therefore remarkable that in the solid state a rather unstable heptacoordinated structure is found.

Concerning the Mössbauer spectrum the high value of the isomer shift of iron in the solid compound is in agreement with the high coordination number. But the shape of the spectrum is rather surprising. The asymmetric Mössbauer doublet (assumed!) of solid $NaFeEDTA(H_2O)\cdot 2H_2O$ was first reported by Spijkerman *et al*. in 1967.[1] The asymmetry of the quadrupole doublet has been explained by a magnetic relaxation effect. However, whatever type of relaxation may be assumed, it is very hard to explain the very little temperature dependence of the spectral envelope (doublet asymmetry): a well developed magnetic sextet has never been observed even at 4.2 K, while the relaxation distortion of the doublet is present already at room temperature.[1-3] Furthermore, the doublet asymmetry shows up as very substantial *intensity* asymmetry (up to 1.61 for the tetramethylammonium salt[1]), which is in contradiction with the relaxation origin. For the potassium salt, this asymmetry (A1/A2) reaches 3.54 at 4.2 K,[2] that is, lowering of the temperature does not point at all to the direction of a well-resolved magnetic sextet.

This relaxation phenomenon is rather rare but very interesting at the same time and its study may serve for the better understanding of relaxing systems.

8.1.2 Results and Discussion

In order to check arguments on the relaxation origin of the distortion of the Mössbauer doublet of solid NaFeEDTA(H_2O)·$2H_2O$, it is important to recall that the Mössbauer spectrum of the aqueous solution of the Fe^{III}EDTA complex and other iron(III) salts show typical magnetic relaxation in the concentration range of 0.01 to 0.5 M (in frozen solutions).[4] In these cases, the origin of magnetic relaxation is considered as mainly of spin-spin type. As such, temperature dependence is not expected and only the average distance between the Fe^{III} species in the solid system determines the conditions for relaxation. Indeed, in some cases where the relative concentration of some type of FeEDTA species is low, a magnetic sextet can be observed, while at higher concentration, a doublet like spectrum can be seen.

We have measured the Mössbauer spectrum of the concentrated solution of NaFeEDTA(H_2O)·$2H_2O$ in frozen state (c=1 mol/dm^3) and found a very similar line shape to that observed for the solid material at room temperature (Fig. 8.1.1). The doublet is somewhat broadened, instead of being closer to a well-resolved thin pair of lines. Since the average distance between the Fe^{III} species in this solution is much less than in a 0.01–0.05 molar one, it would be reasonable to expect a symmetrical doublet due to fast electronic relaxation, or, if not yet here, at least in the solid state where this distance is the least, roughly 0.9 nm. (In a 1 molar solution, it is about 1.2 nm, in the solid 0.8888 nm). Note that the Mössbauer spectrum of the μ-oxo-dimer O(FeEDTA)$_2$ is a symmetrical quadrupole doublet with narrow lines both in a solution and in the solid state while the Fe-Fe distance is estimated to d=0.3533(1) nm.[5]

The solid samples were all thoroughly grinded in order to avoid eventual texture effects. In addition, several Mössbauer runs have been done on the powder sample in different angles with the γ-ray propagation direction which resulted in the same spectrum, which points out that the spectral asymmetry is not due to texture effect.

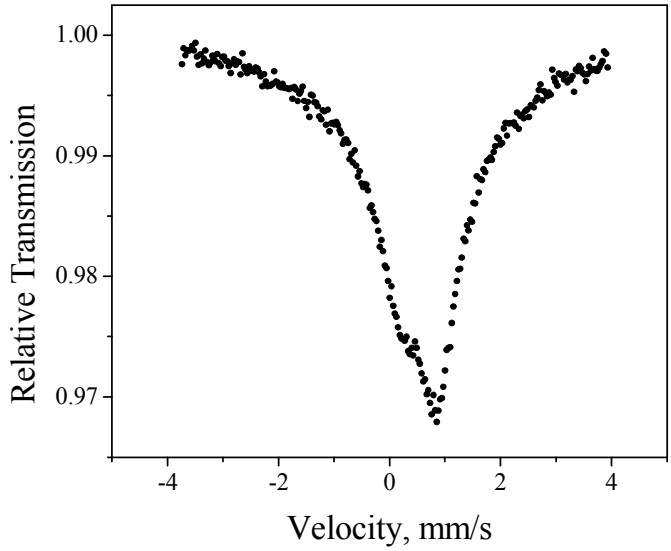

Figure 8.1.1 Mössbauer spectrum of aqueous solution of NaFeEDTA(H_2O)·2H_2O, *c*=1 mol/dm^3, in frozen state at ~90 K.

To check if the relaxation might be of spin-lattice type, we have recorded the Mössbauer spectra of our solid NaFeEDTA(H_2O)·2H_2O sample at various temperatures. As can be seen in Fig. 8.1.2, the overall line shape does not change down to 12 K (some broadening is observed, however, at 12 K), clearly visible change occurs only between 12 K and 5 K.

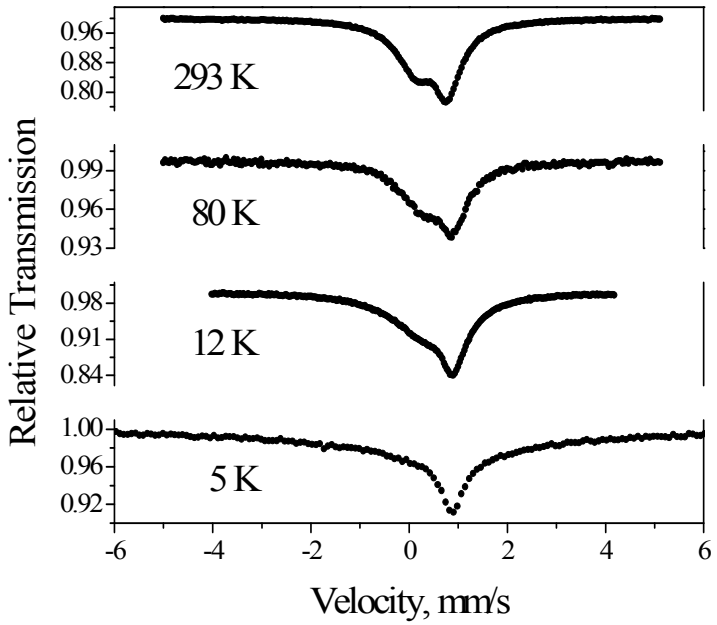

Figure 8.1.2 Mössbauer spectra of NaFeEDTA(H_2O)·2H_2O recorded at different temperatures.

A further argument against spin-lattice relaxation is the fact that after a thermal treatment at 393 K which removes crystal water from the solid sample and therefore results in NaFeEDTA(H_2O) leaves the spectral shape unaffected (Fig. 8.1.3). It is very unlikely that if the lattice has a role in spin coupling, then from a concentrated aqueous solution to a stage where the lattice does not contain water any more, only that which is directly coordinated to the Fe^{3+} centre, the conditions for spin relaxation would remain the same. This fact together with the weak temperature dependence of the spectrum shows that the asymmetry of the doublet of the heptacoordinate Fe^{III}EDTA(H_2O) should be an intrinsic property of the coordination sphere of iron.

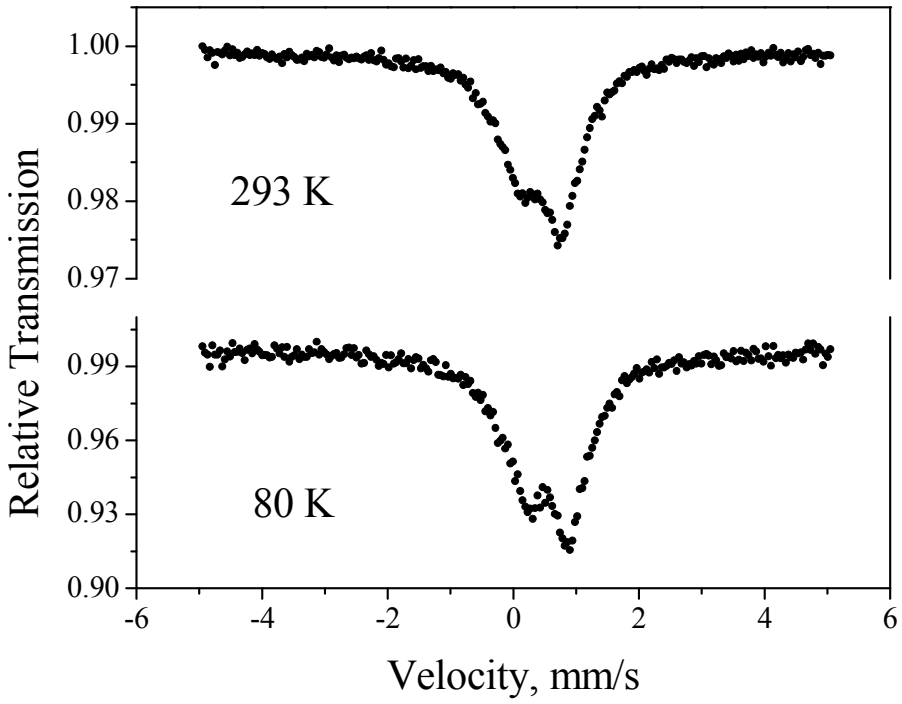

Figure 8.1.3 NaFeEDTA(H_2O) at room temperature and at 80 K.

Another possible explanation of such a doublet asymmetry could be if there were not only one but at least two slightly different lattice positions in the lattice for the iron compound. Although literature data gave no hint of this idea, we have recorded a single crystal XRD of our sample NaFeEDTA(H_2O)·$2H_2O$. The results confirmed (see structure and crystal lattice packing in Fig. 8.1.4 and 8.1.5, respectively) that iron occupies a uniform position in this lattice at 180 K.

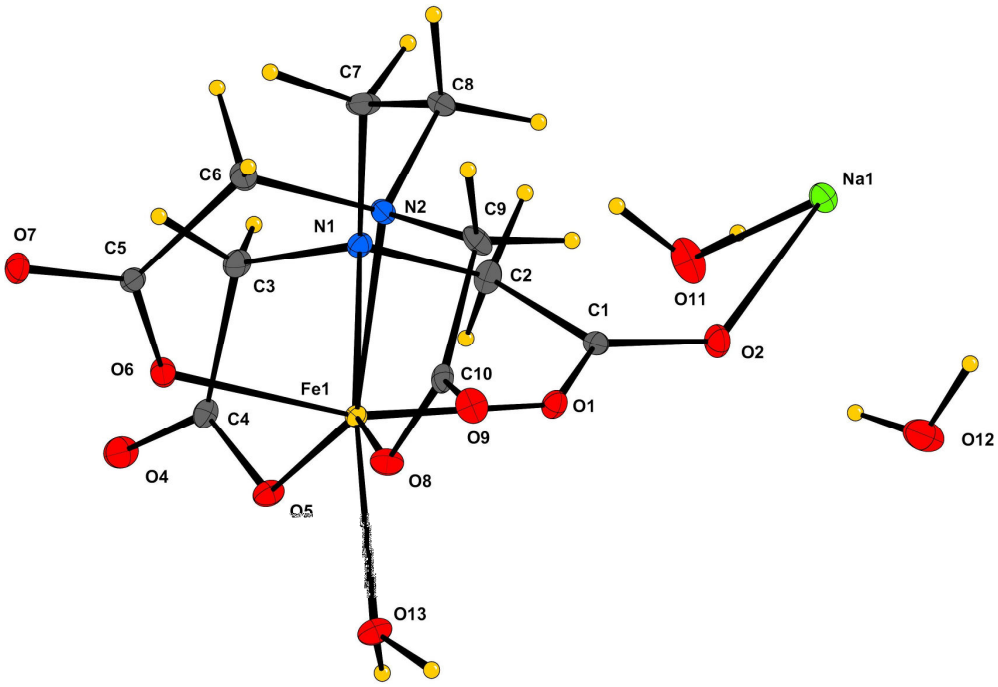

Figure 8.1.4. Structure of NaFeEDTA(H_2O)·2H_2O indicating also the crystal water molecules as determined from a single crystal X-ray diffractogram recorded at 180 K.

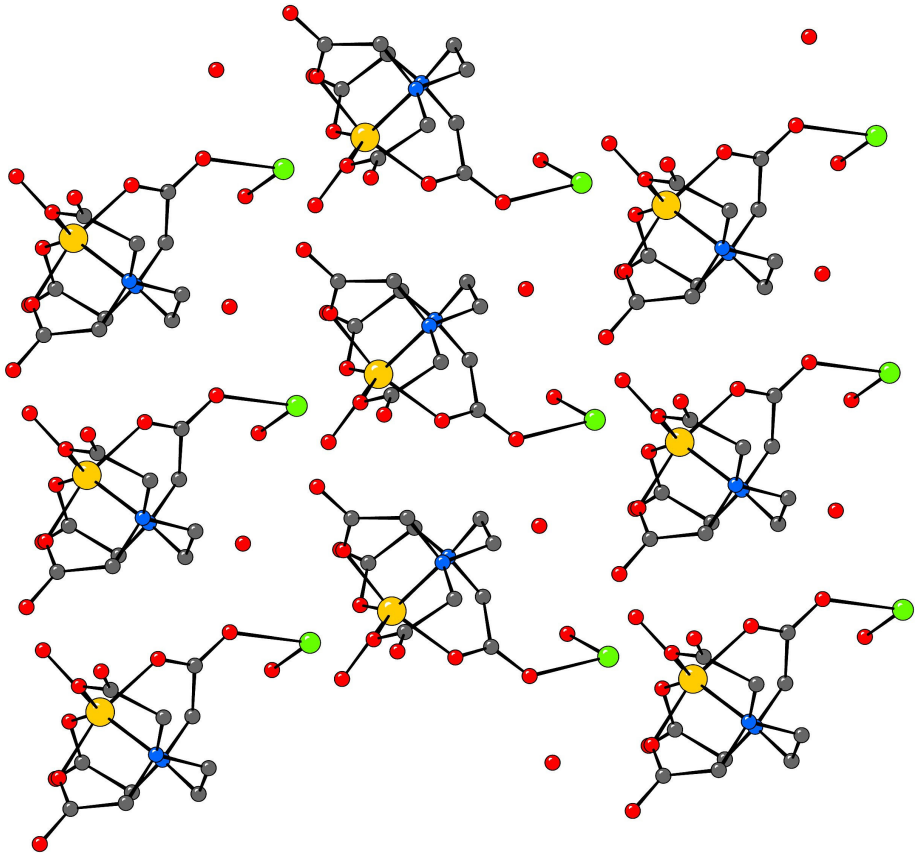

Figure 8.1.5. Crystal structure packing for the NaFeEDTA(H_2O)·2H_2O complex at 180 K.

It is clear that at 180 K there is only one type of ferric species in the crystal lattice, which proves the presence of only one position of the Fe^{III}EDTA complex in the crystal lattice. Therefore the hypothesis that there can be different iron microenvironments in the lattice, such as the dynamical coordination of one of the carboxylate arms, can be safely excluded. In the solid state, molecules of the complex are connected to each other via a system of hydrogen-bonds, forming a three-dimensional network with the shortest iron-iron distance of 8.88 Å.

We can assume here that the distortion of spectral lines in the zero magnetic field Mössbauer spectra is due to a combination of negative single-ion zero-field splitting of the ground sextet of the system and the self-dilute nature of the compound resulting in slow single ion relaxation. The dilute nature is evidenced by the shortest intermolecular Fe^{III}-Fe^{III} distance of ~9 Å, a magnitude which has been shown in a previous study [6] to be large enough to result in long spin-spin relaxation times for high spin iron(III) species. In this complex, we can predict $V_{zz}<0$, *i.e.* stronger axial than in-plane ligation [7]. $V_{zz}<0$ corresponds to $E_\pi<E_\sigma$, where the π quadrupolar transition is $|1/2,\pm1/2\rangle \rightarrow |3/2, \pm 3/2\rangle$ and σ is $|1/2, \pm1/2\rangle \rightarrow |3/2, \pm1/2\rangle$. The theory appropriate [8] to the slow paramagnetic relaxation of an internal field longitudinal (*i.e.*, parallel to the principal axis) electric field gradient tensor predicts that the π transition should suffer the initial and largest line broadening effect with the onset of slow paramagnetic relaxation. This is fully consistent with $V_{zz}<0$.

A possible method to extract more information from the Mössbauer spectrum is applying magnetic field since magnetic patterns offer much more specific parameters for a particular species. We have measured the Mössbauer spectra of both $NaFeEDTA(H_2O)\cdot 2H_2O$ and $NaFeEDTA(H_2O)$ at 50 K and 12 K in 7 T external magnetic field parallel to the propagation direction of the gamma rays. As can be seen in Fig. 8.1.6, first of all, the two sets of spectra (*i.e.* with and without crystal water molecules) look rather similar, giving further support to our finding that the crystal lattice is not responsible for the paramagnetic spin relaxation above ~50 K.

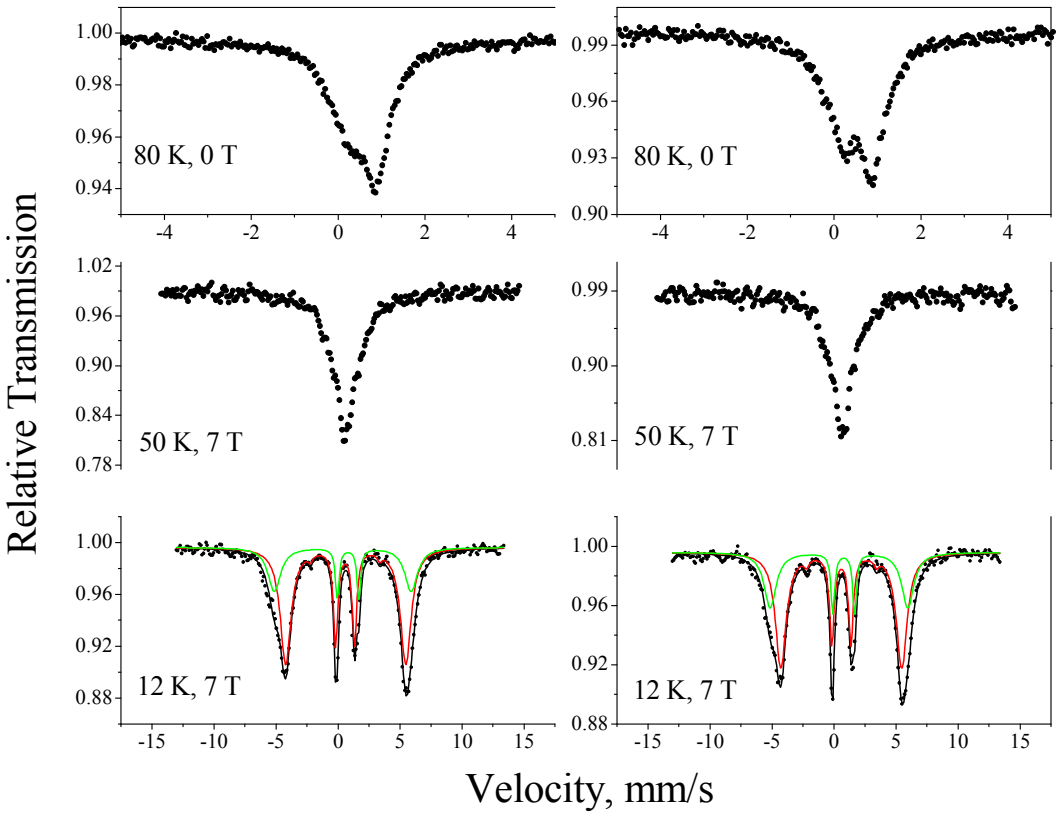

Figure 8.1.6. Mössbauer spectra of NaFeEDTA(H_2O)·2H_2O (left column) and NaFeEDTA(H_2O) (right column). The applied field was parallel with the propagation direction of the gamma rays. Please note the different velocity scales.

At 50 K in applied field there is a broadened line due to magnetic relaxation in the Mössbauer spectra. At 12 K, however, the splitting into two magnetic sextets is clearly visible. One of two sextets is actually a quadruplet since the 2nd and 5th lines of the sextets are missing due to the magnetic field being parallel to the gamma rays, and the intensity of the 2nd and 5th lines of the other sextet is very small as well. This indicates that, formally, such a spectral shape, *i.e.*, where the 2nd and 5th lines (corresponding to the Δm=0 transitions) have zero intensity and there are two different hyperfine magnetic fields, is consistent with a ferrimagnetic behaviour where all the magnetic moments are nearly collinear.[9] The non-vanishing 2nd and 5th lines in the other subspectrum refer to a case when the magnetic moment of one of the components of the ferrimagnetic system is not perfectly parallel or antiparallel to the γ-ray propagation direction. However this angle must be very small, since the intensity of these lines increases with increasing angles (see Appendix 1). A magnetisation measurement down to 2 K indicated simple Curie paramagnetism (Fig. 8.1.7.). The T_c value (paramagnetic Curie temperature) was

found to be 0.0(2), *i.e.* no magnetic ordering can be seen with magnetic susceptibility measurements at low temperatures either. The magnetic moment has a constant value at not too low temperature (μ=5.88 BM) which is close to μ=(4S(S+1))1/2=5.92 BM (when S=5/2), *i.e.* the spin-only value for a high spin Fe^{III} ion.

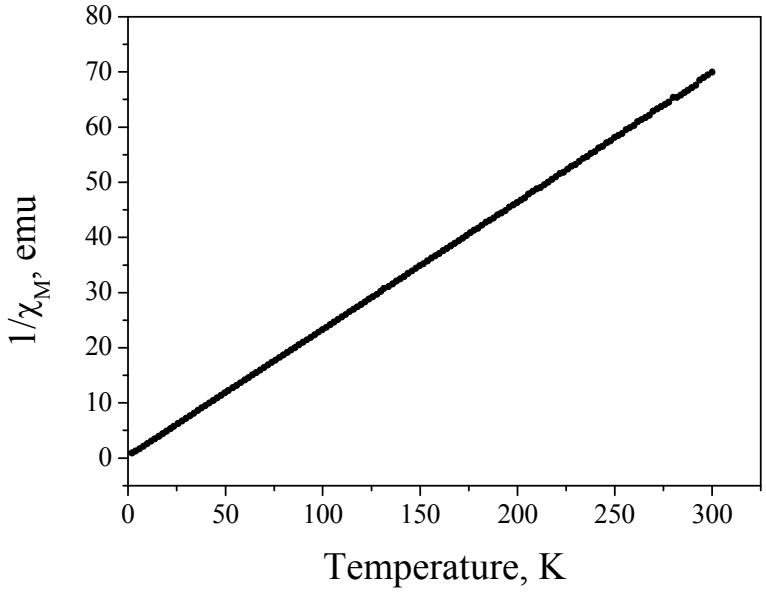

Figure 8.1.7. Temperature dependence of the inverse molar magnetic susceptibility ($1/\chi_M$) of $NaFeEDTA(H_2O)\cdot 2H_2O$.

It is rather remarkable that while using Mössbauer spectroscopy a magnetic ordering can be observed using magnetic susceptibility measurements no trace of such phenomenon can be observed. Two possible explanations can be given for this system. First of all, we have to emphasise that the applied magnetic fields in the two cases were not of the same magnitude, while for the Mössbauer a magnetic field of 7 T, for the magnetic susceptibility measurements a magnetic field of 0.5 T only was applied. On the other hand, the two methods work in different time windows, which means that while using Mössbauer spectroscopy, dynamical effects can be detected as well, using magnetic susceptibility measurements, only long range magnetic orderings are observable. Furthermore, using Mössbauer spectroscopy local as well as macroscopic magnetic interactions can be detected, while magnetic measurements can only detect macroscopic magnetisation. This last difference can be also responsible for the fact that this ferrimagnetic interaction could not be detected using magnetic susceptibility measurements.

It is worth noting that the 1st and 6th lines of the sextets are much broader than the 3rd and 4th. The parameters of the computer evaluations for $NaFeEDTA(H_2O)\cdot 2H_2O$ are given in Table 8.1.1. This indicates a highly frustrated magnetic system probably due to the very effective isolation of the Fe^{3+} centres from each other by the bulky EDTA ligands (the same "dilute nature" as discussed in ref. [6]). A similar case was found by Fourquet *et al.*[10] for triguanidinium hexafluoroferrate(III) although only with a single magnetic component.

Table 8.1.1. Results of the evaluations of the Mössbauer spectra of $NaFeEDTA(H_2O)\cdot 2H_2O$ at 12 K in 7 T external field parallel to the propagation direction of the gamma rays.

Temperature (K)	δ (mm/s) ±0.01	Δ (mm/s) ±0.05	B (T) ±0.5	Prop (%) ±2	$\Gamma_{1\text{-}6}$	$\Gamma_{2\text{-}5}$	$\Gamma_{3\text{-}4}$
					(mm/s) ±0.05		
12	0.60	-0.01	30.3	65.6	1.05	0.45	0.45
	0.60	-0.38	34.5	34.4	1.17	-	0.36

It is very remarkable that at 12 K, (i) the isomer shifts of the two components are identical, (ii) the quadrupole interactions are very different: practically zero for one component and substantial for the other, (iii) the relative intensities are not equal but are roughly 2:1. The two different subspectra in the spectrum recorded at 12 K and in an applied magnetic field of 7 T must refer to two different species. The isomer shifts of these two subspectra show that the coordination environments of the two species are identical regarding the number and type of the coordinating ligands, but the arrangement of these ligands has to be different resulting in different quadrupole shifts. The complex with higher quadrupole shift (lower absolute value) is the more symmetrical.

Korendovych *et al.* investigated a very similar system, however, their complex displayed an antiferromagnetic ordering without applying an external magnetic field, and this ordering could be seen with magnetisation measurements as well.[11]

It is clear that at 180 K there exists only one species in the crystal lattice, however, from the in-field Mössbauer measurements it was established that there has to be two different species with identical ligands. There are two possible scenarios describing the appearance of another species in the crystal lattice.

i) It is known that upon decreasing the temperature, one can trigger magnetic and phase transitions.

ii) Applying an external magnetic field might be necessary to induce this phenomenon. This is expected at relatively high applied magnetic fields. This explanation may be surprising, nevertheless, it has been suggested by theory that the application of an external magnetic field may also change the type of bonding between ligand and central atom.[12]

According to our results obtained so far, we cannot yet decide whether scenario i) or scenario ii) is correct. The persisting problem of relaxing lines in the zero-field spectra as well as the 50 K in-field spectrum makes the spectrum evaluations difficult and therefore we cannot safely exclude either of these two scenarios. Therefore further studies on this system are necessary.

8.1.3 Conclusions

According to Mössbauer measurements and a single-crystal X ray study, it was evidenced that the NaFeEDTA·3H_2O complex has one ferric microenvironment at 180 K. The NaFeEDTA·3H_2O complex was found to be paramagnetic, obeying the Curie-law, however, the in-field Mössbauer measurements revealed ferrimagnetic behaviour at 12 K, in an applied magnetic field of 7 T. The Mössbauer spectra of the compound without an applied external magnetic field display paramagnetic spin relaxation (from room temperature down to 4K!), which can be stopped at low temperatures (between 50 and 12 K) by an applied magnetic field (B=7 T). The in-field experiments resulted in spectra displaying two subspectra due to two ferric microenvironments present in the powder sample, with the same ligands but with different coordination symmetry (as shown by identical isomer shifts and different quadrupole shifts). Two possible explanations have been given for this phenomenon; to decide which is correct further studies are necessary.

8.2 Study of the Thermal Stability of the $Fe^{III}EDTA$ Complex in its Monomeric Form

8.2.1 Introduction

Several studies have been carried out regarding the thermal behaviour of the NaFeEDTA complex, especially because of the possible applications in dissolving iron oxides by ethylenediaminetetraacetic acid containing solutions [14-20] [17]. These methods are more efficient at higher temperatures but the possible degradation of the chelating agent or the complex should be taken into account. Studies found in the literature dealt with the investigation of the thermal behaviour in solution phase [21-22] but there have also been trials to describe the thermal behaviour of the complex in solid state [23,24]. For the solutions, thermoanalytical measurements were carried out in an autoclave, and two phases were analysed after the heat treatment, the gas phase was analysed by gas chromatography, while the remaining solid phase was analysed by powder X-ray diffraction [22], the observed decomposition products are CO_2, H_2, CH_2O and amines (mainly ethylenediamine) in the gas phase, while in the solid state several iron oxides could be observed. Diatlova *et al.* [25] have found the intensive decomposition of the complex at the temperature range of 140-280 °C and the final product of the heat treatment was found to be magnetite. (This shows reductive circumstances for the iron oxide formation.) In ref. [26], ferric hydroxide with ethylenediaminetetraacetic acid was mixed and the ligand concentration in solution was followed and its strong decrease was detected between 180 °C and 275 °C. At 275 °C no more free chelating agent has been detected in the solution and at the same time, the strong decrease of the concentration of free ferric ion has been detected as well. The final product was found to be magnetite just as in the previous example. T. H. Margulova *et al.* [27] have found that magnetite forms only in case when free iron (non chelated ferric ion) was present in the system. In ref. [28], it has been suggested that CO_2 and amines can be resulted from the decomposition in the gas phase. A dependence of the thermolysis products on various parameters like the temperature of the heat treatment, on the presence of additional salts

[17] See also in Chapter 6 –Tuning the oxidation state: Study of the $Fe^{III}EDTA$-photodegradation phenomenon and of the autoxidation of the $Fe^{II}EDTA$ complex in solid state and in solution phase.

in the solution, additional redox agents in the solution, initial pH of the solution, etc., have been detected in ref [28]. Nevertheless, no evidence has been given for these dependences. In ref. [22], the initial pH of the solutions was 4. Thermal treatments were carried out at 140, 245 and at 275 °C. After decomposition, no iron species has remained in the solution and its pH increased to 5-8. CO_2 could be observed in the gas phase after each treatment, but H_2 gas only has been produced in the course of heat treatments at 245 and at 275 °C. Heating the solutions to 100-130 °C, reactions occurred following these equations:

$$2\ NaFeEDTA + H_2O \leftrightarrow Na_2FeOHEDTA + HFeEDTA$$

$$3\ Na_2FeOHEDTA + H_2O \leftrightarrow 2\ Na_3Fe(OH)_2EDTA + HFeEDTA$$

No precipitate could be observed even after the starting of the decomposition of the complex at 140 °C, dark brown precipitate started to appear when the temperature reached 180 °C and at 200 °C it became crystalline. At 140 °C, the formation of CH_2O and of Fe^{2+} was detected. Analysing the solid phase, the following assumptions were made: 180 °C, 5hs amorphous ferric oxides; 200 °C, 3/5 hs, haematite; 3 hs, magnetite in the presence of free iron; 250 °C, 5hs, haematite; 275 °C 5 hs FeO, Fe_2O_3.

In previous studies [23,20-23], the thermal properties of $NaFeEDTA \cdot 3H_2O$ were investigated, and the degradation steps were found to be as follows: first the structural and secondly the ligand (coordinated) water molecules are eliminated followed by the detachment of an carboxylate arm of EDTA, which is oxidised and ejected from the complex as a CO_2 molecule, leaving a reduced, ferrous species behind. This is followed by further ejection of CO_2 molecules, until the complete decomposition of the EDTA chelating agent. However, the temperatures measured for these degradation steps are different for each study. Since the results of the previous studies were contradictory, the thermal treatment and study was repeated and Mössbauer technique was used to characterise the degradation products.

8.2.2 Results and Discussion

8.2.2.1 Thermal Analysis of the Monomeric NaFeEDTA·3H_2O

The study of thermal behaviour of the dark yellow coloured NaFeEDTA·3H_2O complex had two steps; firstly, DTG/TGA measurements were carried out to determine the decomposition steps and the corresponding mass loss and secondly, the decomposition products were analysed using Mössbauer spectroscopy. DTG and TGA measurements of the NaFeEDTA·3H_2O salt were carried out in an STD 2960 Simultaneous DTA-TGA apparatus (TA Instruments Inc., USA), at a heating rate of 10 K/min and in an air flow rate of 130 ml/min. Initial sample masses were between 10-12 mg, and an open Al crucible was used. The decomposition curves are displayed in Figure 8.2.1.

The relative mass losses indicate that at 125.6 °C two water molecules are ejected from the crystal lattice, which is followed by the ejection of the third water molecule at 199.0 °C. This difference in the temperatures is reasonable, since the first two H_2O molecules are only bound in the lattice, while the third one is bound to the ligand sphere of iron. The third step, at 259.2 °C, can be assigned to the loss of a CO_2 molecule, the source of which is a carboxylate arm of the EDTA chelating agent. This latter step should be followed by a change in the oxidation state of the iron ions (reduction step), since the formation of a carbon dioxide molecule from a carboxylate ligand needs an electron transfer. It is obvious, that the three first steps are reproducible since the TGA curve displays a plateau, *i.e.* they are not concave peaks in the temperature difference curve, unlike the fourth step, which displays the complete decomposition of the complex, a series of decomposition reactions which cannot be probably distinguished using available methods.

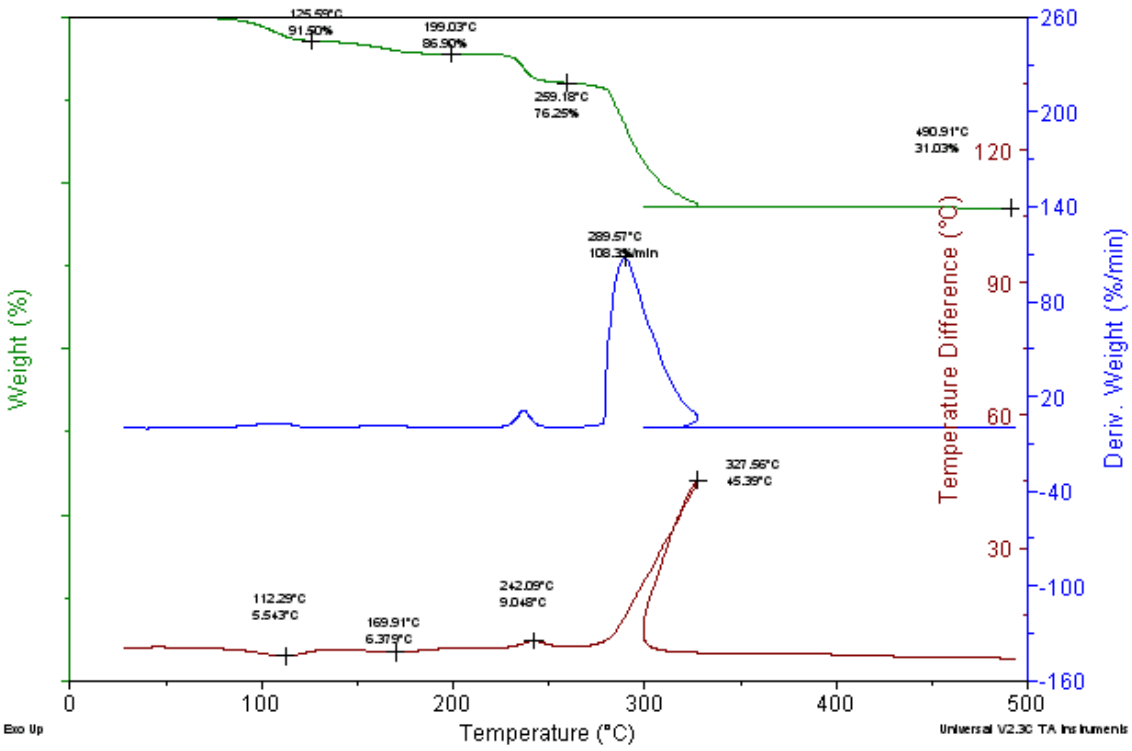

Figure 8.2.1 TGA/DTG curves of the NaFeEDTA·3H_2O complex.

8.2.2.2 Study of the degradation products of NaFeEDTA·3H_2O

As can be seen from the thermal analysis curves, three degradation products are distinguishable, namely, the $NaFe^{III}EDTA·H_2O$, without any crystal water molecules, the fivefold coordinated $NaFe^{III}EDTA$ complex, after the loss of its coordination water molecule, and a Fe^{2+} complex resulting from the loss of CO_2 of the $NaFe^{III}EDTA$ complex. Thermal treatments were carried out in a temperature controlled furnace. The temperature and duration of the treatments were 130 °C for 20 minutes, 200 °C for 20 minutes and 220 °C for 40 minutes, following the thermal analysis curve. The mass losses were verified before and after each treatment using a balance, and a part of the resulting powder was placed into molten paraffin to avoid contact with moisture and oxygen, while the rest was kept as a powder sample to study further reactions of the degradation products. The colour of the heated powder changed after the heat treatment at 220 °C to brown.

Mössbauer spectra recorded before and after the heat treatment at 130 °C during twenty minutes are shown in Figure 8.2.2. Spectrum parameters and errors are listed in Table 8.2.1.

Table 8.2.1 Mössbauer parameters and their errors in parentheses for spectra of the $NaFe^{III}EDTA{\cdot}3H_2O$ complex before (1) and after (2) the heat treatment at 130 °C during 20 min.*

Spectrum / Parameters	δ (mm/s)	eQV_{zz} (mm/s)	ν (1/s)	Γ (mm/s)
8.2.2.a)	0.45(1)	−0.70(1)	9.86(2)	0.60(1)
8.2.2.b)	0.46(2)	−0.62(1)	9.64(2)	0.50(1)

*Spectrum evaluations were done using the Blume−Tjon magnetic relaxation model, therefore the asymmetry parameter was fixed to η=−3 in both cases. Because of the strong correlation of the hyperfine magnetic field with the frequency of the spin fluctuation and with the baseline the value of the hyperfine magnetic field was constrained to be B=40 T in both cases. This value corresponds well to this type of complexes (previous static experiments).

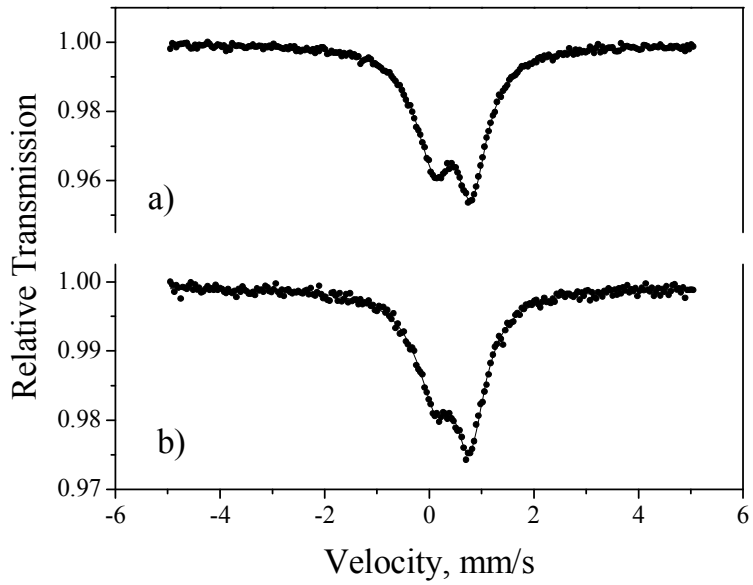

Figure 8.2.2 Mössbauer spectra of the $NaFe^{III}EDTA{\cdot}3H_2O$ complex before (a) and after (b) the heat treatment at 130 °C during 20 min. (Spectra recorded at room temperature)

The relaxation lineshape of the spectra was discussed earlier.

As can be seen, the loss of the two crystal water molecules does not affect the resultant spectrum, the hyperfine parameters remained the same after the heating. This means that the presence or absence of the water molecules in the crystal lattice does not affect the hyperfine interactions of the ^{57}Fe nucleus.

Mössbauer spectra recorded before and after the heat treatment at 200 °C during 20 minutes are shown in Figure 8.2.3. Spectrum parameters and errors are listed in Table 8.2.2.

Table 8.2.2 Mössbauer parameters (and errors) of the $NaFe^{III}EDTA{\cdot}3H_2O$ complex before (1) and after (2) the heat treatment at 200 °C for 20 min.

Spectrum / Parameters	δ (mm/s)	Δ / eQV_{zz} (mm/s)	v	Γ (mm/s)
8.2.3.a)*	0.54(1)	−0.67(1)	9.70(3)	0.53(2)
8.2.3.b)	0.35(1)	1.12(1)	-	0.58(1)

*Spectrum evaluation was done using the Blume−Tjon magnetic relaxation method, therefore the asymmetry parameter was fixed to η=−3; because of the strong correlation between the hyperfine magnetic field and the frequency of the spin fluctuation and the baseline the value of the hyperfine magnetic field was constrained to be B=40 T. This value corresponds well to this type of complexes (previous static experiments).

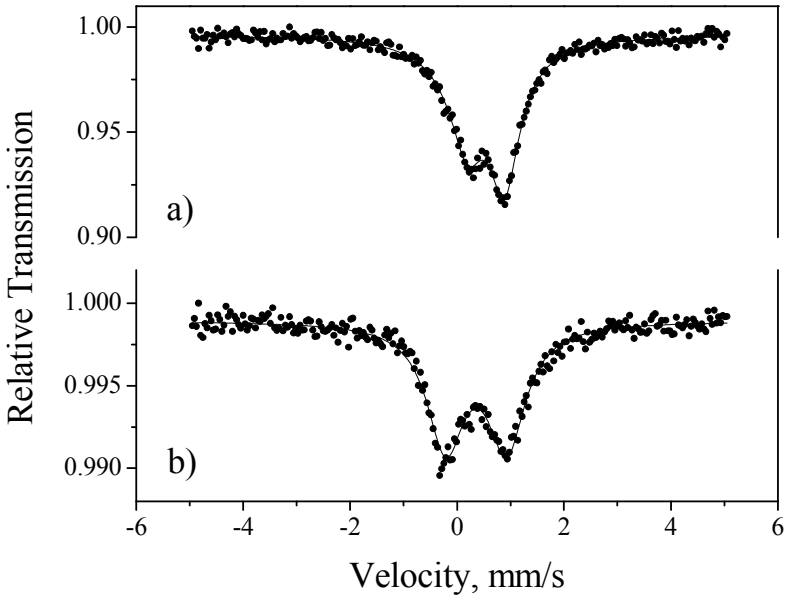

Figure 8.2.3. Mössbauer spectra of the $NaFe^{III}EDTA{\cdot}3H_2O$ complex before (a) and after (b) the heat treatment at 200 °C during 20 min.

The lower isomer shift of the subspectrum displaying the $NaFe^{III}EDTA$ species in Figure 8.2.3.b) corresponds well to the fact that one water molecule has been ejected from the ligand sphere of iron because of the decrease of the 3*d* electron density compared to the case of the $NaFe^{III}EDTA{\cdot}3H_2O$ complex, see in Figure 8.2.3.a).

The spectrum recorded after the heat treatment at 220 °C for 40 minutes is displayed in Figure 8.2.4.a). A fraction of the resultant powder was placed in molten paraffin to preserve it from contact with moisture and carbon dioxide, while, to study its degradation reactions, another fraction was kept in air and Mössbauer spectra were recorded one and ten days after the heat treatment, which are shown in Figure 8.2.4.b) and in Figure 8.2.4.c), respectively. Spectrum parameters and errors are listed in Table 8.2.3.

Table 8.2.3 Mössbauer parameters (and errors) of the $NaFe^{III}EDTA \cdot 3H_2O$ complex before immediately, one and ten days after the heat treatment at 220 °C during 40 min.

Spectrum / Parameters	Spectrum Component	N/N %	δ (mm/s)	Δ (mm/s)	Γ^* (mm/s)
8.2.4.a)	A	48.9	1.08(1)	2.08(1)	0.56(1)
	B	51.1	1.13(1)	2.76(1)	0.56(1)
8.2.4.b)	A	35.9	1.12(1)	2.03(2)	0.53(1)
	B	40.0	1.12(1)	2.87(2)	0.53(1)
	C	24.1	0.40(2)	1.22(8)	0.53(1)
8.2.4.c)	A	14.1	1.19(3)	1.96(8)	0.54(1)
	B	20.7	1.2(2)	2.7(2)	0.54(1)
	C	65.2	0.35(1)	1.41(1)	0.54(1)

*Linewidth were constrained to be all the same within each spectrum evaluation.

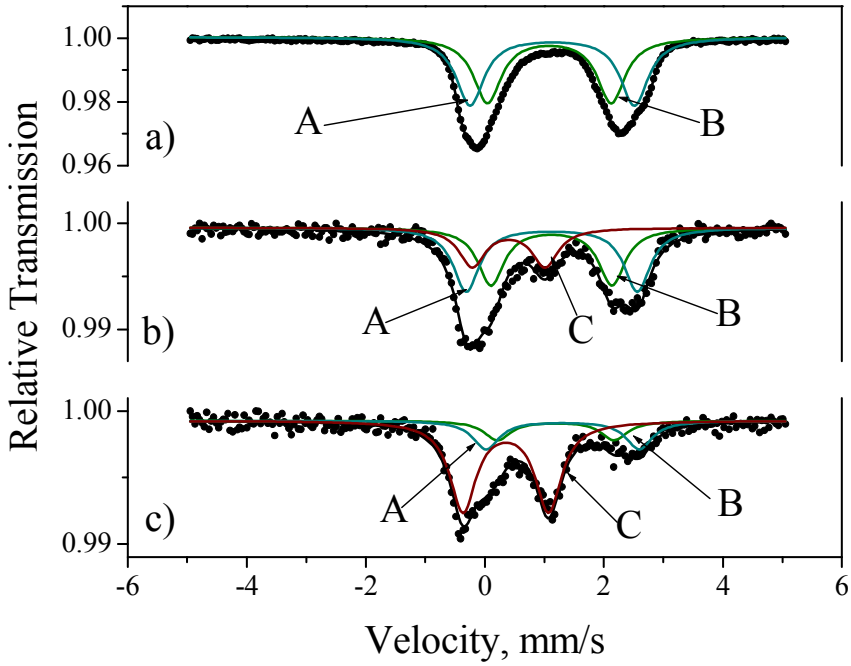

Figure 8.2.4. Mössbauer spectra of the $NaFe^{III}EDTA \cdot 3H_2O$ complex after the heat treatment at 220 °C for 40 min. (a)): sample placed into molten paraffin immediately after the heating process; powder sample let in air. (b)): spectrum recorded one day after the heat treatment. (c)): powder sample in air, spectrum recorded ten days after the heat treatment. (All spectra recorded at room temperature.)

Figure 8.2.4.a) shows two quadrupole doublets, both referring to high spin, Fe^{2+}-bearing species. However, according to the degradation pathway, namely that one carboxylate arm gets detached in the course of the decomposition of the $NaFe^{III}EDTA \cdot 3H_2O$ complex, the formation of only one ferrous degradation product was expected. The isomer shifts of the two distinct subspectra are the same and their ratio is nearly 1:1. Since the thermal analysis curve does not display any other mass change, and the two subspectra differs only in their quadrupole splittings, we can assume that these two species represented by subspectra A and B formed simultaneously and are configurational isomers of each other. This scenario explains the identical isomer shifts and the different quadrupole splittings.

This hypothesis is also supported by the fact that letting the degraded system to relax in air, the resultant oxidation product is identical for both components.

This latter fact led to the hypothesis that the isomer shifts of subspectra A and B may be the same, since on a pure mathematical basis, another line assumption would be

possible, namely, the two distinct subspectra would have approximately the same quadrupole splitting, but different isomer shifts (for this spectrum evaluation see Appendix 3) but in such case, the degradation products should have a completely different composition, therefore their oxidation products should be different as well. Furthermore, in this case a second mass loss at different temperature should have been noticeable in the TGA curve.

The iron(II) compounds resulted from the ejection of a CO_2 molecule from the EDTA chelating agent, which has to be followed by a reduction step converting the ferric into ferrous ion. The oxidation of the ferrous compounds was carried out by aerial oxygen. The mechanism of this reaction might be similar to the one described in Chapter 6, for the autoxidation of ferrous ethylenediaminetetraacetate (Fe^{II}EDTA), *i.e.* one oxygen molecule binds to the ligand sphere of iron, oxidises it, then it binds another ferrous entity composing a bridge, oxidises that part as well, and one oxygen atom is then ejected from the bound, leaving a μ-oxo bridged dimer behind, in the crystal lattice. This latter hypothesis is reinforced by the hyperfine parameters of the subspectrum describing the oxidised form of the degradation products being very close to those of the dimeric Fe^{III}EDTA (δ=0.36 mm/s, Δ=1.60 mm/s at room temperature and δ=0.44 mm/s, Δ=1.60 mm/s at 80 K), to those of the dimeric Fe^{III}CDTA (δ=0.44 mm/s, Δ=1.70 mm/s at 80 K) and to those of the dimeric Fe^{III}EDDA (δ=0.46 mm/s, Δ=1.33 mm/s at 80 K). The relatively high quadrupole splitting value for these spectra is probably due to the angle of the Fe-O-Fe bonds leading to the bridging oxygen atom, being nearly 180°, thus representing a very highly distorted symmetry of the ligand environment.

8.2.3 Conclusions

The thermal degradation products of the monomeric ($NaFeEDTA \cdot 3H_2O$) complex as well as their oxidation products were identified. First the crystal water molecules evaporated, then the coordinated water molecule evaporated. The third step of the thermal decomposition is the detachment of a coordinated carboxylate arm, followed by the formation of a CO_2 molecule, this process is known to result in a change in the oxidation number of the iron ion, *i.e.* when the carbon atom is oxidised, the ferric ion is reduced into ferrous ion. Two ferrous species have been found to form in the course of this degradation step. These two species are probably configurational isomers. This hypothesis is based upon the reasoning that the isomer shifts of the two doublets representing the two ferrous compounds are identical, but another fact supports this finding as well, namely that the oxidation product of the two ferrous compounds is the same ferric species. The further oxidation product of the two resultant ferrous degradation products has been recognised as a μ-oxo dimeric species, with a possibly straight Fe-O-Fe bite angle, just like in the case of the well-known $\{O(FeEDTA)_2\}^{4-}$ anion. This latter assumption could be made because of the very similar hyperfine parameters of the two systems. Reaction pathway for this oxidation has also been proposed. The observed degradation steps were found to be the same as they have been proposed by previous literature data, however, the temperature values corresponding to these degradation steps were slightly different from all data published before, even if these data have already been contradictory.

8.3 References

[1] J. J. Spijkerman, L.H. Hall, J. L. Lambert *J. Am. Chem. Soc,* **1968**, *90*, 2039-2043.

[2] M. Takeda *Hyp. Inter*. **1986**, *28*, 737-740.

[3] V. K. Sharma, P. Á. Szilágyi, Z. Homonnay, E. Kuzmann, A. Vértes *Eur. J. Inorg. Chem.* **2005**, *21*, 4393-4400.

[4] A. Vértes, D. L. Nagy *Mössbauer Spectroscopy of Frozen Solutions*, Akadémiai Kiadó, *Budapest*, **1990**.

[5] P. Gomez-Romero, G. B. Jameson, J. J. Borras-Almenar, E. Escriva, E. Coronado, D. Betran *J. Chem. Soc. Dalton Trans*. **1988**, *11*, 2747-2751.

[6] J. W. G. Wignal *J. Phys*. **1968**, *44*, 2462.

[7] T. C. Gibb *Principles of Mössbauer Spectroscopy*; Chapman and Hall, *London*, **1976**.

[8] M. Blume, J. A. Tjon *Phys. Rev*. **1968**, *165*, 446-461.

[9] C. E. Johnson *J. Phys. D: Appl. Phys*. **1996**, *29*, 2266-2273.

[10] J. L. Fourquet, F. Plet, Y. Calage, R. De Pape *J. Sol. State. Chem*. **1987**, *69*, 76-80.

[11] I. V. Korendovych, R. J. Staples, W. M. Reiff and E. V. Rybak-Akimova *Inorg. Chem*. **2004**, *43*, 3930-3941.

[12] G. V. Gadiyak, Yu. E. Lozovik, M. S. Obrecht *J. Phys. C : Solid State Phys*. **1983**, *16*, 5823-5828.

[13] L. H. Hall, J. J. Spijkerman, J. L. Lambert *J. Am. Chem. Soc*. **1968**, *90*, 2044-2048.

[14] M. I. Litter, E. C. Baumgartner, G. A. Urrutia and M. A. Blesa *Environ. Sci. Technol.* **1991**, *25*, 1907-1913.

[15] M. I. Litter and M. A. Blesa *J. Colloid Interface Sci*. **1988**, *125*, 679-687.

[16] R. Torres, M. A. Blesa and E. Matijević *J. Colloid Interface Sci*. **1989**, *131*, 567.

[17] G. Karametaxas, S. J. Hug and B. Sulzberger *Environ. Sci. Technol*. **1995**, *29*, 2992-3000.

[18] E. Baumgartner, M. A. Blesa, H. A. Marinovich, A. J. G. Maroto *Inorg. Chem*. **1983,** *22*, 2224-2226.

[19] M. A. Blesa, H. A. Marinovich, E. C. Baumgartner, A. J. G. Maroto *Inorg. Chem.* **1987,** *26*, 3713-3717.

[20] O. I. Martynova, B. V. Zhadanov, B. P. Golubev, E. P. Miklashevskaya and B. M. Larin, Mosk. Energ. Inst., Deposited Doc. **1974**, (VINITI 2031-74).

[21] N. I. Kuz'menko and E. M. Yakimets *Zh. Khim*. **1973**, *190*, 76-83

[22] E. M. Yakimets, N. A. Berg and N. I. Kuz'menko, *Teploenergetika* **1971**, *18*, 84-85.

[23] J. Garcia-Oricain and A. Fuster *Afinidad* **1982**, *XXXIX*, 541-542.

[24] F. A. Nour El-Dien *Spectroscopy Letters* **1999**, *32*, 407-419.

[25] N. M. Diatlova, B. I. Bikhman, L. B. Belskaya, M. Z. Gurevich and S. A. Tevlin, *Teploenergetika*, **1966**, *13*, 56.

[26] In: *Energia*, edited by T. H. Margulova, **1965**, 204-226

[27] T. H. Margulova and S. V. Bogatyreva, *Elektricheskie Stanzii*, **1964**, *10*, 14.

[28] In: *Energia*, edited by T. H. Margulova, **1969**.

9 Summary

This work has been devoted to the investigation of the ferric-ethylenediaminetetraacetate and its analogues, such as the ferric CDTA and EDDA complexes. The reactions of iron(III)-ethylenediaminetetraacetate (Fe^{III}-EDTA) system are very important in biochemistry and environmental chemistry. The main method used was Mössbauer spectroscopy, which is an extremely powerful tool for iron compounds and even solutions using the "fast quench" technique.

In frozen aqueous solutions, the EDTA system displays ferrimagnetic behaviour at low pH values, the two components of the ferrimagnet differ in their coordination number due to the coordination or to the lack of coordination of a water molecule in the ligand sphere of the ferric ion. The angle of the two spin components of the ferrimagnet displayed a slight change as a function of the pH of the solution, but the origin of this property could not be determined by Mössbauer spectroscopy, because of the possibility for several line assumptions, as the spectra obtained were rather complicated. When raising the pH of the solutions, the known μ-oxo dimer, $[O(Fe^{III}EDTA)]^{4-}$ is formed. The same observation has been made for the CDTA complex, but the ferric EDDA complex did not form the same dimeric species, which can be explained by the differences in its coordination environment. Structures for the species represented by the subspectra have been proposed. For the EDTA species, a protolytic reaction between pH=0.6 and 4.1 has been recognised, which reinforces the possibility of different reaction quantum yields for the photodegradation of the ferric ethylenediaminetetraacetate at pH=6 and at pH=3.

This latter phenomenon, just like the autoxidation of the Fe^{2+}/EDTA system in solid state and in solution phase have been studied. Interestingly, the ferrous ethylenediaminetetraacetate complex had not been detected in aqueous solution in any of these cases (contrary to what is reported in the literature). However, the solid complex has been synthesised. Studying the autoxidation reaction, in both cases a direct μ-oxo dimer formation has been observed, which has not been seen before. Photodegradation of the dimeric Fe^{III}EDTA has been observed as well, which was a new finding since so far it has been established that the μ-oxo dimer is not photosensitive. Besides, in our studies no photoreduction of the ferric

ethylenediaminetetraacetate has been observed without previous precipitation. It is known that the ferric oxides/hydroxides can catalyse the photodegradation of $Fe^{III}EDTA$, but after our experiments it can be concluded that generating some precipitation is the only way to photoreduce the ferric complex.

The effect of the photodegradation of $Fe^{III}EDTA$ on the reaction of the complex with hydrogen peroxide has also been studied as well as the reaction itself without photodegradation. Reaction pathways have been proposed for both cases as well as the structures for the detected intermediate species. This latter reaction has also been studied by substituting EDTA with CDTA or EDDA. In the CDTA case, the reaction pathway has been recognised to be similar to the EDTA one, but when using EDDA, another reaction pathway has been observed. Proposed reaction mechanisms have been given for every case and for every possible intermediate species, structures have been proposed.

Magnetic properties of the solid $NaFeEDTA \cdot 3H_2O$ have been studied using temperature dependent and in-field Mössbauer spectroscopy as well as magnetic susceptibility measurements and X-ray crystallography. According to the X-ray data, there is only one type of ferric species in the crystal lattice. The complex displays in a large temperature range paramagnetic spin relaxation phenomenon: from 297 K down to 4.2 K where relaxation still can be observed, which is rather rare. This relaxation is of spin-spin relaxation nature. The material was found to be paramagnetic obeying the Curie-law, however, a ferrimagnetic interaction was observed at T=12 K in a B=7 T applied external magnetic field, using Mössbauer technique. The situation is similar to the case of the acidic aqueous solution samples, but the effect is much weaker, which is rather surprising that in a crystalline material less magnetic ordering can be observed than in a frozen solution. Our in-field Mössbauer results pointed out that at low temperature (12 K) and in applied magnetic field (7 T), two distinct iron microenvironments are present, with identical isomer shift and differing quadrupole splittings. To decide on the origin of this structural phase transition, further experiments are needed.

The thermal behaviour of the solid ferric ethylenediaminetetraacetate has also been studied using Mössbauer spectroscopy on the samples after heat treatments carried out at temperature values following the thermal analysis data. The further aerial degradation

of the decomposition products has also been studied in order to obtain more information about their structures and reactivity. Two ferrous species, probably configurational isomers, have been formed in the course of the thermal degradation of the ferric ethylenediaminetetraacetate and both undergo aerial oxidation. The mechanism of their oxidation has been investigated and it was found that both compounds result in a μ-oxo dimeric species after exposing them to air, thus a pathway for the oxidation process has been proposed.

Many interesting physical and chemical properties of the Fe^{III}EDTA and analogous systems have been observed in this work. Our studies on the solution phase structures of the ferric ethylenediaminetetraacetate complexes may serve to elucidate some of the problems related to this system. This, in conjunction with our results on the photodegradation of the Fe^{III}EDTA and on the autoxidation of the Fe^{2+}/EDTA system may be applied in wastewater treatment. Furthermore, these results might contribute to the understanding of analogue systems as well. Our results on the reaction of Fe^{III}EDTA with hydrogen peroxide pointed out that Mössbauer spectroscopy can be also used to investigate relatively fast reactions qualitatively and one can also obtain information about short-lived intermediate species. As enzyme-*mimics*, the identification of the intermediate species can enlighten many biological processes, such like the enzymatic activity of the superoxidise and dismutase.

10 Appendix

1A General Theories for describing the paramagnetic spin relaxation

Methods for describing relaxing systems were developed by Blume, Wegener, Van der Woude and Dekker, and Bradford and Marshall. The first approach for this phenomenon was developed by Afanas'ev and Kagan, who used diagrammatic techniques in order to derive the effect of one-phonon electronic relaxation on Mössbauer spectra. Although those authors discussed no spectra, their results correspond well with those obtained by the Anderson stochastic model of motional narrowing, which method was also used by Blume, and Van der Woude and Dekker.

The relaxation function and its notion are very important in any theory of relaxation line shapes. For a reasonable frequency spectrum $I(\omega)$, a Fourier expansion may be written as:

$$I(\omega) = \int_{-\infty}^{\infty} \varphi(t) e^{i\omega t} dt \tag{10.1}$$

and $\varphi(t)$ is known as the relaxation function characterising $I(\omega)$. For any function $f(t)$ whose value fluctuates in time one may define a correlation function $\psi_f(\tau)$ by:

$$\psi_f(\tau) = \langle f^*(t+\tau) f(t) \rangle. \tag{10.2}$$

The quantum mechanical relaxation function for the Mössbauer spectrum may be derived following the method of Blume, Wegener, or Bradford and Marshall. The total Hamiltonian for the ground and excited levels are written as

$$\mathcal{H}_{tot} = \mathcal{H} + \mathcal{H}_{rad}, \tag{10.3}$$

where $\mathcal{H}$ is the Hamiltonian for the entire system, exclusive with the interaction $\mathcal{H}_{rad}$ with the radiation field. The eigenstates of $\mathcal{H}$ representing initial and final states are $|\alpha\rangle$ and $|\beta\rangle$, respectively. The absorption process is described by the operator $\mathcal{H}_{rad} \equiv \mathcal{H}^+$. The probability absorption of a photon of energy ω whose polarisation and propagation direction are parallel, is given by

$$P(\omega) = \sum_{\alpha,\beta} p_\alpha \frac{|\langle \beta | \mathcal{H}^+ | \alpha \rangle|^2}{\left(\omega + \omega_\alpha - \omega_\beta\right)^2 + \Gamma^2/4}, \tag{10.4}$$

where p_α is the Boltzmann factor for the initial ground state $|\alpha\rangle$, and $\omega_\alpha = \frac{E_\alpha}{\hbar} = \hbar^{-1}\mathcal{H}|\alpha\rangle$, and

$$(\omega^2 + \tfrac{\Gamma^2}{4})^{-1} = \left(\tfrac{2}{\Gamma}\right) \mathrm{Re} \int_0^\infty dt\, e^{i\omega t - \Gamma t/2} = \Gamma^{-1} \int_{-\infty}^{\infty} dt\, e^{i\omega t - \Gamma|t|/2}, \tag{10.5}$$

thus

$$P(\omega)\Gamma^{-1}\int_{-\infty}^{\infty} dt\, e^{i(\omega+\omega_\alpha-\omega_\beta)t-\frac{\Gamma|t|}{2}}\sum_{\alpha,\beta} p_\alpha\langle\alpha|\mathcal{H}|\beta\rangle\langle\beta|\mathcal{H}^+|\alpha\rangle = \Gamma^{-1}\int_{-\infty}^{\infty} dt\, e^{i\omega t-\frac{\Gamma|t|}{2}}\Phi \times$$

$$\sum_\alpha p_\alpha\left\langle\alpha\left|\mathcal{H}^- e^{-\frac{i\mathcal{H}t}{\hbar}}\mathcal{H}^+ e^{+\frac{i\mathcal{H}t}{\hbar}}\right|\alpha\right\rangle = \Gamma^{-1}\int_{-\infty}^{\infty} dt\, e^{i\omega t-\frac{\Gamma|t|}{2}}\langle\mathcal{H}^-\mathcal{H}^+(t)\rangle. \qquad (10.6)$$

$\mathcal{H}^- = (\mathcal{H}^+)^\dagger$ and the Heisenberg representation for is $\mathcal{H}^+$, which represents a scalar interaction processing multipole expansion, here, only dipole radiation, therefore, using the Wigner–Eckart theorem,

$$P(\omega) = \int_{-\infty}^{\infty} dt\left\{(\Gamma^{-1}e^{-\frac{|t|}{2}})\sum_{q,q'} D(q,q')\langle\hat{I}_q^1,\hat{I}_{q'}^1(t)\rangle\right\}e^{i\omega t} \qquad (10.7)$$

is given, where the $\hat{I}_q^1$ are the spherical components and the $D(q,q')$ contain the angular dependence.

The central problem is to determine the time-dependent correlation function enclosed in angular brackets. Bradford and Marshall use a perturbation approach, while Wegener derives an expression equivalent to this latter one and also uses an expansion technique. The Anderson stochastic model, as developed for the Mössbauer case by Blume, may be utilised as follows, the Hamiltonian, $\mathcal{H} = \mathcal{H}_0 + V(t)$, where *V*(*t*), the time-dependent operator will have one of a finite number of forms, at a given moment. $|\alpha\rangle$ and $|\beta\rangle$ are the eigenstates of $\mathcal{H}$ for the various possible forms of the fluctuating *V*(*t*). In this case a finite number of frequencies $\omega_i = \omega_\beta - \omega_\alpha$ may be associated with *V*(*t*), Furthermore, *V*(*t*) and $\mathcal{H}_0$ are effectively diagonal in the angular moment eigenstates.

$$(\langle\mathcal{H}^-\mathcal{H}^+(t)\rangle)_{av} =$$

$$\sum_{m_1 m_0}\frac{1}{2I_0+1}|\langle I_1 m_1|\mathcal{H}^+|I_0 m_0\rangle|^2 \times (\langle I_0 m_0|U(t)|I_0 m_0\rangle\langle I_1 m_1|U^+(t)|I_1 m_1\rangle)_{av} \qquad (10.8)$$

Parentheses represent a stochastic averaging, as distinguished from an ensemble average denoted by angular brackets, convenient to define

$$a = \langle I_0 m_0|U(t)|I_0 m_0\rangle \equiv \left\langle I_0 m_0\left|e^{\frac{i\mathcal{H}_0 t}{\hbar}}e^{i\int_0^t V(t')dt'}\right|I_0 m_0\right\rangle =$$

$$e^{\frac{iE_0 t}{\hbar}}\left\langle I_0 m_0\left|e^{i\int_0^t V(t')dt'}\right|I_0 m_0\right\rangle \qquad (10.9)$$

$$b = \langle I_1 m_1|U^+(t)|I_1 m_1\rangle = e^{-\frac{iE_0 t}{\hbar}}\left\langle I_1 m_1\left|e^{i\int_0^t V(t')dt'}\right|I_1 m_1\right\rangle \qquad (10.10)$$

Consequently,

$$(\langle ab\rangle)_{av} = e^{i(E_1-E_0)t/\hbar}\left(e^{i\int_0^t \omega(t')dt'}\right)_{av}, \tag{10.11}$$

where $(E_1 - E_0)$ is the nuclear γ-ray energy and $\omega(t')$ assumes, as a random function of time, the finite set of frequencies or energy spectrum of $V(t)$. Since $V(t)$ was diagonal in m_1 and m_0, the Bloch equations apply here:

$$(\langle ab\rangle)_{av} = e^{\frac{i(E_1-E_0)t}{\hbar}}\sum_{m_1,m_0} e^{i\int_0^t \omega_{m_1,m_0}(t')dt'} \equiv e^{\frac{i(E_1-E_0)t}{\hbar}}\sum_{m_1,m_0} G_{m_1,m_0}(t) \tag{10.12}$$

Once the frequency spectrum is specified, the Anderson method can be used to evaluate $G_{m_1,m_0}(t)$:

$$G_{m_1,m_0}(t) = \zeta \cdot e^{t(i\tilde{\Omega}-\tilde{\pi})\cdot\eta} \tag{10.13}$$

where ζ is a row vector whose components give the relative probabilities of the frequencies of a fixed transition; $\zeta_i = 1/(2I_0+1) \times |\langle I_1 m_1|\mathcal{H}^+|I_0 m_0\rangle|^2$; $\tilde{\Omega}$ is a diagonal matrix with $\Omega_{ii} = \omega_i(m_1, m_0)$; and $\tilde{\pi} = \tilde{\pi}_d + \tilde{P}$, where $\tilde{P}$ is the probability matrix, and $\tilde{\pi}_d$ is a diagonal matrix with $(\tilde{\pi}_d)_{ii} = -\sum_j {}' P_{ij}$; and η is a column vector with all entries equal to 1.

Thus, the final expression is

$$P(\omega) = \int_{-\infty}^{\infty} e^{i\omega t - \Gamma|t|} e^{-i\omega_0 t}\left\{\sum_{m_1,m_0} \zeta \cdot e^{t(i\tilde{\Omega}-\tilde{\pi})\cdot\eta}\right\}, \tag{10.14}$$

For ^{57}Fe:

$$P(\omega) = \left(\frac{2}{\Gamma}\right)\sum_{i=1}^{6} \mathrm{Re}\,\zeta_i \cdot \tilde{A}_i^{-1}\eta, \tag{10.15}$$

Where

$$\tilde{A}_i = [(\omega - \omega_0) - \Gamma/2]\tilde{E}\tilde{\Omega}_1 - \tilde{\pi}. \tag{10.16}$$

E is the n×n matrix; n is the number of possible frequencies. To include source Γ_s and absorber Γ_α line widths Γ has to be taken as $\Gamma = \Gamma_s + \Gamma_\alpha$.

The relaxation models considered so far have assumed that the random fluctuation remains diagonal in m_1 before and after the relaxation event. In more general cases it is necessary to introduce a perturbation approach that describes relaxation and includes off-diagonal elements of the hyperfine interaction. Bradford and Marshall use a perturbation expansion to evaluate, for the case of ^{57}Fe, a correlation function equivalent to $\langle \hat{I}_q^1, \hat{I}_q^1(t)\rangle$ account cross relaxations $\langle \hat{I}_x^1, \hat{I}_y^1(t)\rangle$ and different relaxation rates along the x, y and z directions.

For isotropic relaxation the spin correlation function is taken as

$$\langle S_i(t)S_j(0)\rangle = \delta_{ij}\frac{1}{3}S(S+1)e^{(-i|t|/\tau)},\ \ i,j=x,y,z, \tag{10.17}$$

where S is the spin and τ is the correlation time for electronic relaxation. For the ^{57}Fe Mössbauer spectrum the Kramers doublet is:

$$I(\omega) = \frac{\Gamma\frac{b}{R}}{\omega^2+\left(\Gamma+\frac{b}{R}\right)^2}e^{b/R^2} - \frac{b}{R^2}\frac{(\Gamma+R)}{\omega^2+(\Gamma+R)^2} \tag{10.18}$$

Where

$$b = \frac{S(S+1)}{3\hbar^2}\left\{\frac{15}{4}A_1^2 - \frac{5}{2}A_1A_0 + \frac{3}{4}A_0^2\right\}. \tag{10.19}$$

This latter one is the case for polycrystalline absorber and A_1, A_0 are the hyperfine constants for the ground and excited states of ^{57}Fe; R is $1/\tau$. The perturbation approach requires $b<<R$; the fluctuation rate should be faster than the hyperfine frequencies expressed in frequency units. Inclusion of a time-independent quadrupole interaction in $\mathcal{H}$ leads to an asymmetry in the quadrupole doublet.

Introduction of an anisotropic hyperfine interaction

$$V(t) = A_{\parallel}I_zS_z(t) + A_{\perp}\left[I_xS_x(t) + I_yS_y(t)\right] \tag{10.20}$$

leads to anisotropic relaxation approximated by correlation functions like

$$\langle S_i(t)S_j(0)\rangle = \delta_{ij}\frac{1}{3}S(S+1)\left[\delta_{iz}e^{-|t|/\tau_{\parallel}} + \left\{\delta_{ix}+\delta_{iy}\right\}e^{-|t|/\tau_{\perp}}\right]. \tag{10.21}$$

In the case when an external magnetic field is applied to polarise the spins, fast relaxation amongst the levels ($\tau^{-1}<<A/h$) leads to a Boltzmann distribution over the levels, and the nucleus senses a field proportional to the moment induced in the paramagnet, which is similar to the situation in a magnetically ordered compound. The microscopic rate of spin fluctuations will begin to affect the Mössbauer spectra in a system where $\tau^{-1}\rightarrow A/h$.

After some further approximations, the final formula of the spectrum is given by

$$I(\omega,k) = \sum_{m_1,m_0}|\langle m_0,\omega,k|\mathcal{H}^-|m_1,m_0,\omega\rangle|, \tag{10.22}$$

where

$$l(m_1,m_0,\omega) = \frac{1+2\gamma(m_1,m_0)/\Gamma}{[\omega-\omega(m_1,m_0)-\delta(m_1,m_0)]^2+\left[\frac{\Gamma}{2}+\gamma(m_1,m_0)\right]^2}, \tag{10.23}$$

with

$$\omega(m_1,m_0) = (g_1\beta_Nm_1 - g_0\beta_Nm_0) \tag{10.24}$$

$$\gamma(m_1,m_0) = (g_1\beta_Nm_1 - g_0\beta_Nm_0)^2\overline{h^2}\tau_2 \tag{10.25}$$

$$\delta(m_1,m_0) = (g_1\beta_Nm_1 - g_0\beta_Nm_0)^3\frac{2}{3}\overline{h^3}\tau_3. \tag{10.26}$$

*1B Detection of different types of magnetism by Mössbauer spectroscopy**

a) Random powder (ferromagnetic or antiferromagnetic, without external magnetic field):

Spin orientation:

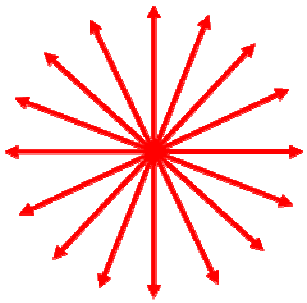

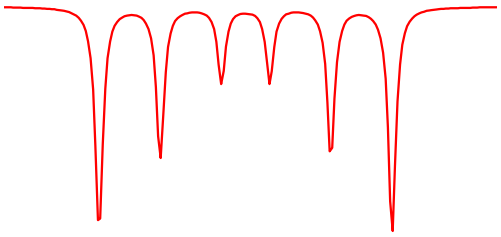

Resultant Mössbauer spectrum:

b) Ferromagnetic system:

1 – parallel case

Resultant Mössbauer spectrum:

Applying an external magnetic field:

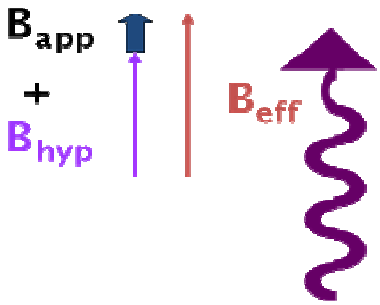

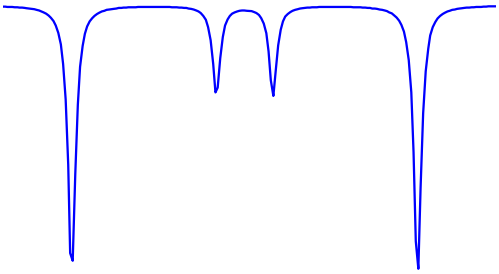

2– antiparallel case

Applying an external magnetic field:

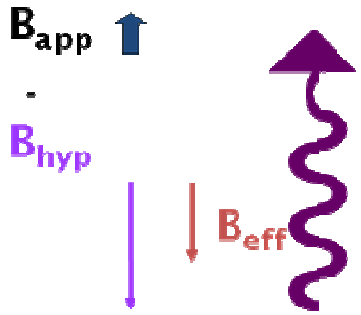

Resultant Mössbauer spectrum:

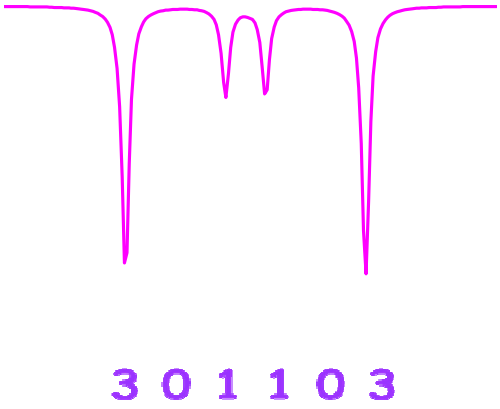

c) Antiferromagnetic system:

Applying an external magnetic field:

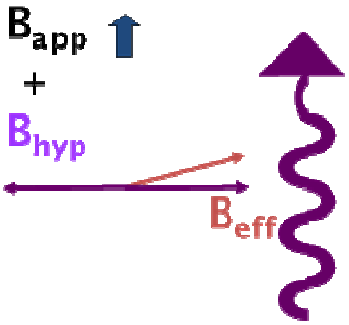

Resultant Mössbauer spectrum:

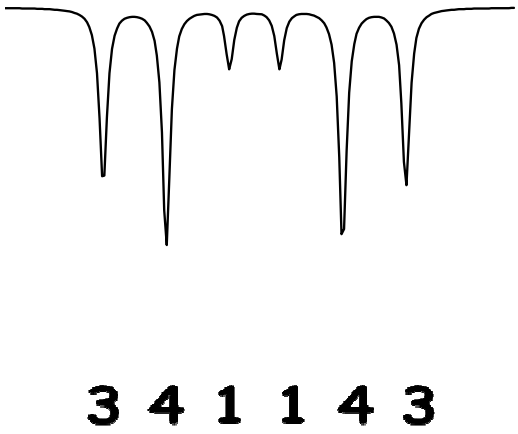

d) Ferrimagnetic system:

Spin orientation:

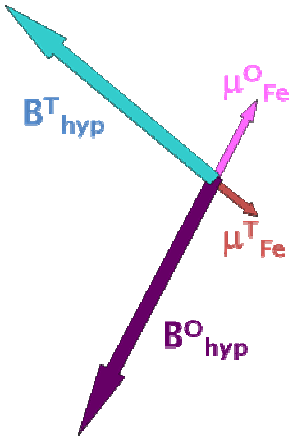

Resultant Mössbauer spectrum:

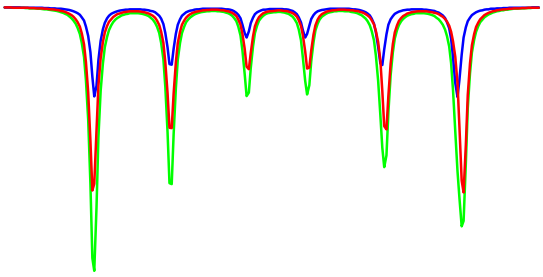

Applying an external magnetic field:

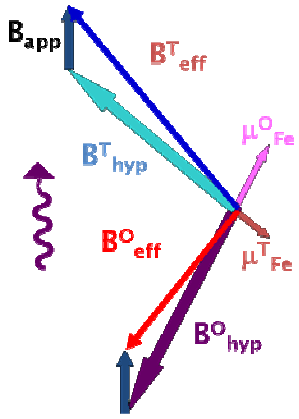

Resultant Mössbauer spectrum:

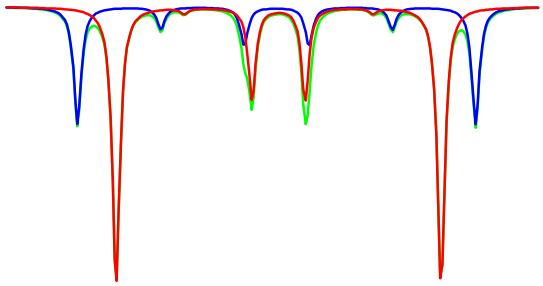

*This demonstration has been done following a personal communication of J.-M. Grenèche and all the spectra refer to a geometry of the Mössbauer set-up when the propagation direction of the γ-rays is identical with the direction of the applied magnetic field.

In case a), the orientation of the spins is random, therefore there is no specific direction and the resultant Mössbauer spectra will display a sextet with line intensities 3:2:1:1:2:3.

Application of an external magnetic field on ferromagnetic systems b/1 and b/2, results in the following effects: the effective magnetic field, which orients the spins a specific direction can increase (case 1, parallel) or decrease (case 2, antiparallel) depending on the direction of the hyperfine magnetic field. The spectral line intensities will be 3:0:1:1:0:3, in both cases, when the direction of the hyperfine magnetic field was identical to the γ-ray propagation direction.

Applying an external magnetic field on an antiferromagnetic system, the two spin components (thus the hyperfine magnetic field) will be oriented perpendicularly to the direction of the applied magnetic field, therefore there will be an angle between the direction of the effective magnetic field and of that the applied magnetic field (*i.e.* γ-ray propagation direction the in this measuring technique). Thus the line intensity ratios in the in-field spectrum will be 3:4:1:1:4:3.

The zero-field Mössbauer spectrum of a ferrimagnetic system, case e), is a magnetic sextet, the superposition of two sextets, with two different spin orientations. The applied field will affect the direction of both spin components, therefore the spectrum will split up into two better resolved subspectra, and the effective magnetic field of one component will increase, while the one of the other will decrease. The intensity of the 2-4 lines gives the value of the angles between the effective and the applied magnetic field for each spin moment, following the equation: $B_{hyp}^2 = B_{eff}^2 + B_{app}^2 - 2 \cdot B_{eff} \cdot B_{app} \cdot \cos\Theta$, hence the hyperfine magnetic field can be calculated.

2 Potentiometric titration of the $Fe^{III}EDTA$ complex

A stock solution of $Fe(NO_3)_3$ of c=1.939·10^{-3} mol/dm^3 was prepared, ionic strength was adjusted to be 0.1 mol/dm^3 by the addition of KNO_3 to the solution. To 9,96 cm^3 of the stock solution, 94.7 µmol Na_2H_2EDTA was added and was titrated by 97.8·10^{-3} mol/dm^3 KOH solution. The obtained titration curve is the following.

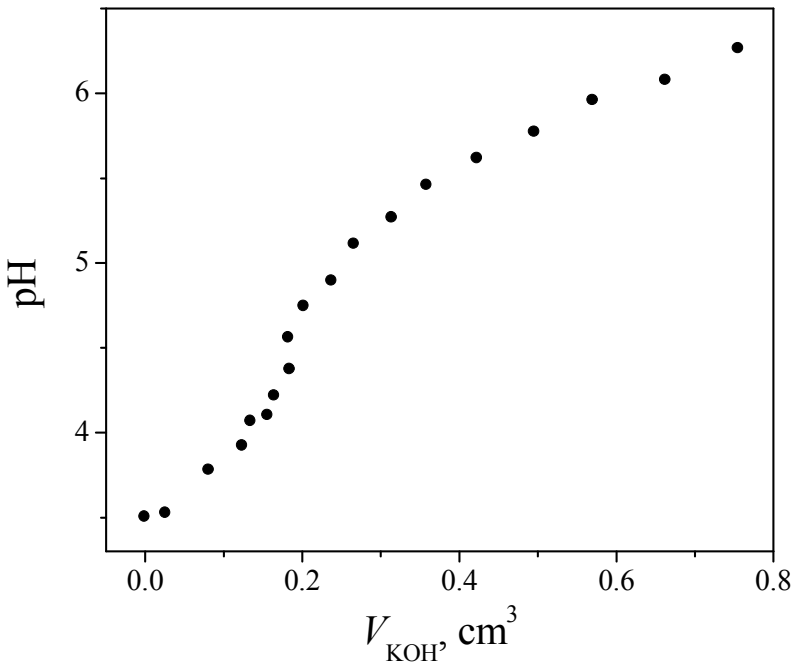

From this curve quantitative conclusions cannot be drawn, but it is clearly visible that apart from the proton exchange reaction which starts to take place at about pH=6 and obviously refers to the equation:

$[Fe^{III}EDTA(H_2O)]^- + OH^- \rightleftarrows [Fe^{III}EDTA(OH)]^{2-} + H_2O$.

There is another proton exchange reaction at about pH=3.

3 Another possible spectral line assumption for the Mössbauer spectrum recorded of the thermal degradation products.

The spectrum with another line assumption is displayed here:

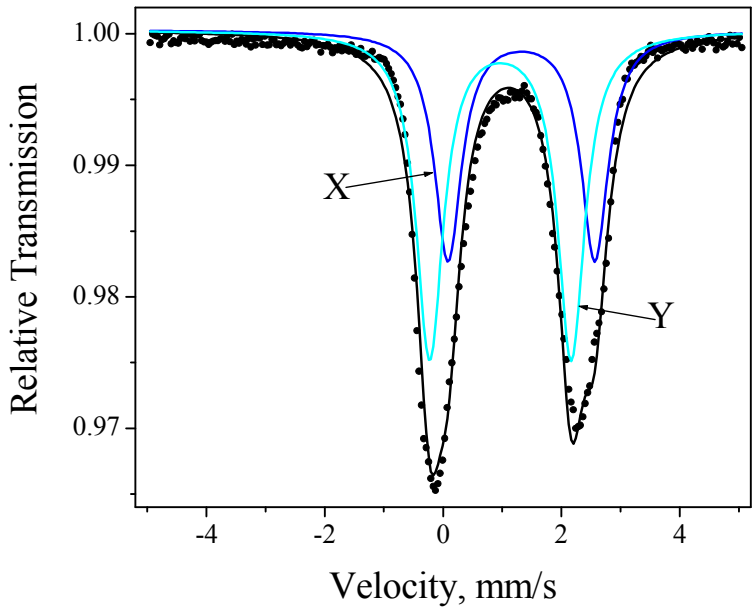

As can be seen, the isomer shifts of the different subspectra are very different, which would obviously mean a very different coordination around the ferrous ion. Parameters are listed below:

Subspectra/Parameters	Relative	δ (mm/s)	Δ (mm/s)	Γ (mm/s)
X	41.2	1.32(1)	2.48(1)	0.55(1)
Y	58.8	0.97(1)	2.39(1)	0.55(1)

An isomer shift of 0.97 mm/s for a high spin ferrous compound, although unusual, could be explained with a very low coordination number. However, in such case, the quadrupole splitting should be considerably different from that of species X as well. Furthermore, such a compound should result in a very different product when oxidised. In our case, the oxidation products of the different compounds were identical, which means that this possible spectrum evaluation remains a mathematical possibility only and has no physical and chemical meaning. Thus the other mathematically possible spectrum evaluation, which was discussed in Chapter 8 is much more credible.